PRODUCTION OF HIGH DENSITY AVIATION FUELS VIA NOVEL ZEOLITE CATALYST ROUTES

UTAH UNIV., SALT LAKE CITY. DEPT. OF FUELS ENGIEERING

23 OCT 1989

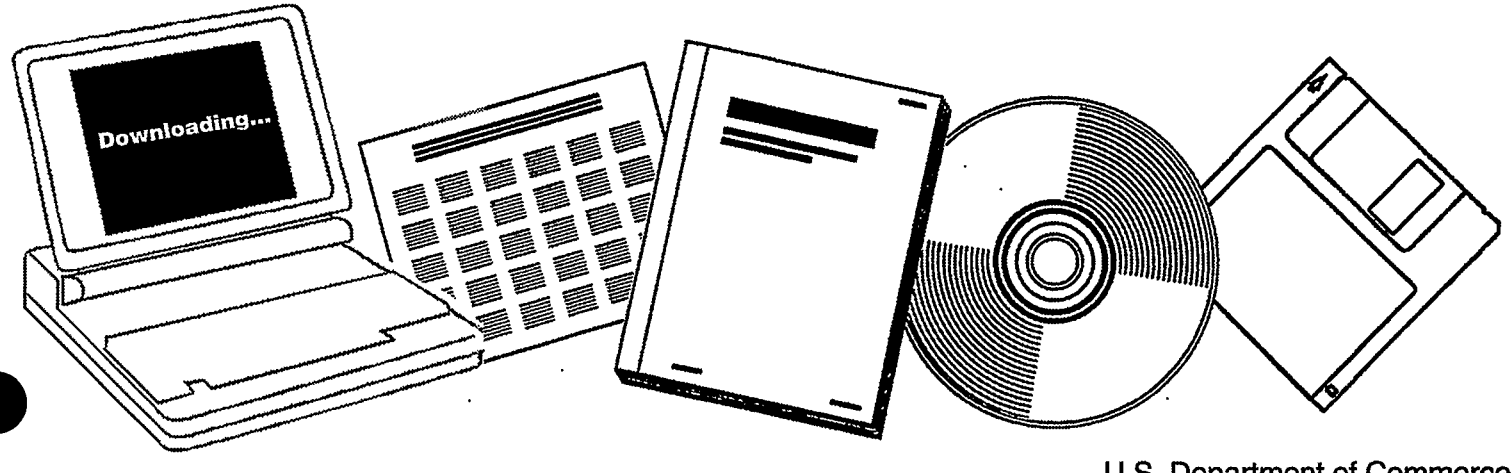

One Source. One Search. One Solution.

NTIS

Providing Permanent, Easy Access to U.S. Government Information

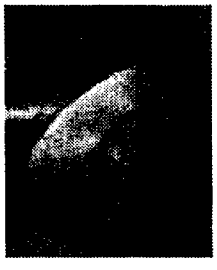

National Technical Information Service is the nation's largest repository and disseminator of government-initiated scientific, technical, engineering, and related business information. The NTIS collection includes almost 3,000,000 information products in a variety of formats: electronic download, online access, CD-ROM, magnetic tape, diskette, multimedia, microfiche and paper.

Search the NTIS Database from 1990 forward

NTIS has upgraded its bibliographic database system and has made all entries since 1990 searchable on **www.ntis.gov.** You now have access to information on more than 600,000 government research information products from this web site.

Link to Full Text Documents at Government Web Sites

Because many Government agencies have their most recent reports available on their own web site, we have added links directly to these reports. When available, you will see a link on the right side of the bibliographic screen.

Download Publications (1997 - Present)

NTIS can now provides the full text of reports as downloadable PDF files. This means that when an agency stops maintaining a report on the web, NTIS will offer a downloadable version. There is a nominal fee for each download for most publications.

For more information visit our website:

www.ntis.gov

U.S. DEPARTMENT OF COMMERCE
Technology Administration
National Technical Information Service
Springfield, VA 22161

WRDC-TR-89-2097

AD-A216 444

PRODUCTION OF HIGH DENSITY AVIATION FUELS VIA NOVEL ZEOLITE CATALYST ROUTES

Dr Francis V. Hanson
Associate Professor of Fuels Engineering
Department of Fuels Engineering
Univresity of Utah
Salt Lake City, Utah 84112-1183

23 OCTOBER 1989

Final Report for Period December 1985 to May 1987

Approved for public release; distribution unlimited.

AERO PROPULSION AND POWER LABORATORY
WRIGHT RESEARCH AND DEVELOPMENT CENTER
AIR FORCE SYSTEMS COMMAND
WRIGHT-PATTERSON AIR FORCE BASE, OHIO 45433-6563

NOTICE

When Government drawings, specifications, or other data are used for any purpose other than in connection with a definitely Government-related procurement, the United States Government incurs no responsibility or any obligation whatsoever. The fact that the Government may have formulated or in any way supplied the said drawings, specifications, or other data, is not to be regarded by implication, or otherwise in any manner construed, as licensing the holder, or any other person or corporation; or as conveying any rights or permission to manufacture, use, or sell any patented invention that may in any way be related thereto.

This report is releasable to the National Technical Information Service (NTIS). At NTIS, it will be available to the general public, including foreign nations.

This technical report has been reviewed and is approved for publication.

Randall B. Howard

RANDALL B. HOWARD, 1Lt, USAF
Fuels Branch
Fuels and Lubrication Division
Aero Propulsion and Power Laboratory

Charles L Delaney

CHARLES L. DELANEY, Chief
Fuels Branch
Fuels and Lubrication Division
Aero Propulsion and Power Laboratory

FOR THE COMMANDER

LEO S. HAROOTYAN, JR., Assistant Chief
Fuels and Lubrication Division
Aero Propulsion and Power Laboratory

If your address has changed, if you wish to be removed from our mailing list, or if the addressee is no longer employed by your organization, please notify WRDC/POSF, WPAFB OH 45433-6563 to help us maintain a current mailing list.

Copies of this report should not be returned unless return is required by security considerations, contractual obligations, or notice on a specific document.

UNCLASSIFIED
SECURITY CLASSIFICATION OF THIS PAGE

REPORT DOCUMENTATION PAGE

Form Approved
OMB No. 0704-0188

1a. REPORT SECURITY CLASSIFICATION UNCLASSIFIED	1b. RESTRICTIVE MARKINGS NONE
2a. SECURITY CLASSIFICATION AUTHORITY N/A	3. DISTRIBUTION/AVAILABILITY OF REPORT Approved for public release; distribution is unlimited.
2b. DECLASSIFICATION/DOWNGRADING SCHEDULE N/A	
4. PERFORMING ORGANIZATION REPORT NUMBER(S) N/A	5. MONITORING ORGANIZATION REPORT NUMBER(S) WRDC-TR-89-2097
6a. NAME OF PERFORMING ORGANIZATION The University of Utah 6b. OFFICE SYMBOL (If applicable)	7a. NAME OF MONITORING ORGANIZATION Aero Propulsion and Power Laboratory(WRDC/POSF) Wright Research and Development Center
6c. ADDRESS (City, State, and ZIP Code) Department of Fuels Engineering Salt Lake City, Utah 84112-1183	7b. ADDRESS (City, State, and ZIP Code) Wright-Patterson AFB, OH 45433-6563
8a. NAME OF FUNDING/SPONSORING ORGANIZATION 8b. OFFICE SYMBOL (If applicable)	9. PROCUREMENT INSTRUMENT IDENTIFICATION NUMBER F33615-85-C-2567
8c. ADDRESS (City, State, and ZIP Code)	10. SOURCE OF FUNDING NUMBERS PROGRAM ELEMENT NO. 62203F; PROJECT NO. 3048; TASK NO. 05; WORK UNIT ACCESSION NO. 55

11. TITLE (Include Security Classification)

Production of High Density Fuels via Novel Zeolite Catalyst Routes

12. PERSONAL AUTHOR(S)
Dr Francis V. Hanson

13a. TYPE OF REPORT	13b. TIME COVERED	14. DATE OF REPORT (Year, Month, Day)	15. PAGE COUNT
Final	FROM Dec 85 TO May 87	1989 October 23	484

16. SUPPLEMENTARY NOTATION

NONE

17. COSATI CODES			18. SUBJECT TERMS (Continue on reverse if necessary and identify by block number)
FIELD	GROUP	SUB-GROUP	High Density Fuels, Catalysis, Zeolite, Aviation Fuels
21	04		

19. ABSTRACT (Continue on reverse if necessary and identify by block number)

The production of high density aviation fuels from reliable, domestic fossil fuel sources is of considerable importance to the United States Air Force. The production of high density aviation fuels can be achieved by a number of alternative process sequences, for example, shape selective cracking of normal paraffins from an appropriate boiling range fraction of a naphthenic crude; saturation of an aromatic FCC cycle stock of the appropriate boiling range; saturation of an appropriate boiling range fraction from a hydrocracker recycle stream when the feed to the hydrotreater is aromatic in nature; synthesis of the appropriate boiling range aromatic species from oxygenates over crystalline aluminosilicates followed by hydrogenation of the aromatic species; and direct synthesis of the aromatic hydrocarbons from hydrogen and carbon monoxide over crystalline aluminosilicate-supported metal catalysis followed by hydrogenation of the aromatic species. This report summarizes a research program aimed at developing catalyst and processing concepts for the production of high density aviation turbine fuels via novel zeolite catalyst routes.

20. DISTRIBUTION/AVAILABILITY OF ABSTRACT ☐ UNCLASSIFIED/UNLIMITED ☒ SAME AS RPT. ☐ DTIC USERS	21. ABSTRACT SECURITY CLASSIFICATION UNCLASSIFIED
22a. NAME OF RESPONSIBLE INDIVIDUAL RANDALL B. HOWARD, 1Lt, USAF	22b. TELEPHONE (Include Area Code) (513) 255-7423 22c. OFFICE SYMBOL WRDC/POSF

DD Form 1473, JUN 86 *Previous editions are obsolete.*

SECURITY CLASSIFICATION OF THIS PAGE
UNCLASSIFIED

SYNOPSIS

The production of high density aviation turbine fuels from reliable, domestic fossil fuel resources is of considerable importance to the United States Air Force. The initial benchmark high density aviation turbine fuel which led to establishment of the various United States Air Force research programs was the high density Soviet aviation turbine fuel acquired during the mid 1970s. Detailed analysis of this fuel indicated an average molecular structure consisting of a two-ring naphthene containing four substituent methyl groups. The average empirical formula of this high density fuel was determined to be:

$$(CH_3)_{3.48}\ (CH)_{8.72}\ (CH_3)_{3.93}.$$

The production of turbine fuels of this average structure can be achieved by a number of alternative process sequences, for example, shape selective cracking of normal paraffins from an appropriate boiling range fraction of a naphthenic crude; saturation of an aromatic FCC cycle stock of the appropriate boiling range; saturation of an appropriate boiling range fraction from a hydrocracker recycle stream when the feed to the hydrotreater is aromatic in nature; synthesis of the appropriate boiling range aromatic species from oxygenates over crystalline aluminosilicates followed by hydrogenation of the aromatic species; and direct synthesis of the aromatic hydrocarbons from hydrogen and carbon monoxide over crystalline aluminosilicate-supported metal catalysts followed by hydrogenation of the aromatic species.

A research program (contract number F33615-85-C-2567) aimed at developing catalyst and processing concepts for the production of high density aviation turbine fuels via novel zeolite catalyst routes was initiated in the Department of Fuels Engineering at the University of Utah during November of 1985.

The original, primary objectives of the program were as follows:

1. to design and fabricate an automated laboratory catalyst testing unit capable of continuous operation and of conducting catalyst screening/evaluation studies and process variable/catalyst aging investigations;
2. selective synthesis of methyl-substituted mono- and dicyclic aromatic hydrocarbons in the aviation turbine fuel boiling range;
3. hydrogenation of alkyl-substituted mono- and dicyclic aromatic hydrocarbons and selected aromatic feedstocks to the corresponding mono- and dicyclic naphthenes in the aviation turbine fuel boiling range; and
4. to conduct an exhaustive survey of the technical and patent literature related to the specific research tasks to be performed under this contract.

The aromatics hydrogenation studies were deemphasized at the instruction of the Technical Project Officer since it was determined that those aspects of the Air Force high density aviation turbine fuel research problem could be accomplished under other sponsored research programs, whereas the zeolite work could only be accomplished as part of the University of Utah program.

The accomplishments of the program through the termination of United States Air Force funding included the following:

- The procedures for the reproducible laboratory synthesis of crystalline aluminosilicates of the ZSM class of zeolites were developed and proven.

- ZSM-5 (methyl-substituted monoaromatics hydrocarbon selectivity) was successfully prepared and characterized in the laboratory. Selectivity and activity data for the conversion of alcohol feedstocks were obtained.
- ZSM-48 (low molecular weight olefin selectivity) was successfully prepared and characterized in the laboratory. Selectivity and activity data for the conversion of methanol were obtained.
- A processing scheme involving the utilization of both ZSM-48 and ZSM-5 was devised for the production of methyl-substituted dicyclic aromatic hydrocarbons and preliminary evaluation of the process concept was carried out in the catalyst testing unit.
- The catalyst testing unit was designed, constructed, and used in the evaluation of catalysts and processing schemes.
- A BET surface area apparatus was designed and fabricated. The operating procedures were developed and tested for a variety of high surface area oxide materials and zeolites, including the ZSM class of zeolites.
- A literature survey database and retrieval system were developed and the assembly of pertinent citations was initiated.

Subsequent to the termination of funding by the United States Air Force an attempt was made to complete the studies in part by using other sources of funding; in particular, unrestricted development funds and grants from industrial research laboratories were used to complete the dissertation studies of Dr. H.P. Wang and the thesis studies of Mr. D.C. Longstaff. Unfortunately, it was not possible to complete all aspects of an anticipated three year research program with limited private sector funds available in the second and third years of the program. Hydrodewaxing studies were incorporated into the program and completed after the discontinuance of the United States Air Force Funding.

The project status and the results of the various elements of the original and expanded research program are discussed in detail in the body of the report.

TABLE OF CONTENTS

TABLE OF CONTENTS (Continues)

TABLE OF CONTENTS (Continues)

TABLE OF CONTENTS (Continues)

TABLE OF CONTENTS (Concluded)

LIST OF FIGURES

LIST OF FIGURES (Continues)

LIST OF FIGURES (Continues)

LIST OF FIGURES (Continues)

LIST OF FIGURES (Continues)

LIST OF FIGURES (Concluded)

LIST OF TABLES

LIST OF TABLES (Concluded)

Section I: INTRODUCTION

Aviation turbine fuels have been traditionally manufactured by distillation of petroleum crudes followed by mild hydrogen treatment to remove organic sulfur and nitrogen species and to impart thermal stability to the fuel. In order to significantly increase the range of volume limited military aircraft, the United States Air Force has contemplated changing over to higher density aviation turbine fuels. The increased range results from increasing the specific gravity of aviation turbine fuels, and, thus, the volumetric heating value as illustrated in Figure 1. Higher density aviation turbine fuels can be produced by expanding the boiling range of the fuel by raising the endpoint; however, increasing the availability of higher density jet fuels through the adjustment of distillation boiling ranges may be limited not only by existing specifications with regard to freeze point but also by the demand for the same boiling range fraction to produce other products.

The past 15 years have revealed the vulnerability of the United States liquid fuels markets to international events. Events beyond the control or influence of the United States have altered the uniform course of domestic economic progress by influencing the availability and cost of traditional energy sources. Thus, it would be desirable to develop stable, domestic sources of the high density aviation turbine fuels.

Aviation Turbine Fuels

Fuels developed for aviation turbine applications must meet certain established specifications. Many of these specifications can be met by the addition of specific compounds or additives to the fuel in low concentrations. However, there are some specifications that cannot be economically met by blending additives and can only be met by adjusting the boiling range of the fuel.

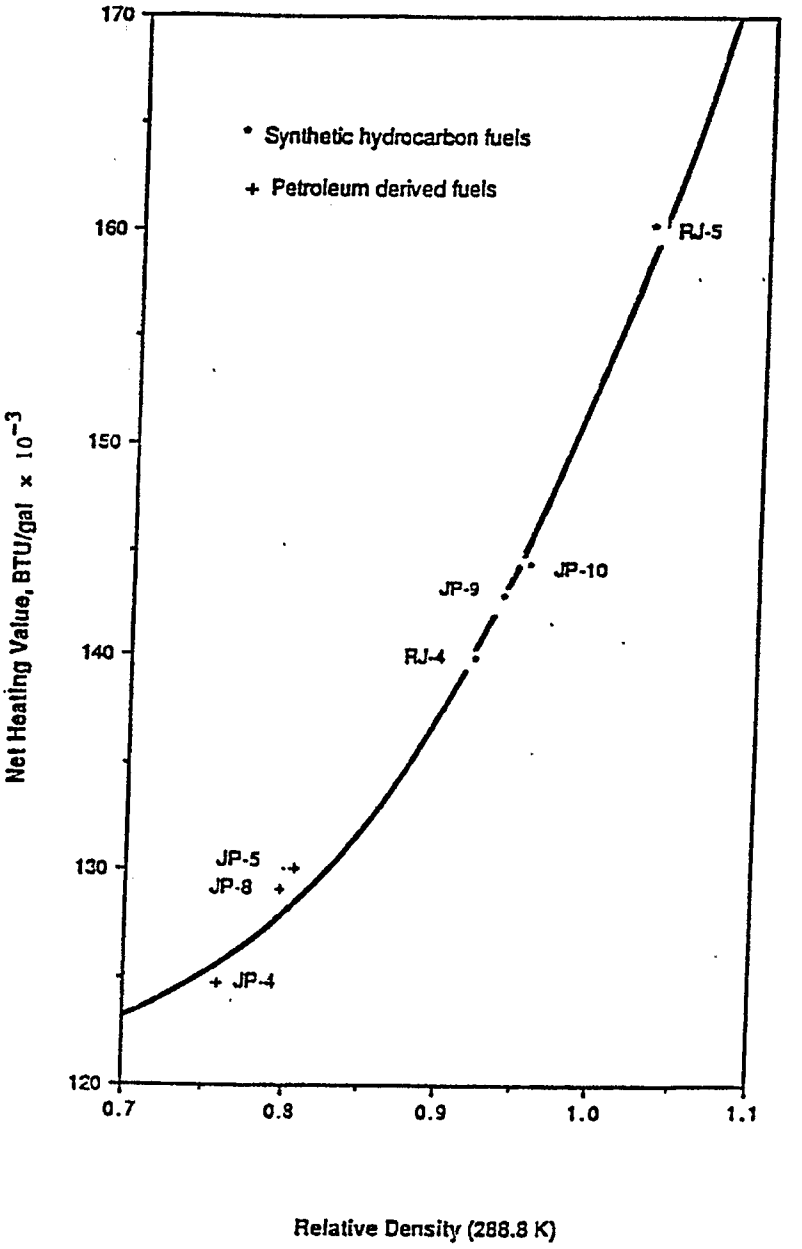

Figure 1. Fuel Density vs. Net Heating Value

A number of the typical specifications for civilian and military jet fuels are listed in Table 1. An indication of the means by which these and other specifications can be met are listed in Table 2; that is, by blending an additive with the straight run fuel or by selecting the proper distillation fraction from an appropriate crude oil.[1]

The most critical specifications are those on freeze point, vapor pressure, and aromatics. Fuels for aviation turbines are usually produced from straight run distillation cuts rather than from cracked stocks to meet the specifications on aromatics and olefins. The specification on viscosity is important, but it is only important for very low freeze point fuels which operate at temperatures below 213 K (-60°C). Generally, the low temperature properties of a fuel are defined according to its freeze point, rather than its low temperature viscosity.

Aromatics concentrations must be less than 20 volume percent[2] because high aromatic fuels produce smoke which excessively heats jet engine components. There exists an added complication for military aircraft related to the visible contrail behind the plane, due to the smoke produced from the combustion of aromatics. Soot in the exhaust gas also makes the jet more vulnerable to heat seeking missiles, due to the higher luminosity of the turbine exhaust gases.

The freeze points of conventional jet fuels range from 233 K to 213 K (-40 to -60°C). If the composition of an aviation turbine fuel is such that the freeze point is too high, then paraffin crystals may form in the fuel stored in the unheated, on-board fuel tanks. These paraffin crystals can deposit in fuel filters and may damage fuel pump components.

Vapor pressure must be low for safety and conservation reasons. However, the vapor pressure must not be too low to avoid aircraft cold starting problems. This is particularly crucial for military jets which are sometimes parked on extremely cold runways.[2]

Table 1

Selected Specifications for Aviation Turbine Fuels[3]

Turbine Fuel Property	Civilian Fuels		Military Fuels		
	Jet A	Jet B	JP-4	JP-5	JP-8
Density (g/cm^3)	0.78-0.84	0.75-0.80	0.75-0.85	0.78-0.85	0.78-0.84
Freeze Point (maximum, °F)	-40	-50	-58	-46	-50
Flash Point (minimum, °F)	100	NA	NA	140	100
Aromatics (maximum, vol%)	20	20	25	25	25
Sulfur (maximum, wt%)	0.3	0.3	0.4	0.4	0.4
H_2 Content (minimum, wt%)	NA	NA	13.6	13.5	13.6
Heat Content (MJ/kg, minimum)	42.8	42.8	42.8	42.6	42.8
Stability Test Temperature (minimum, °f)	473	473	500	500	500

Table 2

Aviation Turbine Fuel Specifications

Specification	Key
Low Aromatic Content	c
Low Freeze Point	c, d
Low Vapor Pressure	c, d
Stability (olefin content)	c, t, a
Sulfur Content	c, t, a
Low Temperature Viscosity	c, d
Water Solubility	a
Electrical Conductivity	a

Key

a - specification can be met by blending of an additive.

c - specification can be met by choice of crude

d - specification can be met by choosing the proper distillation cut

t - specification can be met by chemical treatment of jet fuel

The stability specification for jet fuels requires that the olefin content of the fuel be less than one or two percent. Even though jet fuels are stored in unheated tanks in aircraft, they are used as a coolant for jet engine lubricating oil and the fuel may reach a temperature of 573 K (300°C) or higher in the injection nozzle. For this reason the olefin content must be kept low to avoid polymerization of the olefins and gum formation which can eventually plug some of the fuel injection nozzles.

Aviation turbine fuels need to be low in sulfur and metals because metal sulfates formed in the combustion process can corrode jet engine components. Fuels that contain too much sulfur can be lightly hydrotreated to remove mercaptan sulfur, thus lowering the sulfur content.

Glycol ether is added to the fuels to increase the solubility of water which may condense or freeze in cold fuel tanks. A biocide is also added to restrict the growth of microorganisms at water-hydrocarbon interfaces. This is necessary because microorganisms growing in fuel tanks may form an organic sludge which can plug fuel filters.

Jet fuels can develop static electrical charges during handling and transfer of the fuel from storage tanks to the on-board fuel tanks. If static electrical charges are not dissipated, an electrical arc may occur between the fuel and an electrical ground, thus igniting the fuel vapors. Consequently additives are placed in the fuel to increase its electrical conductivity and to circumvent the build-up of static charge.

The requirement for a low freeze point and low volatility is a dilemma for producers of jet fuels. Only specific cuts of kerosene boiling range materials from specific crudes (which may be of limited availability) can satisfy this dual requirement. Economic considerations dictate that such cuts be either untreated or only lightly hydrogenated to remove nitrogen, sulfur, and olefins.

The requirement that the concentrations of aromatics, olefins, and paraffins be below certain levels limits the possible crudes available for the production of jet fuels to those crudes which have high naphthene content in the 423-523 K (150-250°C) boiling range. These restrictions raise the possibility that the United States could be vulnerable to crude oil supply disruptions during a war involving OPEC oil supplies or an oil embargo. One objective of aviation turbine fuel research and development activities is to produce a naphthenic jet fuel with a normal paraffin content which is low enough so that the freeze point specification will be met. A second objective is to produce these fuels from secure, domestic resources.

Possible Processing Schemes for the Production of High Density Aviation Turbine Fuels

The production of high density aviation turbine fuels can be accomplished by a number of conventional processing schemes[4,5] as well as by several unconventional schemes. The processing schemes which make use of commercially practiced concepts include the following: shape selective cracking of normal paraffins from an appropriate boiling range fraction of a naphthenic crude; saturation of an aromatic FCC cycle stock of the appropriate boiling range; and saturation of an appropriate boiling range fraction from a hydrocracker recycle stream when the feed to the hydrotreater is aromatic in nature. The unconventional processing schemes include synthesis of the appropriate boiling range aromatic species from oxygenates over crystalline aluminosilicates followed by hydrogenation of the aromatic species; and direct synthesis of the aromatic hydrocarbons from hydrogen and carbon monoxide over crystalline aluminosilicate-supported metal catalysts followed by hydrogenation of the aromatic species.

Hydrogenation of Aromatic Refining Feed Streams

The production of high density aviation turbine fuels could be achieved by the hydrogenation of aromatic FCC cycle stocks[4] (Figure 2); that is, a naphthenic, high density aviation turbine fuel could be produced from an expanded boiling range jet fuel fraction produced from aromatic petroleum crude oils that have been reacted over conventional fluid zeolite cracking catalysts. The aromatic jet fuel fraction obtained from an FCC liquid recycle stream should be mostly methyl substituted aromatic hydrocarbons which, upon hydrogenation of the aromatic core over a supported noble metal catalyst, would be an excellent high density turbine fuel candidate. The hydrogenation step would also saturate the olefin species and reduce the sulfur and nitrogen heteroatom concentration to comply with the specifications.

Removal of Normal Paraffins from Naphthenic Refinery Feed Streams

An alternate route for the production of high density aviation turbine fuels would be the removal of normal and slightly branched paraffins from an expanded boiling range jet fuel fraction from a naphthenic crude oil or from the second stage recycle stream of a hydrocracker processing an aromatic feed stock composited from various refinery process streams such as coker gas oils, FCC cycle stocks, and/or primary or secondary furfural extracts.

Solvent Extraction

Normal paraffins could be removed by solvent dewaxing from waxy naphthenic distillation cuts of the proper boiling range. Solvent dewaxing consists of chilling the material to be dewaxed in the presence of a solvent to remove normal paraffins.[6] This process is a step in the manufacture of conventional low pour point lube oils and could be used to selectively remove

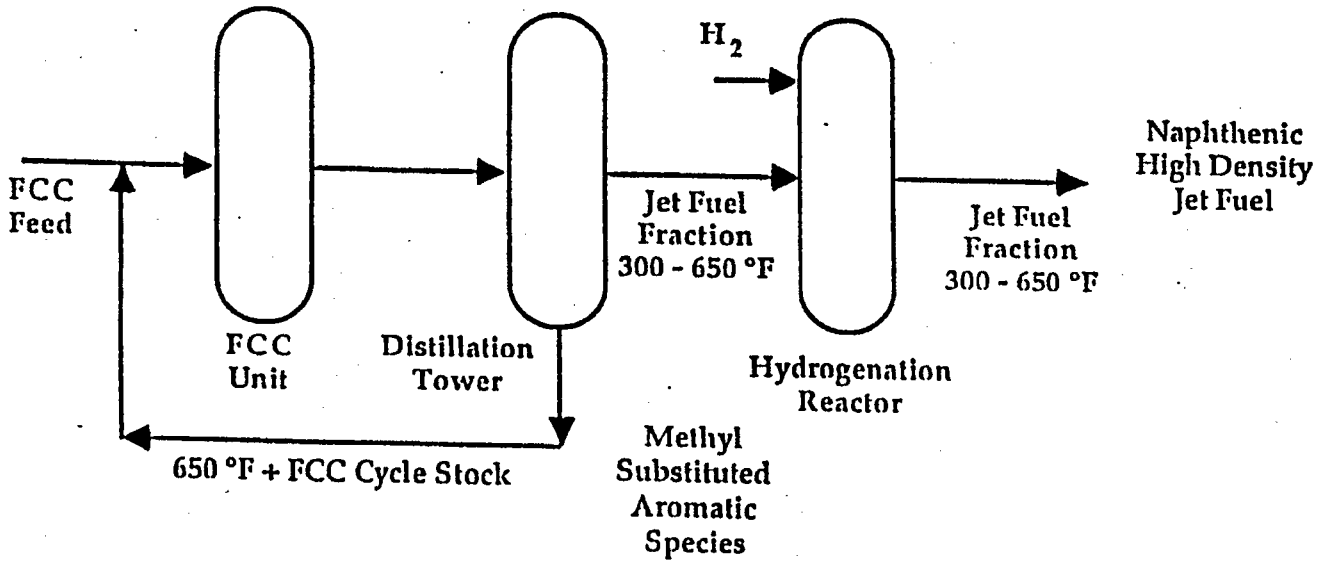

Figure 2. Proposed Conventional Route to High Density Aviation Turbine Fuel Hydrogenation of Aromatic FCC Cycle Stocks

normal paraffins from these expanded boiling range fractions to reduce the freeze point to meet the fuel specification. The normal paraffins precipitate and the crystals are removed by filtration. This process is expensive due to refrigeration costs.[7] In the case of dewaxing jet fuels this process would be particularly expensive due to the lower crystallization temperatures of paraffins in the jet fuel boiling range.

Shape Selective Catalytic Dewaxing

An alternative to solvent dewaxing is shape selective cracking of the normal paraffins in an expanded boiling range waxy naphthenic petroleum distillate. The expansion of the boiling range results in an increased freeze point, a larger average ring structure, and a higher density in the jet fuel fraction. The shape selective cracking catalyst will selectively convert the normal paraffins and slightly substituted paraffins to the light and intermediate naphtha boiling range resulting in a reduction of the freeze point. Catalysts suitable for this application include the acid form of ZSM-5[8-10] and platinum supported on H-Mordenite.[11]

This process concept can be applied to straight run naphthenic crude oils (Figure 3) or to hydrocracker jet fuel fractions (Figure 4). The cracked naphtha is then distilled to the original initial boiling point of the uncracked feed. If the wax is completely converted to cracked products, only naphthene molecules will remain in the boiling range of the original feed, which would then be suitable as a jet fuel. It is not likely that 100 percent conversion of the normal paraffins will need to be accomplished for the product to meet jet fuel specifications.

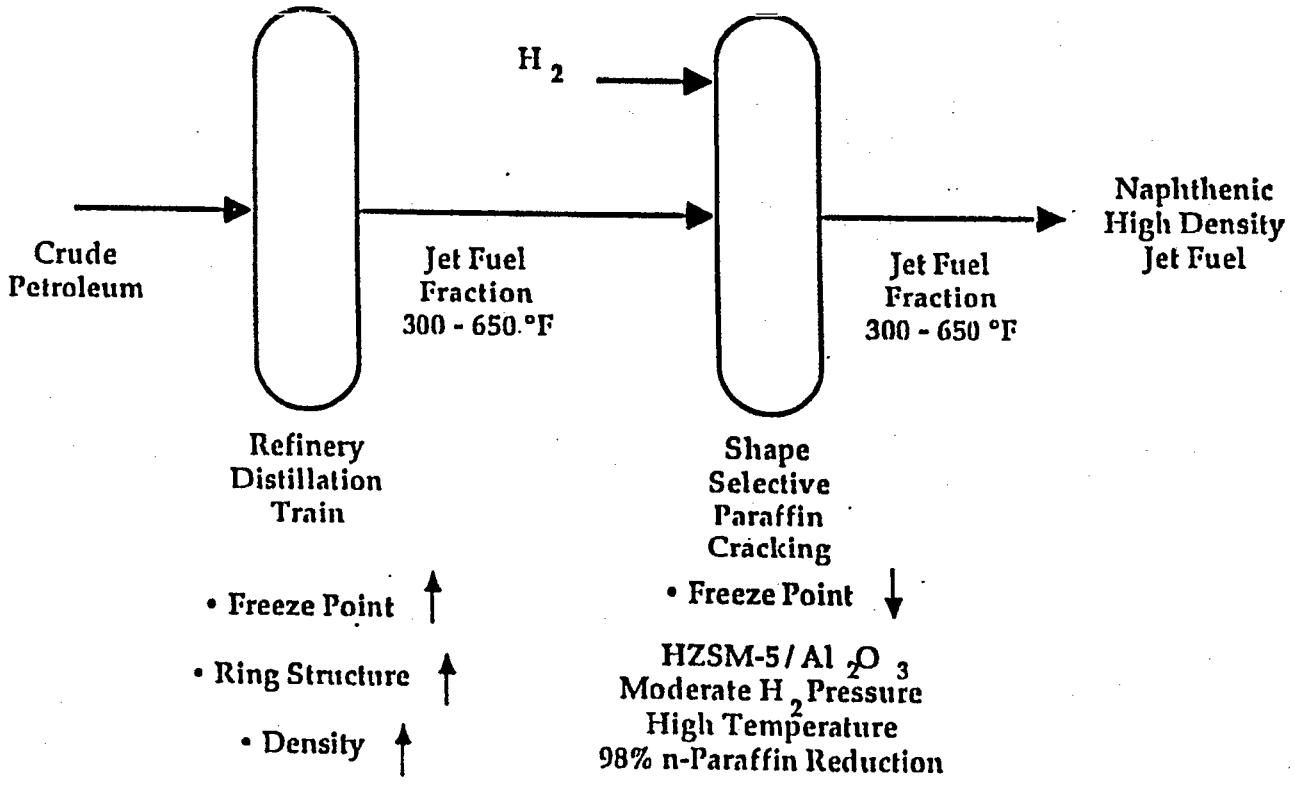

Figure 3. Proposed Conventional Route to High Density Aviation Turbine Fuel. Shape Selective Cracking of n-Paraffins in Naphthenic Aviation Turbine Fuel Fraction.

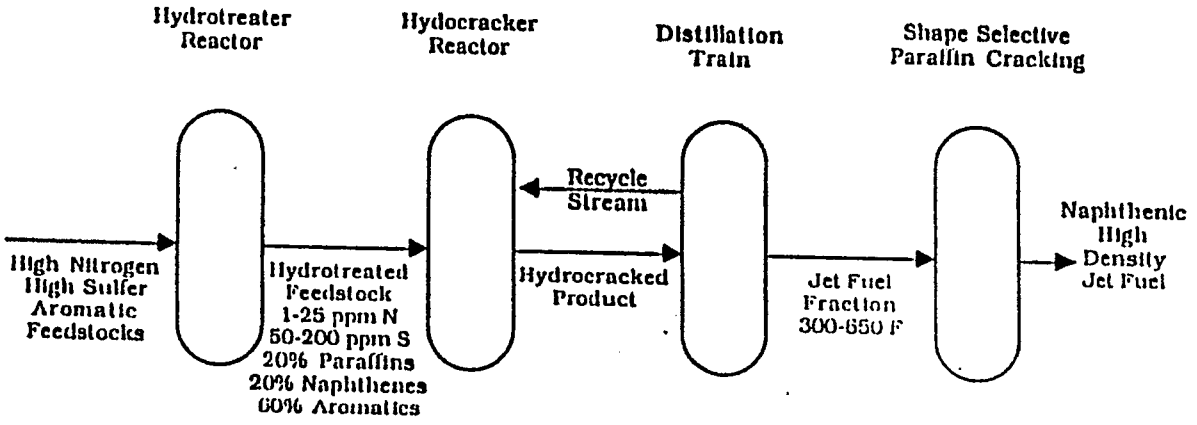

Figure 4. Proposed Conventional Route to High Density Aviation Turbine Fuel.
Shape Selective Cracking of n-Paraffins in Hydrocracker Aviation Turbine Fuel Fractions.

This method of low freeze point jet fuel production requires a shape selective cracking catalyst which will permit normal paraffin and slightly branched molecules to diffuse to active cracking sites but still restrict the diffusion of naphthenic molecules to the active sites. Certain zeolite catalysts such as ZSM-5 exhibit the appropriate shape selective behavior.[12]

Shape Selective Formation of Aromatic Hydrocarbons, Followed by Hydrogenation to the Corresponding Naphthene

An unconventional route to the production of high density aviation turbine fuels involves the use of shape selective catalysts to form the appropriate methyl-substituted aromatic hydrocarbons from oxygenates, followed by hydrogenation of the aromatic core to produce the corresponding naphthene. If feasible, this concept could provide a secure, albeit expensive, domestic source of high density fuels, since the oxygenates can be produced from domestic coal resources via commercially practiced Fischer-Tropsch technology. A schematic of the concept is presented in Figure 5.

A primary objective of this research project was to evaluate the potential of this concept for the production of high density fuels with an emphasis on the aromatic formation reactor system.

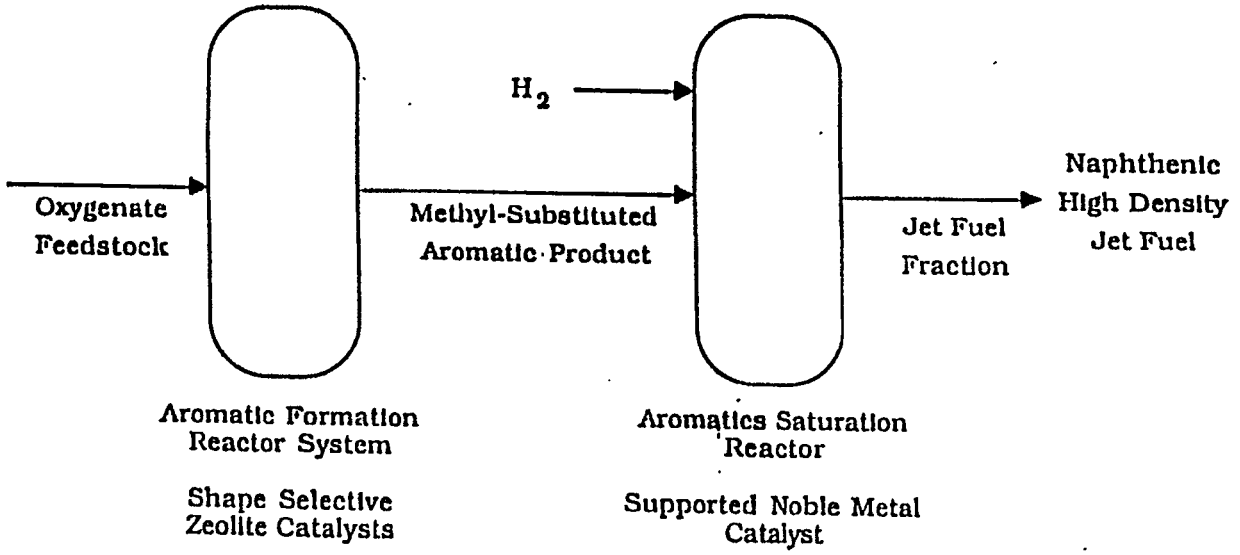

Figure 5. Proposed Novel Catalytic Route to High Density Aviation Turbine Fuel.
Oxygenate Conversion to Aromatic Hydrocarbons Followed by Hydrogenation to the Naphthenes

Section II: ANALYSIS OF AVIATION TURBINE FUEL SAMPLES

Research Personnel: Chia J. Wang
Graduate Student

Hong P. Wang
Graduate Student

Francis V. Hanson
Associate Professor

The initiation of a research program at the University of Utah aimed at producing high density aviation turbine fuels required the development of a data base on aviation turbine fuel properties. This was accomplished by analyzing a series of samples provided by the Air Force Wright Aeronautical Laboratories at Wright-Patterson Air Force Base. The samples included three petroleum-derived fuels, JP-4, JP-5, and JP-8, and a shale oil derived fuel, JP-4. Three samples of a pyrolysis oil product were also included in the analysis program. Since the objective of the research program was to develop catalyst and processing concepts leading to the production of high density aviation turbine fuels, a high density fuel was also incorporated into the analytical program. A secondary objective of the analysis studies was to evaluate the analytical capabilities of the Laboratory of Coal Science, Synthetic Fuels and Catalysis at the University of Utah. The samples provided by the Air Force Wright Aeronautical Laboratories are identified in Table 3. In addition, a sample of an aromatic solvent, 2040 solvent, was analyzed as a potential feedstock for the production of high density aviation turbine fuel by hydrogenation of the aromatic rings.

The analyses performed on the aviation turbine fuel samples, the pyrolysis oils, and the aromatic solvent included both physical and chemical properties, as well as spectroscopic characterization in the case of the high density fuel:

Table 3

Identification of Aviation Turbine Fuel Samples

USAF Sample Code	Sample Identification	Quantity (Quarts)	Color
82-POSF-1028	Soviet MIG 25 Jet Fuel	1	Clear
82-POSF-0541	JP-4 (Petroleum Derived)	2	Faint Yellow
83-POSF-1431	JP-4 (Shale Oil Derived)	3	Clear
83-POSF-1030	JP-5 (Petroleum Derived)	2	Yellow
83-POSF-0462	JP-8 (Petroleum Derived)	2	Clear
82-POSF-0162	Pyrolysis Oil (2%)[a]	1	Slightly Yellow
83-POSF-0801	Pyrolysis Oil (30%)[b]	1	Yellow
84-POSF-1949	Pyrolysis Oil[c]	1	Yellow

[a] 2% aromatic hydrocarbons
[b] 30% aromatic hydrocarbons
[c] 500°F minus cut of 82-POSF-0162 (HDI)

- specific gravity
- viscosity (as a function of temperature)
- flash point
- fire point
- simulated distillation
- heat of combustion
- elemental analysis
  - carbon
  - hydrogen
  - sulfur
  - nitrogen
- infrared spectra
- molecular weight
- nuclear magnetic resonance
  - proton
  - carbon 13

The specific gravities were determined using a vibrating U-tube density meter. The viscosities were measured as a function of temperature using the Wells-Brookfield Model LVT Micro-viscometer. The pour point, flash point, fire point, and the heat of combustion were determined according to the accepted ASTM methods. The elemental analyses and the molecular weights were determined by Galbraith Laboratories of Knoxville, Tennessee. The infrared spectra and nuclear magnetic resonance analysis were performed in the Chemistry Department at the University of Utah.

Simulated distillation data were obtained using a Hewlett-Packard Model 5830A gas chromatograph equipped with a dual flame-ionization detector. The packing material was 3 percent Dexsil 300 on Anakrom Q.

Analysis of the High Density Aviation Turbine Fuel

The high density Soviet aviation turbine fuel was analyzed to provide a basis for the research and development studies on high density fuels. Duplicate tests were performed in each

instance to evaluate and monitor our analytical procedures and to determine the reproducibility of the procedures.

The physical inspections are presented in Table 4, and the simulated distillation analysis is presented in Table 5 and Figure 6. The chromatogram for the high density Soviet jet fuel is reproduced in Figure 7. The elemental analysis and the molecular weight are presented in Table 6. The viscosity is plotted as a function of the inverse temperature in Figure 8.

The Soviet jet fuel had an API gravity of 36.3° API, a pour point of -103°F, a flash point of 175-180°F, and a relatively high volumetric energy content (138,320 Btu/gal). Inspection of the data in Tables 4 and 5 and Figures 6 and 8, indicated that the experimental analytical procedures employed in this project gave excellent reproducibility.

The infrared spectra presented in Figure 9 were run on a PE-283 spectrometer. The spectra exhibited strong bands in the C-H stretch, the C-CH_2 inplane scissor, C-CH_3 in-place bending, and the CH_2 rocking regions of the spectra. Furthermore, the spectra did not indicate the presence of unsaturated carbon-carbon bonds nor the presence of heteroatoms in this sample. According to Yen et al.,[12] the absorption at 2920 cm^{-1} attributed to C-H stretching vibrations of methylene groups, whereas the absorption band at 1380 cm^{-1} is due to C-H symmetric bending vibrations of methyl groups. The absorbance ratio of the 2920 cm^{-1} to 1380 cm^{-1} bands was determined, and the value of the ratio was approximately unity indicating a high degree of methyl substitution in the Soviet high density jet fuel.

The proton and carbon-13 nuclear magnetic resonance analysis indicated that the Soviet jet fuel contained essentially no alkanes and no long chain paraffins and only minor amounts of aromatic carbons (<2.4 percent). The majority of the aromatic components are 1-ring structures such as toluene, xylenes, and tetralins. The samples also contained a vanishing small concentration

Table 4

Physical Properties of Soviet High Density Jet Fuel

Physical Property	Run Number 1	Run Number 2
Specific Gravity (60°F/60°F)	0.84334	0.84334
API Gravity, °API	36.3	36.3
Viscosity, cps		
20°C	3.10 ± 0.05	3.12 ± 0.05
30°C	2.50 ± 0.05	2.59 ± 0.05
40°C	2.09 ± 0.05	2.10 ± 0.05
50°C	1.72 ± 0.05	1.74 ± 0.05
Pour Point, °F	-103	-103
Flash Point, °F	179.6	176.0
Fire Point, °F	190.4	186.8
Heat of Combustion		
Kcal g^{-1}	10.83	11.01
Btu lb_m^{-1}	19,500	19,810
Btu gal^{-1}	137,225.5	139,417

Table 5

Simulated Distillation of Soviet High Density Jet Fuel

Distillation Fraction	Run Number 1	Run Number 2
IBP, °F	190.4	185
5	332.6	329
10	376.7	370.4
20	416.3	413.6
30	441.5	438.8
40	463.1	458.6
50	483.8	480.2
60	503.6	500
70	521.6	518
80	545	540.5
90	578.3	578.3
95	599	600.8
99	644	654.8
Gasoline Fraction 125-400°F, wt%	15.7	15.7
Middle Distillate 400-650°F, wt%	83.3	82.5
Heavy Gas Oil 650-1000°F, wt%	1.1	1.8
Residue 1000°F, wt%	0	0
Volatility 1000°F, wt%	100	100

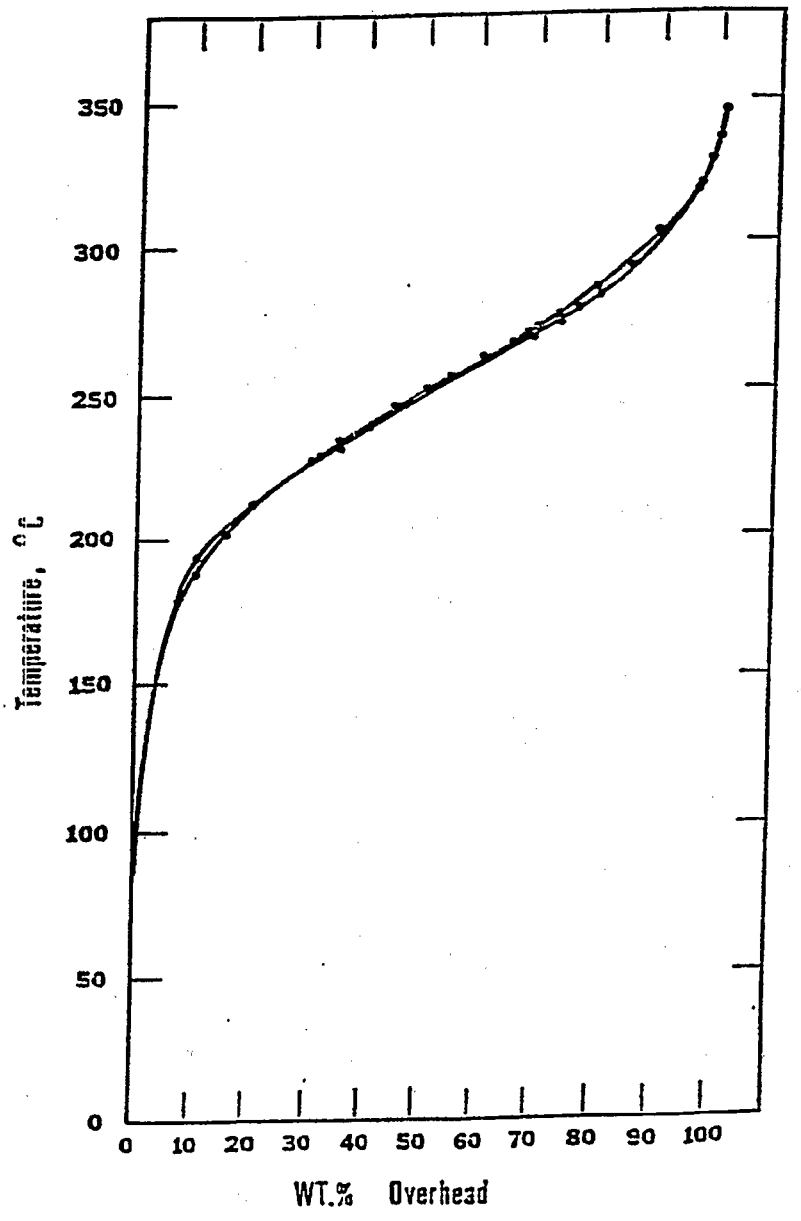

Figure 6. Simulated Distillation Curves for High Density Fuel (82-POSF-1028)

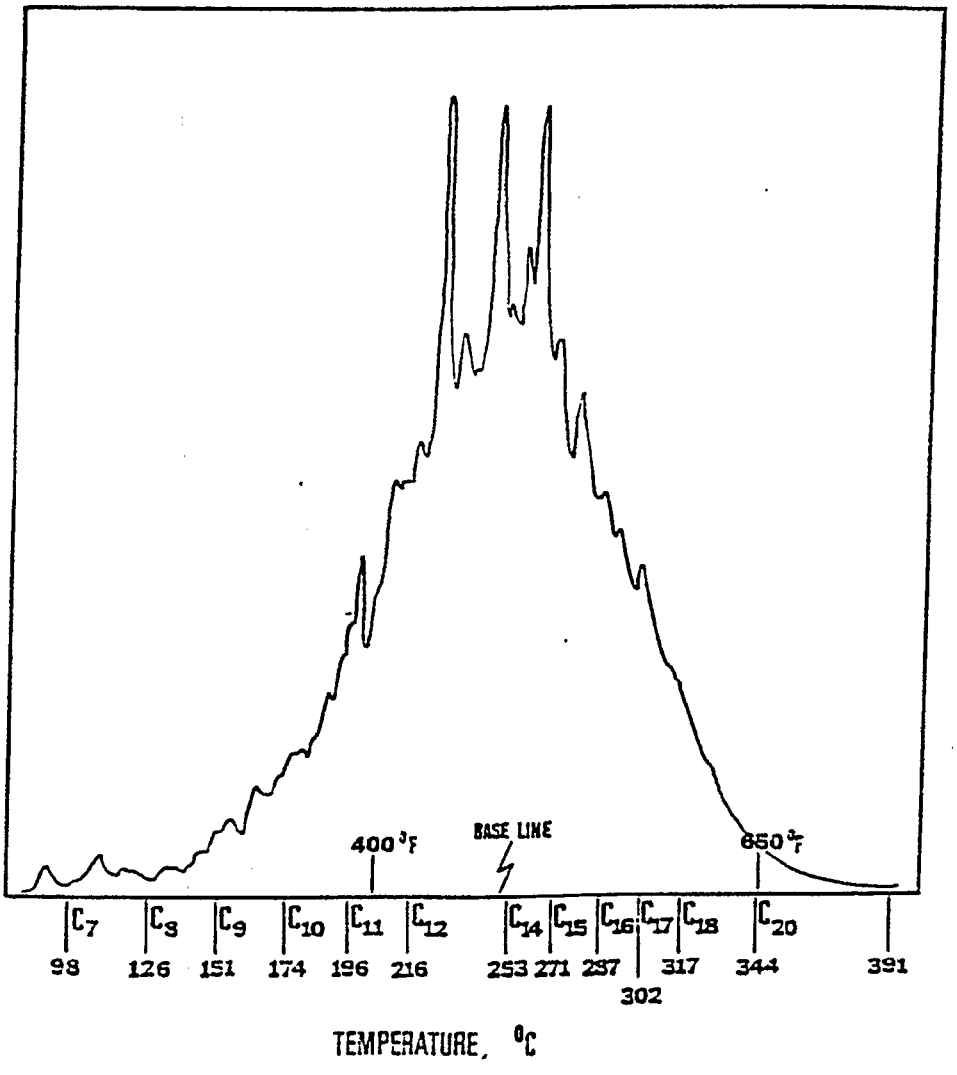

Figure 7. Simulated Distillation Chromatogram
High Density Fuel (82-POSF-1028)

Table 6

Elemental Analysis of Soviet High Density Jet Fuel

Elemental Analysis	
Carbon, Wt%	86.3
Hydrogen, Wt%	13.7
Nitrogen, ppm	6
Sulfur, ppm	16
Atomic Hydrogen/Carbon Ratio	1.89
Molecular Weight, g mol^{-1}	225

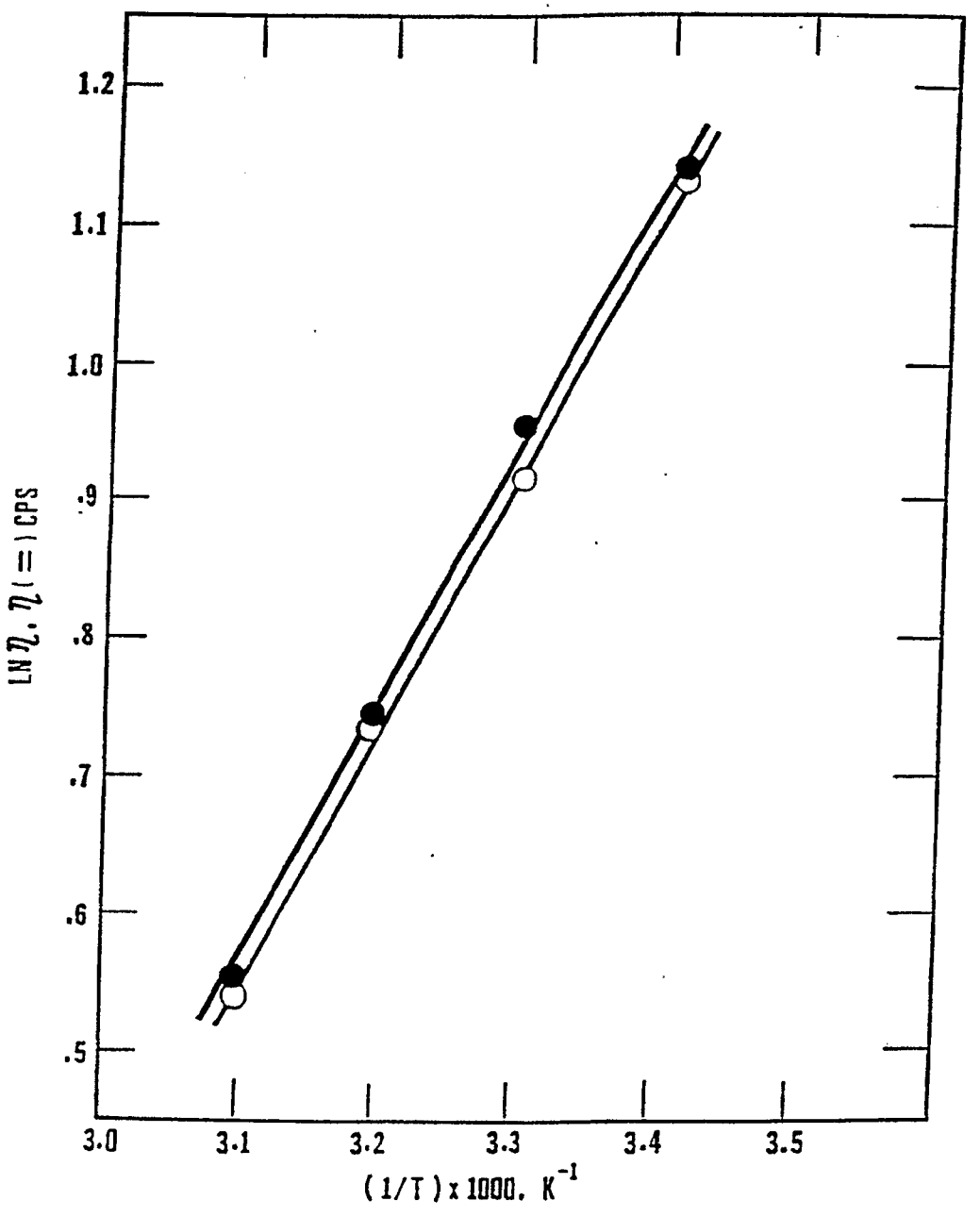

Figure 8. Viscosity-Inverse Temperature Plot
High Density Fuel (82-POSF-1028)

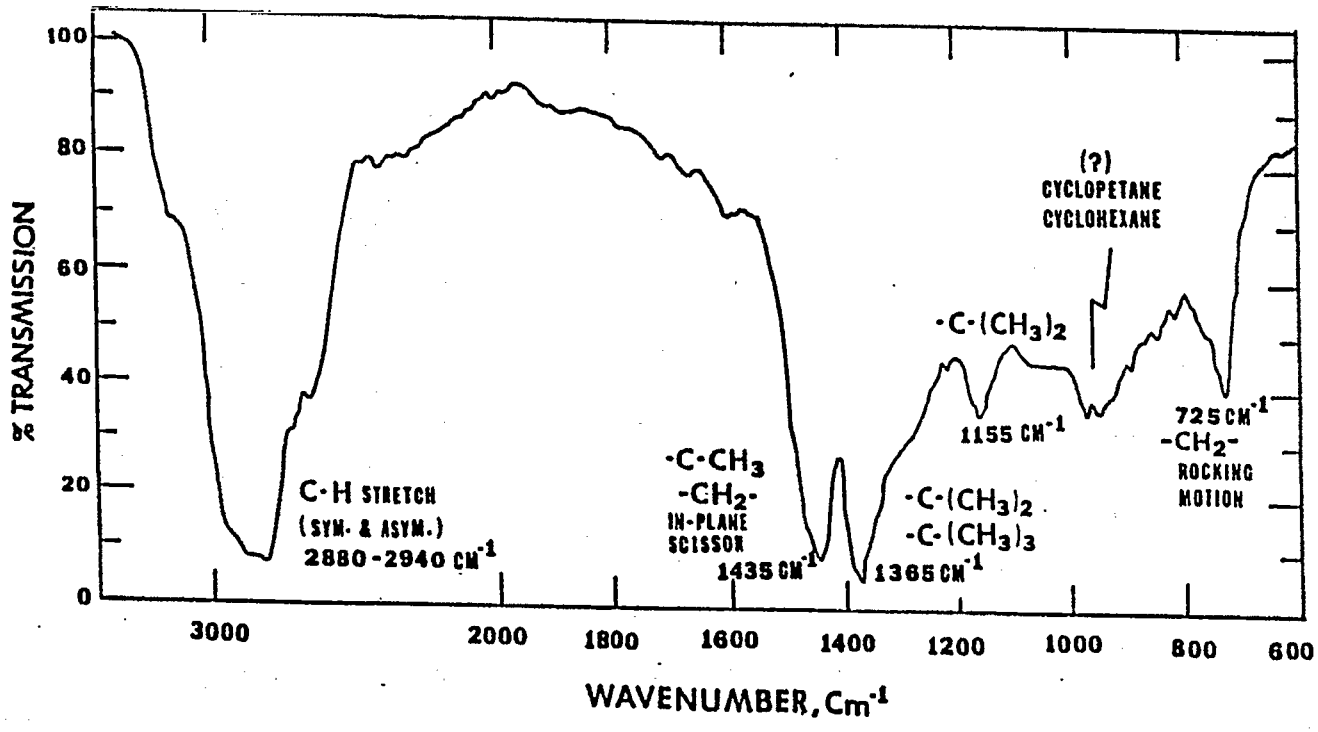

Figure 9. Infrared Spectrum of High Density Fuel (82-POSF-1028)

of 2-ring aromatics. Approximately 35 percent of the protons/hydrogens in the sample were methyl (CH_3) hydrogens. The high degree of methyl substitution was confirmed by the atomic hydrogen to carbon ratio, 1.89, calculated from the elemental analyses. The molecular entities comprising this high density jet fuel are methyl substituted naphthenes (1 and 2 rings), having approximately four methyl groups attached to the fused carbon rings, and isopranes. These species were determined to have an average empirical formula given by

$$(CH)_{3.48}(CH_2)_{8.72}(CH_3)_{3.93}$$

The absence of normal paraffins and the low concentration of aromatics in the Soviet fuel led to the speculation that it might be a hydrogenated catalytic cracker cycle stock or light gas oil,[4] to which front end specialty hydrocarbon additives had been added.

Analysis of Conventional Aviation Turbine Fuels and Pyrolysis Oils

The results of the physical and chemical analyses of the jet fuel samples are presented in Tables 7 through 13 and in Figures 10 and 11. The standard properties of the aviation turbine fuel samples are compared in Table 14. In general, the data appear to meet the reported specifications[13] (Table 15) and data from the literature for the various jet fuel samples.

Analysis of the Aromatic 2040 Solvent

A sample of the 2040 solvent was obtained from the Air Force Wright Aeronautical Laboratories for possible use in the aromatics hydrogenation studies. A limited amount of analysis

Table 7

Specific Gravities of Aviation Turbine Fuel Samples

	RUN I		RUN II	
Sample Code	**Specific Gravity (60°F/60°F)**	**API Gravity**	**Specific Gravity (60°F/60°F)**	**API Gravity**
82-POSF-0162	0.87523	30.2	0.87523	30.2
82-POSF-0541 (JP-4-P)	0.76181	54.2	0.76181	54.2
83-POSF-0462 (JP-8)	0.79605	46.3	0.79605	46.3
83-POSF-0801	0.89652	26.3	0.89652	26.3
83-POSF-1030 (JP-5)	0.81356	42.4	0.81356	42.4
83-POSF-1431 (JP-4-S)	0.76661	53.1	0.76661	53.1
84-POSF-1949 (HD-1)	0.87221	30.7	0.87231	30.7
82-POSF-1028 (SJF)	0.84334	36.3	0.84334	36.3

Table 8

Viscosity as a Function of Temperature
Aviation Turbine Fuel Samples

Sample Code	Temperature (°C)	Viscosity (cps) Run I	Viscosity (cps) Run II
82-POSF-0162	20	2.54 ± 0.05	2.52 ± 0.05
	15	2.94 ± 0.05	2.97 ± 0.05
	10	3.32 ± 0.05	3.33 ± 0.05
	5	3.80 ± 0.05	3.85 ± 0.05
82-POSF-0541 (JP-4)	20	0.78 ± 0.05	0.80 ± 0.05
	15	0.82 ± 0.05	0.86 ± 0.05
	10	0.90 ± 0.05	0.90 ± 0.05
	5	0.96 ± 0.05	0.98 ± 0.05
83-POSF-0462 (JP-8)	20	1.18 ± 0.05	1.20 ± 0.05
	15	1.34 ± 0.05	1.37 ± 0.05
	10	1.47 ± 0.05	1.48 ± 0.05
	5	1.65 ± 0.05	1.66 ± 0.05
83-POSF-0801	20	2.62 ± 0.05	2.60 ± 0.05
	15	2.97 ± 0.05	3.01 ± 0.05
	10	3.32 ± 0.05	3.34 ± 0.05
	5	3.85 ± 0.05	3.95 ± 0.05
83-POSF-1030	20	1.74 ± 0.05	2.60 ± 0.05
	15	2.97 ± 0.05	3.01 ± 0.05
	10	3.32 ± 0.05	2.23 ± 0.05
	5	2.54 ± 0.05	2.56 ± 0.05
83-POSF-1431 (JP-4)	20	0.86 ± 0.05	0.89 ± 0.05
	15	0.90 ± 0.05	0.93 ± 0.05
	10	0.98 ± 0.05	0.98 ± 0.05
	5	1.05 ± 0.05	1.10 ± 0.05
84-POSF-1949 (HD-1)	20	2.31 ± 0.05	2.28 ± 0.05
	15	2.63 ± 0.05	2.66 ± 0.05
	10	2.88 ± 0.05	2.92 ± 0.05
	5	3.34 ± 0.05	3.38 ± 0.05
82-POSF-1028 (SJF)	50	1.72 ± 0.05	1.74 ± 0.05
	40	2.09 ± 0.05	2.16 ± 0.05
	30	2.50 ± 0.05	2.59 ± 0.05
	20	3.10 ± 0.05	3.12 ± 0.05

Table 9

Viscosities of Jet Fuel Samples at 253 K

Sample Code	Viscosity[a] (cps)	(cst)
82-POSF-0162	8.3	9.4
82-POSF-0541 (JP-4-P)	1.7	2.2
83-POSF-0462 (JP-8)	3.7	4.7
83-POSF-0801	8.5	9.5
83-POSF-1030 (JP-5)	5.9	7.2
83-POSF-1431 (JP-4-S)	1.9	2.4
84-POSF-1949 (HD-1)	7.9	9.0
82-POSF-1028 (SJF)	8.2	9.7

[a]Viscosity: temperature data extrapolated to -20°C.

Table 10

Flash Point/Fire Point Data for Jet Fuel Samples

Sample Code	Flash Point		Fire Point	
	°C	°F	°C	°F
82-POSF-0162	110	230	115	239
82-POSF-0541 (JP-4-P)	--	--	--	--
83-POSF-046 (JP-8)	98	208.4	104	219.2
83-POSF-0801	92	197.6	97	206.6
83-POSF-1030 (JP-5)	109	228.2	115	239
83-POSF-1431 (JP-4-S)	--	--	--	--
84-POSF-1949 (HD-1)	92	197.6	98	208.4
82-POSF-1028 (SJF)	82	179.6	88	190.4

Table 11

Gross Heat of Combustion for Jet Fuel Samples

Sample	Run Number	Heat of Combustion cal/g	Btu/lb	Btu/gal
82-POSF-0162	1	10,720	19,295	140,622
	2	10,679	19,222	140,089
82-POSF-0541 (JP-4-P)	1	10,889	19,601	124,312
	2	10,953	19,715	125,037
83-POSF-0462	1	10,920	19,656	130,276
	2	10,801	19,442	128,856
83-POSF-0801	1	10,613	19,103	142,610
	2	10,509	18,916	141,216
83-POSF-1030 (JP-5)	1	10,776	19,396	131,383
	2	10,613	19,104	129,404
83-POSF-1431 (JP-4-S)	1	11,004	19,807	126,531
	2	11,010	19,818	126,601
84-POSF-1949 (HD-1)	1	10,750	19,351	140,547
	2	10,781	19,406	140,951
82-POSF-1028 (SJF)	1	10,830	19,500	137,226
	2	11,010	19,810	139,417

Table 12

Simulated Distillation Data

Percent Recovered	82-POSF-0162 °C	82-POSF-0162 °F	82-POSF-0541 °C	82-POSF-0541 °F	83-POSF-0462 °C	83-POSF-0462 °F	83-POSF-0801 °C	83-POSF-0801 °F	83-POSF-1030 °C	83-POSF-1030 °F	83-POSF-1431 °C	83-POSF-1431 °F	84-POSF-1949 °C	84-POSF-1949 °F	SOVIET JET FUEL °F
0.5 (IBP)	115	239	<37	<98.6	104	219.2	97	206.6	115	239	<37	<98.6	98	208.4	190.4
1.0	129	264.2	<37	<98.6	115	239	115	239	129	264.2	<37	<98.6	115	239	--
5.0	180	356	52.5	126.5	143	289.4	181	357.8	164	327.2	45	113	174	345.2	332.6
10	186	366.8	76	168.8	155	311	193	379.4	177	350.6	64	147.2	185	365	376.7
20	200	392	97	206.6	172	341.6	204	399.2	195	383	102	215.6	199	390.2	416.3
30	205	401	117	242.6	181	357.8	212	413.6	205	401	122	251.6	204	399.2	441.5
40	213	415.4	128	262.4	191	375.8	223	433.4	217	422.6	142	287.6	212	413.6	463.1
50	222	431.6	148	298.4	199	390.2	232	449.6	225	437	162.5	324.5	220	428	483.8
60	229	444.2	171	339.8	208	406.4	241	465.8	237	458.6	179	354.2	226	438.8	503.6
70	239	462.2	191	375.8	217	422.6	250	482	243	469.4	195	383	234	453.2	521.6
80	249	480.2	211	411.8	226	438.8	260	500	255	491	210	410	243	469.4	545
90	262	503.6	230	446	237	458.6	273	523.4	266	510.8	228	442.4	253	487.4	578.3
95	270	518	239	462.2	243	469.4	280.5	536.9	272	521.6	237	458.6	259	498.2	599
99	282.5	540.5	251	483.8	251	483.8	290	554	279	534.2	246	474.8	262.5	504.5	644
99.5 (FBP)	284	543.2	252	485.6	253	487.4	292	557.6	280	536	249	480.2	264	507.2	
Gasoline, wt%		26.07		78.39		56.34		19.3		27.83		75.25		25.56	15.7
Middle Distillate, wt%		73.93		21.61		43.66		80.7		72.17		24.75		74.44	83.3
Heavy Gas Oil, wt%		---		---		---		---		---		---		---	1.1
Volatility <1000°F, wt%		100		100		100		100		100		100		100	100

Table 13

Elemental Analysis of Aviation Turbine Fuel Samples

Sample Code	C (wt%)	H (wt%)	H/C (atomic ratio)
82-POSF-0162	86.96	12.69	1.74
82-POSF-0541 (JP-4-P)	85.77	14.5	2.01
83-POSF-0462 (JP-8)	86.18	13.99	1.93
83-POSF-0801	86.93	12.31	1.69
83-POSF-1030 (JP-5)	85.82	13.44	1.87
83-POSF-1431 (JP-4-S)	85.28	14.41	2.01
84-POSF-1949 (HD-1)	86.81	12.60	1.83
82-POSF-1028 (SJF)	86.3	13.7	1.89

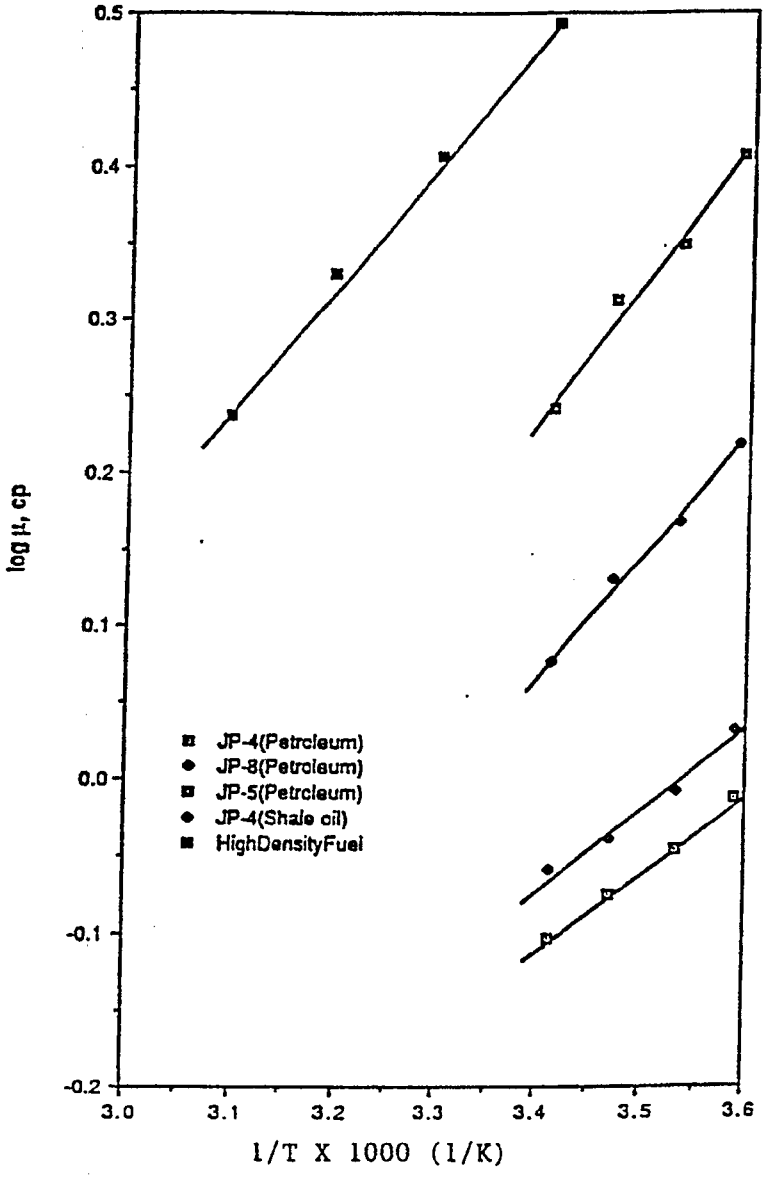

Figure 10. Arrhenius Temperature Dependence for Aviation Turbine Fuel Viscosities

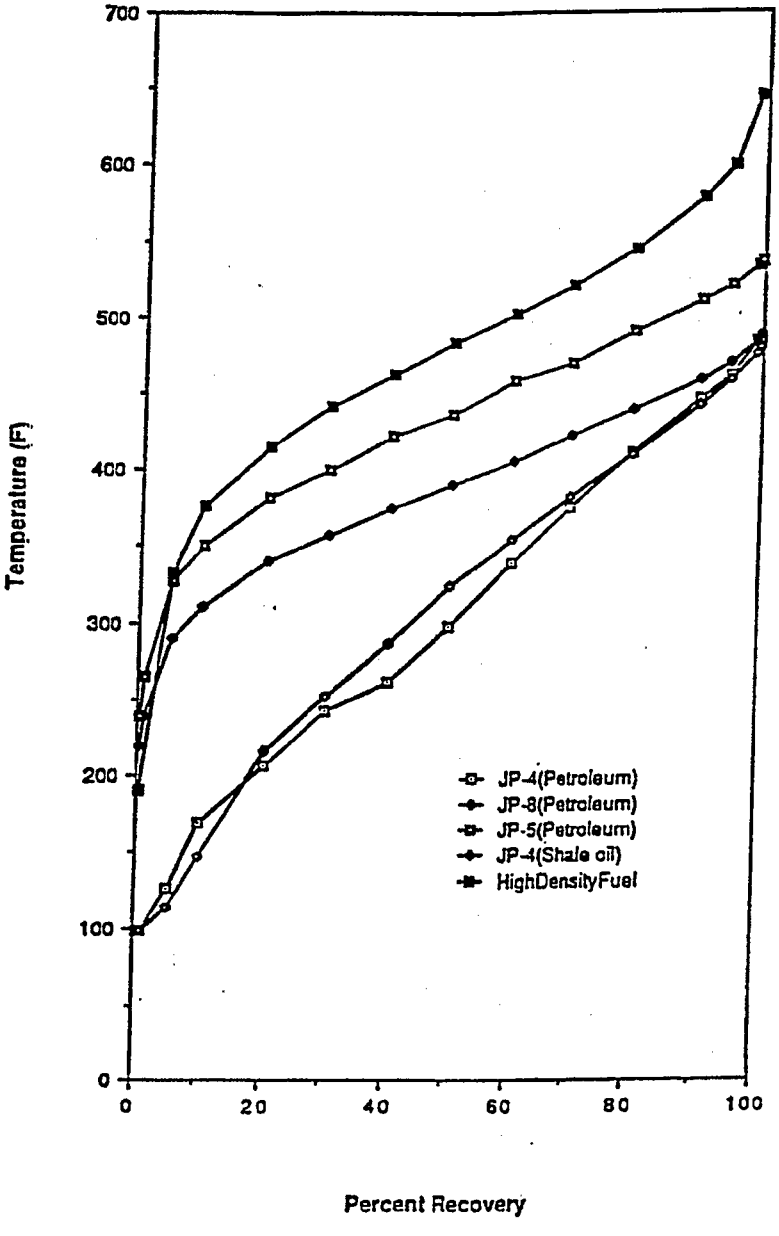

Figure 11. Simulated Distillation Curves
Aviation Turbine Fuel Analysis

Table 14

Comparison of Physical Properties of Aviation Turbine Fuels

Identification	JP-4 Petroleum Derived	JP-4 Shale Derived	JP-5 Petroleum Derived	JP-8 Petroleum Derived	High Density Fuel
CODE	82-POSF-0541	83-POSF-1431	83-POSF-1030	83-POSF-0462	83-POSF-1028
Properties					
Gravity, °API	54.2	53.1	42.4	46.3	36.3
Viscosity @ 253K, cps	2.2	1.9	5.9	3.7	8.2
Simulated Distillation					
Gasoline, wt%	78.4	75.2	27.8	56.3	15.7
Mid Distillate, wt%	21.6	24.8	72.2	43.7	82.8
Gas Oil Fraction, wt%	–	–	–	–	1.5
Flash Point, °F	–	–	228.2	208.4	177.8
Heat of Combustion, Btu/gal	124,675	126,556	130,394	129,566	138,320
Atomic H/C Ratio	2.0	2.0	1.87	1.93	1.89

Table 15

Aviation Turbine Fuel Specifications[13]

Fuels Identity	JP-4	JP-5	JP-8
Specifications			
Gravity, °API	45-57	36-48	39-51
Specific Gravity, 60/60°F	0.751-0.802	0.788-0.845	0.775-0.830
Distillation, °F (°C)[a]			
IBP	---	---	---
10% Ovhd	---	400 (204.4)	400 (204.4)
20% Ovhd	290 (143.3)	---	---
50% Ovhd	370 (187.8)	---	450 (232.2)
90% Ovhd	470 (243.3)	---	---
End Point	---	550 (278.8)	550 (278.8)
Flash Point, °F (°C)[b]	---	140 (60)	110 (43.2)
Reid Vapor Pressure, psi	2.0-3.0	---	---
Freeze Point, °F (°C)[a]	-72 (-58)	-51 (-46)	-51 (-46)
Luminometer Number[b]	60	50	45
Smoke Point, mm[b]	---	19.0	25
Net Heat of Combustion,[b] Btu/lbm	18,400	18,300	18,400

[a] Maximum permitted values.

[b] Minimum permitted values.

was performed on this solvent due to the deemphasis of the aromatics saturation work after receipt of the sample. The 2040 solvent was also considered as a candidate feedstock for a process concept in which an aromatic feedstock would be passed over ZSM-5 in the presence of methanol to produce a permethyl substituted high density aviation turbine fuel. The simulated distillation data are presented in Table 16, and selected, measured properties are reported in Table 17.

Table 16

Simulated Distillation Analysis of 2040 Solvent

% Recovered	°C	°F
0.5 (IBP)	160	320
1.0	164	327
5.0	177	351
10.0	193	379
20.0	212	414
30.0	225	435
40.0	238	460
50.0	242	468
60.0	251	484
70.0	263	505
80.0	273	523
90.0	288	550
95.0	293	559
99.0	334	633
99.5 (FBP)	375	707

Gasoline Fraction 125-400°F, wt%	17.4
Middle Distillate 400-640°F, wt%	81.4
Heavy Gas Oil 650-1000°F, wt%	1.2
Residue 1000°F, wt%	0.0
Volatility 1000°F, wt%	100.0

Table 17

Selected Physical Properties of 2040 Solvent

Specific Gravity (15°C)	0.973
API Gravity, °API	13.95
Viscosity, cps	
15°C	2.82
20°C	2.35
Pour Point, °C	-23.0

Section III: SHAPE SELECTIVE CATALYSIS

Research Personnel: Hong P. Wang
Graduate Student

Daniel C. Longstaff
Graduate Student

Francis V. Hanson
Associate Professor

Introduction

The conversion of methanol to aromatic hydrocarbons followed by hydrogenation to the corresponding naphthenes as a route for the conversion of coal or synthetic or natural gas to high density or endothermic jet fuels has at least two advantages. First, high selectivity for a particular product can be achieved by adjusting the catalytic properties of zeolites and/or the process operating conditions. Second, the starting material, methanol, can be produced from alternative nonpetroleum resources via Fischer Tropsch type technologies from domestic coal resources.

It is proposed that high density aviation turbine fuels can be produced by the synthesis of methyl substituted, two-ring aromatic hydrocarbons followed by hydrogenation of the aromatic species to the corresponding naphthene.[14]

The advent of shape selective catalysis, first discovered and reported by Weisz and Frilette in the early 1960s,[15] has created new opportunities to direct and control catalytic reactions involving hydrocarbons. Zeolites not only regulate those reactant materials that can diffuse into them but can also regulate those products that can readily diffuse out because of their unique pore structures and shape selectivity, thus controlling the product selectivity.

In the early 1970s, it was found that methanol could be converted to high octane number gasoline over the shape selective zeolite ZSM-5 in excellent yields and with long catalyst cycle

life.[16] Additional research has shown that ZSM-5 can selectively produce specific hydrocarbon classes through variations in operating conditions and by modification of the catalyst preparation scheme.[17-18]

The unique catalytic and shape selective properties of ZSM-5 zeolites have been attributed to their crystalline structure. Zeolite ZSM-5 is a pentasil zeolite which possesses pore openings intermediate between those of small pore zeolites such as zeolite A and erionite and large pore zeolites such as faujasite. The 10-membered ring opening of ZSM-5, compared to eight for zeolite A and 12 for the faujasites, permits molecules that are intermediate in size to enter its channels.

A new zeolite designated ZSM-48 was synthesized in the early 1980s.[19] This zeolite, having SiO_2/Al_2O_3 ratio >5, can be used in conjunction with zeolite ZSM-5 for the conversion of methanol or higher alcohols to hydrocarbons in the jet fuel or diesel fuel boiling ranges.

The major objective of this work was to synthesize zeolite catalysts and to evaluate novel processing schemes using these catalysts for the production of methyl-substituted aromatics from oxygenated species. Zeolite structures related to ZSM-5 and ZSM-48 were investigated and explored. An investigation of the reactions of methanol and higher alcohols over synthetic zeolites was also conducted.

Zeolite Catalysts

Zeolites are crystalline, hydrated aluminosilicates. Their chemical composition can be represented by the empirical formula $M_{2/n}O \cdot [Al_2O_3 \cdot xSiO_2] \cdot yH_2O$, where x is generally equal to or greater than two and n is the valence of the cation M. When M is a proton, the zeolite is a strong Brönsted acid. As x approaches infinity, the framework will, of course, be electronically neutral.

Structurally, zeolites are framework aluminosilicates based on an infinitely extending three-dimensional network of AlO_4 and SiO_4 tetrahedra linked to each other by shared all oxygen atoms. Cations are introduced into the structure to preserve the electronic neutrality since the replacement of tetravalent silicon atoms by trivalent aluminum atoms results in the formation of ionic sites in the vicinity of the aluminum atoms. The cations so introduced are usually readily exchangeable.

Detailed reviews on the structures, physical and chemical properties of the catalytically important zeolites and molecular sieves have been discussed by Breck,[20], Rabo,[21], and Barrer.[22] A loose definition of zeolites has been proposed by Smith:[23] a zeolite is an aluminosilicate with a framework structure enclosing cavities occupied by large ions and water molecules, both of which have considerable freedom of movement, permitting ion exchange and reversible dehydration.

In some synthetic zeolites, aluminum cations are replaced by gallium ions, and silicon ions are replaced by phosphorus or germanium ions. The structure of a zeolite after complete dehydration must remain intact to be used as a molecular sieve.

General Concepts Related to Zeolite Synthesis

The most comprehensive early studies on zeolite synthesis were conducted by Barrer and his co-workers. In 1950 the Union Carbide Corporation initiated a systematic study of zeolite synthesis which resulted in the synthesis of about 20 novel synthetic zeolites by the application of a new field of chemistry involving highly reactive alkaline aluminosilicate gel, metastable crystallization, and low temperature, low pressure crystallization.[24] Zeolite A, discovered by Breck et al.,[25] can be prepared by combining sodium metasilicate and sodium aluminate solutions such that the reaction mixture is aluminum-rich. The powdered crystalline zeolite A can be obtained by refluxing the aluminosilicate gel solution for 3 to 4 hours. Using the same reagents, zeolite X

(SiO_2/Al_2O_3 = 2 -3) and zeolite Y (SiO_2/Al_2O_3 = 3 - 6)[26] can also be synthesized. Both of these zeolites are isostructural with the naturally occurring zeolite, faujasite (SiO_2/Al_2O_3 = 4.5).

In 1961, Barrer and his co-workers[27] first reported the synthesis of N-A (a siliceous analog of zeolite A) by adding tetramethylammonium cations to sodium alumino-silicate gels. The alkylammonium ion appeared to increase the framework Si/Al ratio, that is, the framework composition was enriched in silicon atoms. Kerr and Kokotailo[28] also reported the synthesis of a zeolite designated ZK-4 which was isostructural with zeolite A but whose SiO_2/Al_2O_3 ratio was 3.4.

Wadlinger et al.[29] received a patent in 1967 which described a new zeolite, designated zeolite beta, and its method of preparation. Zeolite beta was synthesized from silicon-rich reaction mixtures containing tetraethylammonium ions and sodium ions and was the first zeolite to have SiO_2/Al_2O_3 ratios greater than 10.

Argauer and Landolt[30] patented a preparation procedure that led to the formulation of a medium-pore class of zeolites known as Zeolite Socony Mobil (ZSM-) and more specifically to the zeolite catalyst known as ZSM-5.[30,31] The discovery of the novel catalytic properties of ZSM-5 during the last decade has been followed by an intensive research effort on the synthesis of other highly siliceous zeolites and catalytic applications of these materials.[32-34] ZSM-5 can be prepared from high SiO_2/Al_2O_3 ratio reaction mixtures containing sodium and tetrapropylammonium ions and at temperatures above 373 K.[30]

A new family of molecular sieves has been disclosed having nonaluminosilicate frameworks. An important example of this expansion is the recent discovery of the novel aluminophosphate ($AlPO_4$) molecular sieves.[35-37] The structures of several of these materials are analogous to the crystalline aluminosilicate zeolites. These materials represent a new class of microporous inorganic solids that are currently being evaluated in catalytic applications.

Characteristic Structures of Catalytically Important Zeolites

The zeolites that have been widely investigated are those that have achieved industrial applications. These zeolites, namely, X, Y, mordenite, the pentasil types, and erionite, have pore openings characterized by 12-, 10-, and 8-rings of oxygen atoms.

Large Pore Zeolites

Faujasite: Faujasite is a naturally occurring zeolite with chemical composition: $(Na_2Ca)[Al_2SiO_4O_{12}]\cdot 8H_2O$. The synthetic zeolites X and Y have framework structures similar to that of the natural mineral faujasite. The faujasite structure is comprised of truncated octahedra (sodalite cage) interconnected via double six-ring (D6R) units. The three-dimensional framework gives rise to the large supercages approximately 13 Å in diameter. There are eight supercages per unit cell. The supercages are interconnected via 12-membered rings of about 7.4 Å in diameter. The unit cells are cubic with a cell dimension of nearly 25 Å. Each unit cell contains 192 AlO_4 and SiO_4 tetrahedra that are linked through shared oxygen atoms.[38,39]

The cation sites that exist inside the supercage or close to the wall of the supercages are probably most important for catalytic purposes.[40] These sites can accommodate hydrogen ions that become framework hydroxyl groups and potential acidic catalytic sites following ion exchange.

Mordenite: Mordenite is a natural, orthorombic aluminosilicate that has the general formula: $(Na_2K_2Ca)[Al_2SiO_{10}O_{24}]\cdot 7H_2O$. The mordenite structure contains no large supercages, in contrast, the dehydrated structure has a two-dimensional small-port channel system. The mordenite structure also contains a one-dimensional pore system (large port) of parallel elliptical channels defined by 12-membered rings of approximately 6.7 Å diameter.[38,39] The natural mordenite mineral appears to be a small pore zeolite because the pore system is partially blocked by amorphous impurities or cations resulting in an effective diameter of about 4 Å.[38-40]

Mazzite: Mazzite (ZSM-4 or zeolite omega) is a member of the cabazite group. Massite has a one-dimensional system of parallel channels defined by 12-membered rings 7.4 Å in diameter.[38,39]

Small Pore Zeolites

Erionite: The erionite structure is hexagonal containing double six-membered rings and single six-membered rings that are arranged in parallel planes perpendicular to the hexagonal axis. This arrangement produces supercages supported by columns of cancrinite type cages linked through double six-membered rings. It results in a three-dimensional pore system consisting of cavities with dimensions of 1.5 x 6.3 Å and eight-membered oxygen ring apertures that have dimensions of 3.6 x 5.2 Å.[38,39]

Erionite is a naturally occurring zeolite having a SiO_2/Al_2O_3 ratio of about six (erionite has the general formula: $(Na_2,Ca,Mg,K_2)O \cdot [Al_2O_3 \cdot SiO_2] \cdot 6H_2O$). It is a thermally stable and acid resistant zeolite. Erionite is commercially used in catalytic cracking and hydrocracking applications. The molecular shape selectivity can be controlled by means of modification of its pore size. The pore system of erionite contains a continuous diffusion path for molecules with a maximum kinetic diameter of 4.3 Å. Thus the structure can adsorb linear hydrocarbons and exclude branched hydrocarbons.[40]

Cabazite: The trigonal structure (possibly triclinic) of cabazite has double six-membered rings linked together through tilted four-membered rings. The framework contains large ellipsoidal cavities, each entered through eight-membered rings. These cavities are joined together via their eight-membered rings to form a three-dimensional channel system having dimensions of 3.6 x 3.7 Å.[38,39]

Offretite: Offretite is structurally related to erionite except in the sequence of six-membered rings. Intergrowths of offretite and erionite, e.g., ZSM-34 and zeolite T, are observed frequently.[38]

ZK-5: Zeolite ZK-5 consists of truncated cuboctahedra joined through double six-membered rings in a body-centered structure. The main channel system is defined by eight-membered rings about 3.9 Å in diameter.[38,39]

Pentasil Zeolites and Molecular Sieves

ZSM-5: The unique catalytic properties of zeolite ZSM-5, as in conversion of oxygenates to hydrocarbon species, have been attributed to its crystal structure.[41,42]

Zeolite ZSM-5 is comprised of orthorhombic unit cells. The framework consists of a set of sinusoidal channels intersecting with a set of straight channels. The channels (Figure 12) are ellipsoidal with 10-membered ring openings, having the approximate free diameters of about 5.4 x 5.6 Å for straight channels and 5.1 x 5.5 Å for sinusoidal channels.[30,43,44]

ZSM-11[44-46] and silicalite are closely related to ZSM-5 in structure. The ZSM-5 and silicalite have orthorhombic unit cells whereas the unit cell of ZSM-11 is tetragonal. Silicalite-2 and ZSM-11 contain two sets of intersecting straight channels with 10-membered ring openings of about 5.1 x 5.5 Å free dimension.

ZSM-48: Zeolite ZSM-48 was found as an impurity phase in zeolite ZSM-39.[47] Zeolite ZSM-48 in a form substantially free from impurities was later synthesized hydrothermally by Mobil scientists.[48] ZSM-48 is a high silica zeolite with orthorhombic or pseudoorthorhombic unit cells. X-ray powder diffraction, electron diffraction, sorption and catalytic characteristics indicate that zeolite ZSM-48 has a framework based on the ferrierite sheet with linear non-interpenetrating

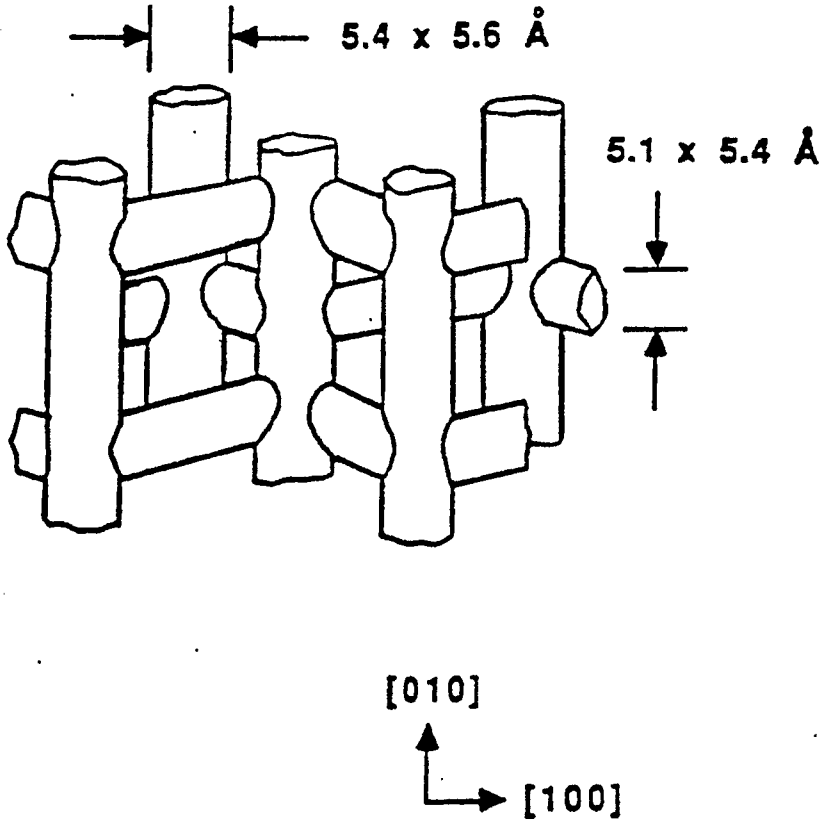

Figure 12. ZSM-5 Channel System

10-membered ring channels (ideal dimensions are 5.3 x 5.6 Å) running perpendicular to the sheet. A possible structure for ZSM-48 has been proposed by Schlenker et al.[49] It is proposed that ZSM-48 has a structure that is based on ferrierite sheets linked via bridging oxygens located in a mirror plane.

Shape Selective Zeolite Catalysis and Catalysts

Preparation of Shape Selective Zeolites

Synthesis of ZSM-type Zeolites

Since the work of Barrer[40] and Kerr,[50] a variety of organic cations have been used in the synthesis of zeolites. The major driving force for the use of organic cations was to synthesize a zeolite material with a high SiO_2/Al_2O_3 ratio. As the SiO_2/Al_2O_3 ratio increases, the acidity, thermal stability and hydrothermal stability also increase.[51] A second objective was to synthesize a zeolite material with a larger intracrystalline pore channel system than those of zeolites X or Y, both of which have been used extensively in catalytic cracking and hydrocracking processes.[27,52] A wider pore structure zeolite was desirable since it would crack more of the heavy end of the petroleum feed.

The cations used in the synthesis of ZSM-type zeolites are usually members of one of the following classes or types of cation: alkylammonium cations, alkyl-phosphonium cations and organic complexes. Alkylammonium organic cations have been more widely used in the synthesis of zeolites than phosphonium cations. The use of organic cations as templates in the synthesis of zeolites has led to the discovery of many new zeolitic materials.[53] The most commercially interesting of these are the ZSM-type zeolites developed by Mobil scientists.[33,34,54-78] These zeolites are usually synthesized in a reaction mixture containing alkali metal cations in the presence of organic cations or complexes.

The organic cations used in the synthesis of ZSM-type zeolites are identified in Table 18.[33,34,54-78] The nomenclature and chemical formulae for these organic cations are presented in Tables 19 and 20. Many of these zeolites are structurally related.

Synthesis of Zeolite ZSM-5

Zeolite ZSM-5 was originally prepared from reaction mixtures containing tetrapropylammonium ions.[30] Other organic bases, for example, other quaternary ammonium ions,[79,80] primary and secondary amines,[81] diamines,[92,93] alcohols[84] were also used for the preparation of ZSM-5. Numerous other compounds, representative of a wide variety of functional groups,[85-88] have been claimed to be effective for preparation of ZSM-5 zeolite under suitable conditions. It is also possible under certain circumstances to crystallize ZSM-5 from reaction mixtures in the absence of an organic base.[84,87,88]

Zeolite ZSM-5 can also be synthesized in the presence of a tetraureacobalt (II) complex with a specifically defined reaction mixture. Depending on the ratio of tetraureacobalt (II) complex to silica in the zeolite synthesis reaction mixture, the crystalline product consists of highly twinned rectangular prismatic crystals exhibiting extreme uniformity in size from about 5 x 10 microns to about 10 x 20 microns.[89]

Zeolite ZSM-5 can also be prepared containing an outer aluminum-free shell by increasing the hydroxide content or by reducing the organic cation concentrations, i.e., the template ion to SiO_2 ratio. The outer shell is essentially SiO_2 that has crystallized on the zeolite surface in the ZSM-5 type configuration. This preparation technique leads to a more selective catalyst for the production of p-xylene.[90]

Table 18

Organic Cations Used in the Synthesis of ZSM-Type Zeolites

Zeolite	Cations	Si/Al	Type	Reference
ZSM-4	Na, TMA or P or C	1.5-10		54
ZSM-5	Na, TPA	>6	Pentasil	30,31
ZSM-6	TMACl	13-150		55
ZSM-8	Na. TEA	5-100		56
ZSM-10	K. DDO	2.5-3.5		57
ZSM-11	TBP, BTPP, TBA	10-45	Pentasil	58
ZSM-12	Na, TEA	10-100		59,60
ZSM-18	Na, HMBTP	<50		61
ZSM-20	Na, TEA	3.5-5	Faujasite	62
ZSM-21	Na. ED, P, C	4-25	Ferrierite	63
ZSM-23	Na, P	12-55		64
ZSM-25	Na, TEA	3-5		65
ZSM-34	Na, K, TMA	4-10	Offretite/Erionite	66
ZSM-35	Na. P, ED	4-25	Ferrierite	67
ZSM-38	Na, C	4-25	Ferrierite	68
ZSM-39	TC, P	>20		69
ZSM-43	Cs, C	5-8		70
ZSM-47	TMACl	8-25		71
ZSM-48	Na, C_3-C_12 ADA	>75		72-77
ZSM-51	TMPP or DMPP	>30		78

Table 19

Nomenclature for the Organic Cations Used in the Synthesis of ZSM-Type Zeolites

TMA	Tetramethylammonium
TPA	Tetrapropylammonium
TEA	Tetraethylammonium
DDO	[1,4-Dimethyl-1,4-diazabicyclo (2,2,2) octane]2+
TBP	Tetrabutylphosphonium
BTPP	Benzyltriphenylphosphonium
TBA	Tetrabutylammonium
HMBTP	1,3,4,6,7,9-Hexahydro-2,2,5,5,8,8-hexamethyl-2H-bensol[1,2-C:3,4-c^{1};5-6-C] tripyrolium
ED	Ethylenediamine
P	Pyrrolidine
C	Choline
TC	Tetraurea Co(II)
ADA	n-Alkyl-diamine

Table 20

Chemical Formulae of the Organic Cations Used in the Synthesis of ZSM-Type Zeolites

TMA	$(CH_3)_4N^+$
TPA	$(C_3H_7)_4N^+$
TEA	$(C_2H_5)_4N^+$
DDO	$(C_8H_{18}N_2)^{2+}$
TBP	$(C_4H_9)_4P^+$
BTPP	$C_6H_5CH_2(C_6H_5)_3P^+$
TBA	$(C_4H_9)_4N^+$
HMBTP	$C_6(C_2H_4N(CH_3)_2)_4^{3+}$
ED	$NH_2(CH_2)NH_2$
P	$NH(CH_2)_4$
C	$(CH_3)_3N(CH_2)OH$
TC	$((NH_2)_2CO)_4$-Co(II)
ADA	$NH_2(CH_2)_nNH_2$

Derouane et al.[91] reported two different crystallization processes for the formation of ZSM-5 crystals. In process A, a limited number of ZSM-5 nuclei are formed at the expense of an amorphous aluminum-rich gel phase. The nuclei grow slowly by a liquid-phase ion transport mechanism by incorporating TPA which may serve as a template during the growth process. In process B small X-ray amorphous ZSM-5 aggregates appear very early in the crystallization process followed by formation of X-ray crystalline ZSM-5 due to a solid to solid phase transformation mechanism.

Zeolites having a structure intermediate between ZSM-5 and ZSM-11 can be synthesized in the presence of tetrabutyl-ammonium cation at temperatures of 423 - 448 K.[56,92] Jablonski et al.[93] indicated that ZSM-5/ZSM-11 intergrowth structures can be synthesized from reaction mixtures with the mole oxide ratio: $4.5(TBA)_2O14.7Na_2OAl_2O_3$ $173.4SiO_22452H_2O9Br$. X-ray powder diffraction and selected area electron diffraction were used to identify the intergrowth structures.[90-93]

Doelle et al.[94] reported that the hydrogen form of Zeolite ZSM-5 can be prepared using 1,6-hexanediamine (C6DN) as the organic cation from a sodium-free gel, which after heating in air at 823 K gives the hydrogen form directly without an intermediate ion exchange step.

Synthesis of Zeolite ZSM-48

Zeolite ZSM-48 can be prepared from a reaction mixture containing a source of silica, optionally alumina, alkali metal oxide, water, and RN (RN is a C_1-C_{20} organic compound having an amine functional group of $pK_a \geq 7$).[72-77] In preparing the highly siliceous form of ZSM-48 no alumina is added. Thus the only aluminum present occurs as an impurity introduced into the reactant mixture.

The preparation of crystalline zeolite ZSM-48 requires the silica/alumina mole ratio of reaction mixture to be at least 500 to avoid product contamination with other silicates, notably crystalline silicates ZSM-5 or ZSM-11. Valyocsik[78] indicated that the silica/alumina mole ratio of the reaction mixture can be much less than 500 (e.g., as low as 180 or less) and still produce relatively pure ZSM-48 if a different organic template (bis(N-methylpyridyl)-ethylinium compound) is used.

High crystallinity zeolite ZSM-48 was prepared from a reaction mixture containing the organic cation, pyrrolidine, by Suzuki et al.[95] The scanning electron microscope image of the ZSM-48 crystal indicated a rod-like structure 0.2 - 0.4 μm in width and 3 - 5 μm in length.

Factors Affecting the Synthesis of the ZSM Family of Zeolites

Zeolite crystallization is believed to be a nucleation-controlled process from a reaction mixture containing alkaline aqueous gels at temperatures between 353 and 523 K. The primary influences of the reaction mixture compositions in zeolite synthesis were reported by Rollmann:[96] (1) framework composition is affected by the SiO_2/Al_2O_3 ratio; (2) crystallization mechanism is affected by the H_2O/SiO_2 ratio; (3) structure and cation distribution are affected by the Na^+/SiO_2 ratio; and (4) framework aluminum content is affected by the R_4N^+/SiO_2 ratio. Generally, addition of the organic cation to a reaction mixture used in zeolite synthesis may affect changes on zeolite structure, crystallization rate, chemical composition, and microscopic texture.[53,96] The organic cation (R_4N^+) is thought to function as a hydroxyl ion donor because of its basicity. The organic cation may also increase the solubility of the aluminate or silicate ions. It has also been postulated that the organic cation serves to organize the water molecules.[52,53,97-99]

Substitutes in the Framework of the ZSM Family of Zeolites

Introducing other atoms to replace aluminum and silicon in the framework of known zeolites has been widely studied. Such efforts could result in new zeolite structures with unique pore channels and cage systems that could result in the synthesis of new catalyst systems which could promote novel reactions.

Framework substitutes such as B, Ge, Fe, Cr, As, and V in the synthesis of pentasil zeolites have been recently reported.[52] A number of investigators[100-104] have prepared a material having a ZSM-5 structure in which boron atoms are claimed to be the zeolitic framework. Evidence for this substitution has been given by Taramasso et al.[100] from measurements of the size of the unit cell, and by Gabelica et al.[104] from magic angle spinning NMR (MAS-NMR) data. It should be noted that metal-containing zeolites must be subjected to careful study to identify the location and type of interaction with the zeolite framework structure, that is, to insure that the atom is actually in the framework and not sited on top of an aluminium atom in the framework.

Modification of Shape Selective Zeolites for Catalytic Use

Most industrial reactions are acid catalyzed reactions. Thus it is necessary to modify the synthetic zeolites to introduce the acidic catalytic sites as well as to improve the thermal and chemical properties. The zeolite catalysts can be modified by treatment in the following ways: (1) ion exchange, (2) thermal and hydrothermal treatment, (3) chemical modification, and (4) metal loading.

Ion Exchange

The synthetic routes for preparing zeolites usually result in final products containing a substantial amount of alkali metal ions. The alkali metal cations can be replaced by other cations.

Most zeolite preparation schemes include an ammonium ion exchange if the end result is intended to be a catalyst. The concept is to exchange the alkali cations for ammonium ions and then generate the hydrogen or acidic form of the zeolite by thermal decomposition. The rate and degree of ion exchange strongly depend on factors such as the nature of the zeolite, the type and nature of the cation to be exchanged, and the reaction condition for the ion exchange process. Higher degrees of exchange can usually be obtained by batchwise repetition of the exchange procedure.

Direct proton exchange requires the use of solutions with a higher proton concentration such as dilute acid. However, since most zeolites are acid sensitive, the potential applications of direct proton exchange are limited. The stability of zeolites to acid increases with increasing silica/alumina ratio. Hence high silica zeolites are more suitable for ion exchange with dilute acid.

Thermal Treatment

Ammonium exchange of zeolites and the subsequent thermal decomposition is an important activation procedure for many commercial catalysts. The thermal treatment of the ammonium exchanged zeolites is usually conducted at temperatures ranging from 700 to 950 K.

An informative study on H-form zeolites[105] using differential thermal analysis indicated that the first observation on heating is the loss of physically bound water, resulting in an endotherm near 423 K. Next, an endotherm is observed near 923 K corresponding to final dehydroxylation. High temperature treatments may result in structural collapse.

Chemical Modification

The dealumination of a zeolite without destruction of the zeolite structure by treating with $SiCl_4$ has been reported by Beyer and Belenykaja.[106] They claimed that the aluminum atoms in

the framework of NaY were replaced by silicon atoms. Klinowski et al.[107] have confirmed this type of dealumination by ^{29}Si-NMR spectroscopy using the sodium-form of mordenite. The dealumination of ZSM-5 with silicon tetrahalides has also been reported by Chang.[108] Namba et al.[109] found that the aluminum atoms on the external surface of ZSM-5 crystallites were removed more selectively than those in the pores by treating NaZSM-5 zeolite with silicon tetrahalide vapors at 723-923 K.[109]

Metal Loading

It is often necessary to incorporate additional active components in a catalyst to accomplish the required catalytic transformation from reactants to products in many industrial processes. Such components are frequently metals, metal oxides, or metal sulfides similar to those used in non-zeolite or amorphous oxide catalyst systems. Metals can be loaded in zeolite containing catalysts in several ways including ion exchange of the zeolite from solution, impregnation from solution, adsorption from the gas phase, and comulling during catalyst formation of the solid metal component or its solution.

Metals such as nickel, cobalt, silver, iron, and chromium can be directly exchanged from aqueous solutions of their salts such as nitrates, chlorides, acetates, and the like. Many of these can also be introduced as the amine complex ion. Palladium and platinum that normally exist in solution as negative ions ($PdCl_2^{2-}$) must be converted into a positive ion before they can be incorporated. Formation of the positively charged tetramine complex from the palladium salts occurs readily in aqueous ammonia to give the $Pd(NH_3)_4^{2+}$ ion. Platinum forms a similar complex. When the exchange capacity of the zeolites is low, e.g., high-silica zeolites and molecular sieves such as silicalite and aluminum phosphates, other methods, such as impregnation, must be used.

Characterization of Zeolites

X-ray Diffraction

Crystal structure determination using X-ray powder data has played an important role in the development of the science and technology of zeolite molecular sieves and catalysts since the advent of synthetic zeolites. Crystallization mechanisms, modification processes, molecular sieve properties and catalytic behavior can be properly understood if the complete crystal structure is known.

Identification of zeolites can be carried out on the basis of X-ray diffraction. Powder patterns are the common method by which the crystallinity of a zeolite can be determined.[110] If a pattern shows no evidence for crystalline or amorphous contaminants, purity is estimated by the comparison of the intensities of reflections at d-spacings smaller than about six Angstroms with those of a highest purity sample of similar composition and crystal size. Quantitative analyses are much more difficult to conduct because there is no absolute 100 percent crystalline zeolite standard. Thus percent crystallinity can only be compared to an arbitrarily defined standard.

Microanalysis

Many techniques in the field of electron optical instrumentation are available to provide information concerning crystal shape and size and as well as other characteristics of zeolites.[111,112] One of the most important techniques applied in zeolite research is transmission electron microscopy (TEM). Scanning electron microscopy (SEM) used in conjunction with scanning microprobe analysis yields a great deal of information on zeolites.[113]

Scanning Electron Microscopy: In scanning electron microscopy an electron probe is used to scan the surface of a specimen using deflection coils. The interaction between the primary beam

and the specimen produces various signals from back scattered electrons, secondary electrons, X-rays, etc. which may be utilized to form an image of the surface. The appropriate signal is detected, amplified, and displayed on a cathode-ray tube screen scanned synchronously with the beam. One important advantage of SEM is that less stringent specimen preparation requirements are necessary and this permits samples to be examined in a largely unaltered state, since only a conducting surface layer is required. Magnification in the range 20-50000 times is normally available with a resolution down to 100 Å. Zeolite samples are usually covered with a thin film of gold to ensure sufficient electrical conductivity the sample so as to prevent the build-up of a surface charge which leads to distorted image pictures. The gold film also serve to protect heat sensitive samples during analysis.

The back-scattered electrons give a signal varying with the respective atomic number of the probing metal species. Measuring the wavelength of the induced characteristic X-ray radiation with special detectors permits elemental analysis of the surface region upon which the beam is focused. This technique is known as electron microprobe analysis. Ballmoos and Meier[114] have studied the distribution of silicon and aluminum in ZSM-5 crystals using the microprobe analysis method. These results are very important in explaining the mechanism of crystallization of the zeolites. The rate of nucleation and crystal growth increases with the silicon content. Furthermore, microprobe analysis has also helped to explain the catalytic activity of zeolites by measuring the number of active centers within the channel system which is a function of the silica-to-alumina ratio.[114,115]

Transmission Electron Microscopy: Transmission electron microscopy can achieve resolutions of about 3 Å at a magnification of approximately 10^6. The resolution can be improved by using special imaging techniques known as bright field, dark field, or lattice imaging. The surface scanning technique and the analysis of the characteristic X-ray radiation can also be applied

in the transmission mode, that is, scanning transmission electron microscopy (STEM). This method has the advantage of better resolution as compared with TEM, but has the disadvantage of difficult sample preparation.[113]

Lyman et al.[116] indicated that particles of ZSM-5 with different silica-to-alumina ratio may have different chemical profiles across the particle. The technique employed was X-ray emission spectroscopy in the STEM. Small particles, silica-to-alumina ratio of 10, indicated either enrichment of silicon near the surface or a near homogeneous composition. Large particles, SiO_2/Al_2O_3 ratio of 40, exhibited more aluminium near the particle surface than in the center.

Thermal Desorption

The acid strength of zeolites can be determined by measuring the heat of adsorption or desorption of a suitable probe molecule. Ammonia meets the requirements for such a probe[117-120]. Firstly it is small enough to enter all the zeolite pores. Secondly it can react both with the Brönsted and Lewis acid sites. Pyridine is much less suitable with regard to the first requirement. Derouane and co-workers[118] have indicated that the concentration of active acidic sites in ZSM-5 is related to the aluminum content of the zeolite and presumed these sites are located at channel intersections. These sites are characterized by an ammonia desorption band near 773 K. Weaker acidic sites are characterized by a desorption band at about 500 K. These weaker sites probably correspond to terminal silanol groups on the external surface of the zeolite or possibly nonzeolitic impurities. However, Haag[121] has reported that a single type of acid site was observed using ammonia temperature-programmed desorption. A single desorption band with a maximum temperature of 673 K was found. If the zeolite is exposed to excess ammonia vapor, three desorption bands are observed and are erroneously thought to indicate the presence of three types of acid sites on zeolite ZSM-5.[117-120]

Vibrational Spectroscopy

Vibrational spectroscopic techniques can furnish direct information about the nature of surfaces and adsorbed surface species. These techniques provide information on a molecular level. During the last decade there has been increasing recognition that infrared spectroscopy can yield information not only on short range bond order and characteristics but on long range order in crystalline solids caused by lattice coupling.

Flanigen et al.[122] have indicated that the mid-infrared vibrations can be classified into two types, named internal and external vibrations. The internal vibrations, including asymmetric stretch (1250-950 cm^{-1}), symmetric stretch (720-650 cm^{-1}), and T-O (TO_4-tetrahedra, T denotes silicon or aluminum atom) bend (500-420 cm^{-1}), are present in the spectra of zeolites with small changes in absorption frequencies regardless of the type of the framework of the zeolite. The external vibrations depend on the structure of zeolites and are assigned to linkages of the TO_4-tetrahedra typical for a special framework topology. Groups of this kind are the pore opening (420-300 cm^{-1}) and double rings (650-500 cm^{-1}), present in a great variety of zeolites and also the various polyhedral units.

The crystal structure of a ZSM-type zeolite has been studied by X-ray diffraction and infrared spectroscopy. Although the X-ray diffraction pattern of the small ZSM-5 zeolite crystal is characteristic of an amorphous material, the infrared spectra along with catalytic measurements indicated that the material behaved like crystalline ZSM-5.[123] The results have been interpreted in terms of the presence of the small ZSM-5 zeolite crystals (diameter less than 80 Å) in an amorphous matrix.

Recently diffuse reflectance spectroscopy has been applied to the study of high silica zeolites. This technique is much more sensitive in comparison with the standard transmittance

infrared spectroscopy. Kanzansky et al.[124] carried out the measurements on ZSM-5 in the near infrared region, which includes fundamental stretching vibrations of O-H bonds, their overtones and combinations of stretching and bending vibrations. They provided evidence for the similarity of Brönsted and Lewis acidic sites in high silica ZSM-5 and provided an interpretation of the difference in their catalytic activities by shape selectivity effects or by the difference in the concentration of acidic active sites.

Ammonia temperature programmed infrared spectroscopy can provide useful information about the assignment of the different temperature programmed desorption bands. Lok et al.[125] indicated that the infrared spectrum for ZSM-5 shows two sharp bands at 3740 and 3610 cm-1 and a broad band around 3475 cm-1. They noted that the only change in the infrared spectrum during thermal desorption of ammonia from ZSM-5 is the reappearance of a small portion of the 3610 cm-1 band. Therefore, the ammonia desorption from ZSM-5 below 528 K is primarily due to physically adsorbed ammonia.

An infrared spectroscopic study of simple alcohols adsorbed on ZSM-5[126] was in agreement with the results from thermal desorption spectroscopy:[127] each of the alcohols adsorbs in the vicinity of the aluminium atoms, as evidenced by the disappearance of the hydroxyl band associated with the hydrogen cations.

Furthermore, the comparison of sequences of site populations with observed reactivities on ZSM-5 suggests that Lewis sites are the origin of catalytic activity in the conversion of CH_3OH to $(CH_3)_2O$.[117] Similar comparisons also indicate that dealuminated Brönsted sites are the principal source of reactivity for the conversion of $(CH_3)_2O$ to hydrocarbons.[128,129] Active acidic sites involving in methanol conversion can be expressed according to the following simplified reaction scheme:

$$CH_3OH \xrightarrow[\text{Lewis Acid}]{} (CH_3)_2O \xrightarrow[\text{Brönsted Acid}]{} \text{Hydrocarbons} \qquad (1)$$

Acid properties of NaHZSM-5 zeolites of various degrees of exchange have been studied by quantitative infrared studies of pyridine adsorption.[130-133] Two kinds of Brönsted acid sites were detected, OH groups vibrating at 3609 cm-1 being strong acid sites and other protonic sites (3740 cm^{-1}) of lower acidity. The concentration of acid sites (determined by infrared spectroscopy) was found to be equal to the concentration of protons introduced into zeolite by ion exchange.[134,135] These results indicate that the introduction of protons into the zeolite does not acidify weaker sites preexisting in the zeolite before ion exchange.

Solid State NMR

NMR spectra can provide information on the bonding of atoms to the silicon and aluminum in the structure and distinguish between different types of species such as Si-4Si, Si-3Si1Al, Si-2Si2Al, Si-1Si3Al, and Si-4Al in the zeolite lattice and external to the lattice structure. The key is the development of the magic angle (54°44') spinning NMR for the measurement of chemical shift in solid samples. The chemical shift values are characteristic of crystallo-graphically and chemically distinct environments.

Correlations between chemical shift and structure were established,[136] and used[137,138] in structural studies of both soluble and insoluble silicates and aluminosilicates. The structure of a wide variety of zeolitic solids has been investigated[137-149] using ^{29}Si, ^{27}Al and several other nuclei.

Kinetic Characterization

α-Test: The catalytically active centers in the H-form of ZSM-5 are believed to be Brönsted acid sites, i.e., bridging hydroxyl groups associated with framework aluminum atoms. The number of catalytically active acidic hydroxyl groups is equal to the aluminum content, if all the aluminum atoms are in tetrahedral framework positions and if they are not poisoned.

The cracking of n-hexane provides a suitable quantitative test reaction for measuring the acidity of a catalyst. At a given temperature the magnitude of the rate constant, k, is obtained from the equation $k = (1/t) \cdot \ln\{1/(1-\varepsilon)\}$, where k is the first order rate constant, ε is the fractional conversion and t is the contact time.[150] The rate constant for cracking is expressed in α-units, α = 1 being the value of a high activity amorphous SiO_2/Al_2O_3.[151,152] Haag et al.[121] indicated that the hexane cracking activity over HZSM-5 is strictly proportional to the aluminum content over more than three orders of magnitude, extending down to aluminum contents in the parts per million range. Extrapolation of the data on a linear plot gave zero activity at zero aluminum content.[121,153] A similar linear relationship was also observed between the α-value and the intensity of the NMR signal due to tetrahedral aluminum.[121]

Isobutane Isomerization: The isomerization of isobutane which proceeds by a bimolecular mechanism over large-pore zeolites has been used as a probe reaction to study the channel structure of the pentasil zeolites.[154,155] The product stream contains propane and pentanes in addition to n-butane over mordenite. In zeolite ZSM-5, there is not enough space in the channel intersection for a bimolecular transition state. As a consequence, pentanes are not present in the products of the reaction.[156] This suggests a mono-molecular mechanism. Haag and Dessau[157] indicated this monomolecular transition state involves a pentavalent carbonium ion intermediate.

Surface Area Measurement: Various means have been used to measure surface areas for molecular sieve zeolites including the BET method. However, the BET method gave much lower results than other techniques. The use of the Langmuir isotherm may be the more appropriate method. A simplified method can be used in which V_m (volume of a monolayer of gas adsorbed) is measured at a low relative pressure on the order of 0.02.

External surface area measurements are of importance in understanding the catalytic activity and adsorption properties, since the external surface contributes only to nonselective reaction or adsorption processes.[158] The external surface area of molecular sieve zeolites has been measured by (a) the filled-pore method,[159-161] (b) modified BET method using large molecules, or (c) electron microscopy. The shape and size of the zeolite crystals can be measured by SEM; however, the external geometric surface area can be calculated only when the crystals are discrete and relatively homogeneous. Benzene or n-hexane, thought to diffuse freely within the pentasil frameworks, can access all the active surface. Thus the external surface area can be measured by the BET method when the pores are filled with benzene or n-hexane so as to exclude the adsorptive from the internal surface of the zeolite.

Intracrystalline Diffusion in Zeolites

When porous materials are exposed to the gas phase, two well-known regimes are defined in classical diffusion theory. One is the ordinary diffusion regime for which the mean free path of the gaseous molecule is smaller than the pore size of the porous material. It turns out that the diffusivities are equal to the ordinary gaseous diffusion coefficients reduced by the porosity. As the pore size becomes smaller than the molecular mean free path, there is a transition to the Knudsen diffusion regime, where the diffusivity is inversely proportional to the pore dimension.

Crystalline zeolites with their regular, rigid, and defined void structures have introduced a third regime. Weisz[162] has termed it as the configurational diffusion regime. Here, intracrystalline diffusion is affected by the matching of the shape, size, and configuration of the diffusing gas to the corresponding parameters of the zeolite framework. It is believed that this type of intracrystalline diffusion plays a major role in shape selective zeolite catalysis. The rate of the shape selective catalysis might be expected to be controlled by the rate of diffusion rather than by any catalytic phenomenon.[163,164]

Molecules with sizes similar to or slightly larger than the zeolite pores can usually diffuse through the pore structure due to the molecular vibrations (molecular shape and configuration can change in time) or breaching of the zeolite pores (bond cleavage followed by reconstruction of the bond).[20]

The size, charge, position in the zeolite framework, and concentration of the exchanged ions may influence the diffusion characteristics of the zeolite framework. The geometry and dimensions of the channel network and crystal shape of the zeolite may also govern diffusion in zeolites.

Shape Selective Zeolite Catalysis

Types of Shape Selective Zeolite Catalysis

Shape selective catalysis using zeolites is based on the locus of active catalytic sites in the intracrystalline pore system, which is very uniform in one or more discrete dimensions. Therefore, shape selectivity may be achieved by virtue of geometric factors, Columbic field interaction, and difference in diffusion rate.[165] Molecular shape selective catalysis can be divided into several major classes: reactant selectivity, product selectivity, restricted transition state selectivity, and molecular traffic control.[38,155,166,167]

Reactant Selectivity: Reactant or charge selectivity occurs when some of the molecules in a reactant mixture are too large to be able to diffuse freely within the intracrystalline volume of the zeolite because of diffusion constraints, selective sorption, or molecular sieving effects.

Product Selectivity: Product selectivity occurs when the products of the reaction formed within the pores are too bulky to diffuse to the exterior surface of the catalyst where they can be observed. The bulky molecules are either converted to less bulky molecules by cracking or equilibration or deactivate the catalyst by blocking the pores.

Restricted Transition State Selectivity: Restricted transition state molecular shape selectivity occurs when local configuration constraints prevent or limit the formation of a given transition state. Reactions requiring smaller transition states proceed unhindered. Neither reactant nor product molecules is prevented from diffusing through the pores.

An example is the high selectivity of the zeolite ZSM-5 based xylene isomerization process.[155] The ratio of the rate constants for the bimolecular disproportionation to trimethylbenzene and toluene compared with the isomerization to other xylenes (k_{isom}/k_{disp}) is higher for ZSM-5 than that for HY or H-Mordenite zeolites by 10 - 100 times. It is clear that the narrower pore zeolites restrict the bimolecular reaction due to steric hindrance.

Molecular Traffic Control: The concept of molecular traffic control shape selectivity developed from studies of single component adsorption measurement in ZSM-5 type zeolites.[168] As discussed previously, zeolite ZSM-5 has two types of channel systems, one system is sinusoidal whereas the other is straight. It was observed that molecules such as p-xylene and 3-methylpentane are restricted to the straight channel whereas linear molecules such as n-pentane and n-hexane can diffuse easily through both types of channels. This has led to the proposal that reactant molecules

may enter zeolite ZSM-5 preferentially through one set of channels and the products leave the zeolite by a different set thus minimizing counter diffusion. The general concept of molecular traffic control still requires definitive experimental evidence before it is generally accepted. Reactions that may exhibit molecular traffic control selectivity include benzene alkylation with ethylene and toluene alkylation with methanol over ZSM-5.[169] The higher activity of p-xylene alkylation by methanol in ZSM-11 compared with ZSM-5 may also be due to molecular traffic control.[170]

Coking on Shape Selective Zeolite Catalysts

The formation of coke is often acid-catalyzed and it is therefore a major concern when using acidic zeolite catalysts. Understanding the mechanisms that control coking, and its effect on catalytic properties such as selectivity and activity, is essential for catalyst selection and process design.

The low rate of deactivation of ZSM-5 in a number of industrial processes has been attributed to the dimensions of the pores that sterically hinder the formation of coke precursors or intermediates and to the relatively low density of acid sites.[171-177] Generally, zeolites with noninterconnecting uniform channels or noninterconnecting nonuniform channels will age more rapidly than their counterparts with interconnecting channels or cages. Interconnected pore networks offer a greater number of pathways to the active sites through which molecules can diffuse randomly, thereby decreasing the number of active sites in the blocked pore. The occurrence of cages in noninterconnecting or interconnecting networks provides room to accommodate initial coke formation without immediate blocking of the pores. These deposits may grow to a size greater than the pore or window aperture, leading to a situation in which the catalyst cannot be regenerated under mild conditions.[175,176] A qualitative description of aging by

pore blockage has been proposed for the case of increasing coke content.[176] The effect of pore mouth blockage is to reduce the rate of entrance of reactants into the crystallites, to increase the tortuosity of diffusion paths to and from the active sites, and to reduce the intrinsic number of accessible sites.[178] The effects of coking modes, pore mouth restriction and bulk restriction (internal coking) are to reduce the diffusivity of reactant and product molecules as a result of the reduction of the effective diameter of the pore.[175]

Applications of Shape Selective Zeolite Catalysts in Industrially Significant Processes

Methanol-to-Gasoline Process

A large variety of acidic catalysts can be used for the conversion of methanol to hydrocarbons.[16] The use of zeolite ZSM-5 as an acid catalyst[17,38,155,179-202] is particularly attractive as it offers a new and variable route for the direct production of high-grade gasoline from methanol which can be produced from coal or natural gas. The shape selective properties of ZSM-5 catalysts are the basis for the Mobil Methanol-To-Gasoline (MTG) process. Among the advantages of ZSM-5 catalyst are the following: it forms less coke than the other catalysts due to transition state selectivity, and it produces hydrocarbons in a rather narrow compositional range. The MTG processes capable of converting methanol to hydrocarbons and water: the maximum hydrocarbon yield is 44 wt. percent with the balance, 56 wt. percent, being water. Hydrocarbons produced over ZSM-5 include paraffins (60-67 percent), olefins (6-8 percent), and aromatics (27-32 percent).

The methanol reaction over ZSM-5 catalyst involves a series of consecutive steps. Chang and Silvestri[190] proposed that the reaction associated with the production of gasoline boiling range hydrocarbons proceeds according to the following simplified reaction scheme:

$$2\ CH_3OH \longleftrightarrow CH_3OCH_3 \longrightarrow C2^{=}\text{-}C5^{=} \longrightarrow \begin{matrix}\text{Paraffins}\\ \text{Aromatics}\\ \text{Cycloparaffins}\\ C_6^{+}\ \text{Olefins}\end{matrix} \qquad (3\text{-}2)$$

Methanol is converted first to dimethylether (DME). This step is very much faster than the subsequent steps. The reaction pathway that accounts for the first C-C bonds formed from methanol or DME, i.e., the creation of a covalent bond between two C_1 units to form a C_2 species, is still unresolved. The species involved in this step is probably a cationic C_1 fragment, and the product is most likely ethylene, or possibly propylene. This initial olefin is further converted to longer aliphatics that later cyclize, dehydrogenate to form aromatics that are alkylated by methanol or shorter olefinic intermediates. These reactions stop at durene because there is no space to form larger polyalkyl-aromatics at ordinary processing conditions. It should be noted that durene formation can be minimized by controlling catalyst and process conditions.[203] Additional research has shown that variations in operating conditions and catalyst modification can selectively produce specific hydrocarbon classes.[16]

Methanol-to-Olefins and Distillates

The methanol conversion process can be modified to produce light olefins (MTO) before the C_2 - C_4 olefinic intermediates are converted to higher molecular weight paraffins and aromatics by using a low acidity ZSM-5.[204] Pentasil borosilicate zeolites and pentasil aluminosilicates treated with HF have also been reported to be effective in the MTO process.[205] The borosilicate catalysts are less active than the aluminosilicate ones and convert methanol to propylene. The fluoridated aluminosilicate pentasil converts methanol to ethylene.

The Mobil Olefins-to-Gasoline and Distillates (MOGD) process converts light olefins to a whole range of liquid products. The products are either gasoline or jet and diesel fuels or even No. 2 fuel oil. Approximately 100 percent high quality gasoline in the "gasoline mode" and 80 - 90 percent jet and diesel fuels plus 10 - 20 percent gasoline in the "distillate" mode can be produced in the MOGD process.[206]

Middle Distillate and Lube Oil Dewaxing

Middle distillate and lube oil dewaxing processes are based on the principle that long-chain linear and slightly branched hydrocarbons are selectively hydrocracked from the feedstock. Thus the concentration of linear paraffins is reduced and the pour point, cloud point, and freeze point of the product liquids are decreased. The reductions in these properties are related to the fact that linear and slightly branched hydrocarbons have higher melting points than highly branched hydrocarbons and hence give rise to higher pour, cloud and freeze points. Shape selective catalysts can remove the normal paraffins without appreciable conversion of the other components.[207]

Hydrodewaxing processes remove waxy paraffins from intermediate and heavy gas oils (diesel fuel and heating oils) and lube oil base stocks by converting them to gasoline and LPG fractions. The Mobil distillate and lube oil dewaxing processes[208-211] use HZSM-5 catalyst. The catalyst may contain a hydrogenation component such as Ni, Zn, or Pt. The catalyst in the similar British Petroleum Process is platinum supported on hydrogen mordenite.[212]

The middle distillate dewaxing process (MDDW) developed by Mobil is a fixed bed process.[210] The process decreases the pour point of the product by 30 - 40 K. The by-product gasoline has a relatively high octane number and therefore it may be added to the gasoline pool without further reforming.

M-Forming Process

The Mobil Selectoforming process,[213] developed in the mid-sixties, introduced an additional processing step to the usual reforming process in which the low octane paraffins are selectively removed by hydrocracking to propane and light gases. The catalyst (erionite) could be placed in the bottom of the last reforming reactor or in a separate reactor.

M-forming,[214] developed by Mobil Oil Corporation, is more sophisticated than Selectoforming. The process is basically the same with the catalyst being changed from erionite to ZSM-5. The ZSM-5 catalyst can admit singly branched paraffins as well as simple aromatics such as benzene and toluene. The larger channel size permits the removal of the second lowest octane components, the single branched paraffins, by hydrocracking. Furthermore, the aromatic species are alkylated by the olefinic component of the cracked product. The alkylaromatics contribute to octane number and reduce the loss of cracked products to gas, thus increasing the liquid yield.

Alkylation of Aromatics

Benzene Alkylation

Alkylation of benzene with ethylene yields ethylbenzene followed by the dehydrogenation process to produce styrene. The Badger-Mobil vapor phase ethylbenzene process uses ZSM-5 catalyst.[215] The process relies on the unique shape selective properties of ZSM-5 catalyst. Multiple beds of catalyst are used with benzene and ethylene being added between the beds for temperature control.

Toluene Alkylation

Toluene can be alkylated with ethylene to give ethyl-toluene over ZSM-5 catalyst. The desired p-ethyltoluene is formed preferentially because the catalyst can direct the reaction based on the very small difference in the molecular dimensions either by rate of formation (controlled by transition state selectivity) or rate of diffusion out of the pores.

Techniques for modifying the pore openings of the ZSM-5 catalyst by means of phosphorus,[216] boron,[217] and magnesium[218] have been reported. It is noted that production of o-ethyltoluene, the largest isomer, was essentially eliminated. The selectivity for p-ethyltoluene is significantly improved with these catalysts.

The formation of p-xylene in excess of equilibrium values from toluene alkylation with methanol has been reported over a phosphorus or magnesium modified ZSM-5.[219,220] Although all three isomers are formed at equilibrium concentrations within the pore structure, the p-xylene can diffuse out of the catalyst approximately 10^4 times faster than the other isomers thus shifting the equilibrium within the catalyst pore structure in favor of p-xylene.

Toluene Disproportionation

Toluene disproportionation, the transalkylation of two moles of toluene to one mole each of xylene and benzene, has been practiced commercially for a number of years.[211,220-222] The catalyst is ZSM-5. Toluene can be converted with high selectivity to benzene and xylene.[223] Shape selectivity of the catalyst also helps to minimize coking and the formation of higher molecular weight hydrocarbons.

Xylene Isomerization

The xylene isomerization process is the conversion of m- and o-xylenes to p-xylene.[224,225] Zeolite ZSM-5 has been applied to this reaction in which it should be possible to influence the direction of the reaction by modifying the pore structure. Modifications of the pore structure by incorporation of boron, magnesium, phosphorus, antimony or by controlled coking can be expected to improve the product distribution due to shape selective effects.[155,226-228] Improvements on the commercial process by steaming the ZSM-5 or adding alkali ions or by using higher SiO_2/Al_2O_3 ratio zeolites have also been reported.[229]

Preparation of Zeolites ZSM-5 and ZSM-48

Preparation of Zeolite ZSM-5

The preparation of the ZSM-5 class of zeolites used in this investigation was based on a method patented by Argauer and Landolt.[30] The general preparation scheme used for the synthesis of ZSM-5 is presented in Figure 13. Silica (22.9 g) was partially dissolved in 100 cm^3 of 1 N tetrapropylammonium hydroxide (TPAOH) or 2.18 N tetrapropyl ammonium bromide (TPABr) by heating the solution to a temperature of approximately 353 K with magnetic stirring. A solution of sodium aluminate and deionized water was added to the silica solution at 353 K with magnetic stirring. The mixture was placed in a Teflon beaker and heated in an autoclave (capacity 1000 liters) at 453 K (or 433 K) for six days (or 10 days) without stirring. The resultant solid product was filtered, washed with about 1000 cm^3 of distilled water and dried at 383 K for 16 hours. A portion of this product was subjected to X-ray diffraction analysis to determine the crystalline nature of the zeolite. The product was then calcined at 813 K in air for 16 hours prior to modification by ion exchange.

Step 1: The organic cation (TPAOH or TPABr) was dissolved in water at 353 K with magnetic stirring to form Solution A.

Step 2: Silica was partially dissolved in Solution A at 353 K with magnetic stirring to form Solution B.

Step 3: Sodium aluminate was dissolved in water at 353 K with magnetic stirring to form Solution C.

Step 4: Solution B was mixed with Solution C at 353 K with magnetic stirring to form Solution D.

Step 5: Sodium hydroxide was added to Solution D to adjust the pH value to ~12 at 353 K to form Solution E.

Step 6: Solution E was transferred to an autoclave and was heated in an oven at 453 K (or 433 K) for 6 days (or 10 days) without stirring to produce the precipitated/crystallized zeolite F.

Step 7: NaZSM-5, as synthesized, was filtered and washed with distilled water. The sodium-form of ZSM-5 was then dried at 383 K for 16 hours and calcined at 813 K for 16 hours to produce Solid G.

Step 8: The NaZSM-5 was exchanged using ammonium nitrate to produce the hydrogen-form of ZSM-5.

Figure 13

Procedure for the Synthesis of ZSM-5

PROCEDURE FOR SYNTHESIS OF HZSM-5

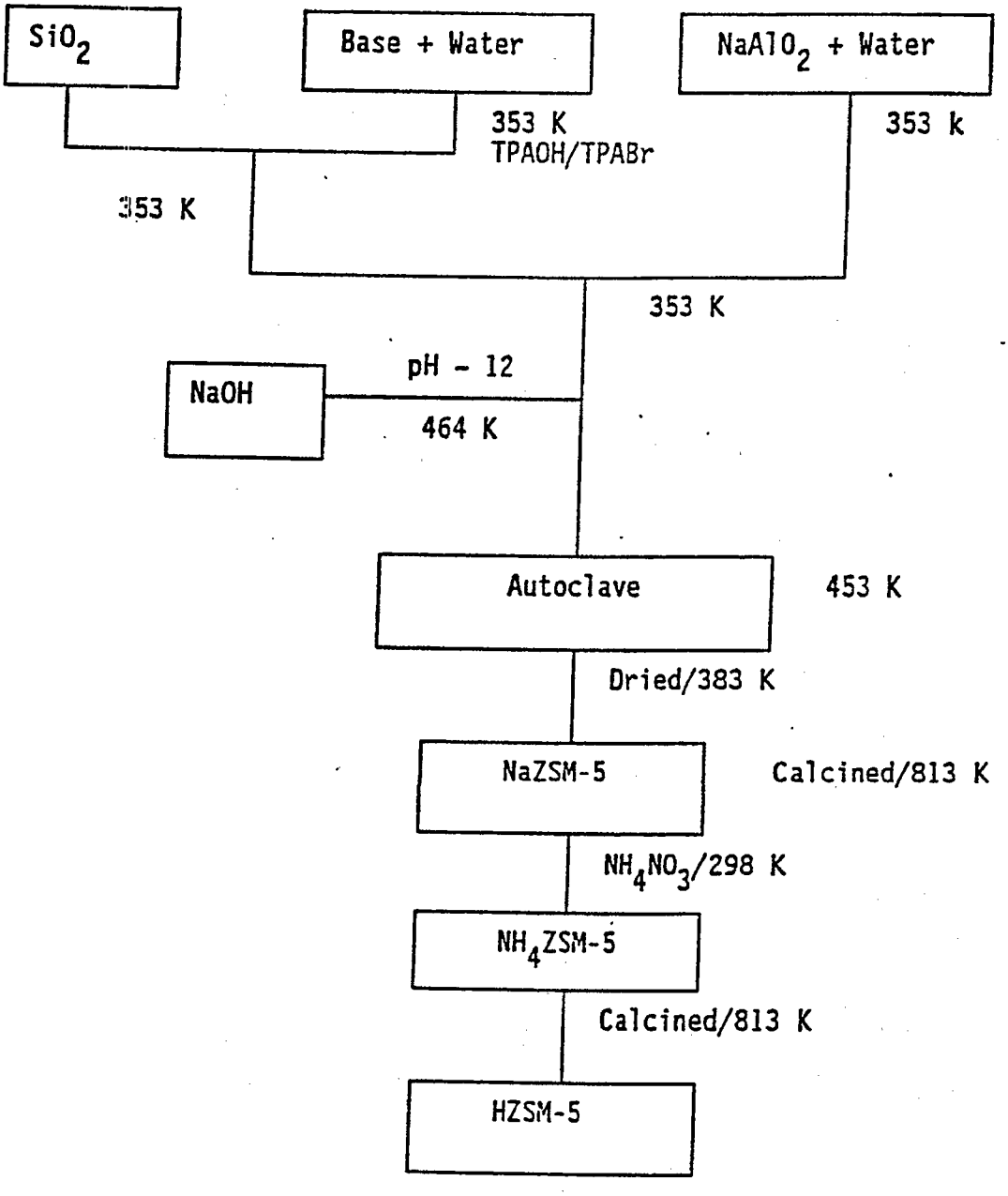

Zeolite ZSM-5 in the hydrogen form was prepared by two procedures. The first method consisted of crystallizing the sodium form of ZSM-5 at 425 K (or 453 K) from a gel containing organic cations (TPABr or TPAOH). The sodium form was subsequently exchanged three times with a 1 N NH_4NO_3 solution at 298 K. The NH_4ZSM-5 was then heated for 16 hours at 813 K to obtain the hydrogen form of the catalyst, HZSM-5.

A direct method for preparing HZSM-5 with the same structure as indicated by X-ray diffraction patterns has also been investigated. The zeolite crystals are formed using 1,6-diamino-hexane (C6DN) as the organic cation from a sodium-free gel, which after calcination in air at 1023 K directly gives the hydrogen form without an intermediate ion exchange. The procedure for the direct synthesis of the hydrogen form of ZSM-5 is presented in Figure 14. The zeolite obtained in this way is designated as HZSM-5D.

Preparation of Zeolite ZSM-48

ZSM-48 can be prepared from a reaction mixture containing a source of silica, an organic compound (1,6 hexane-diamine (C6DN), 1,8-diaminooctane (C8DN) or 1,12-diamino-dodecane (C12DN)) having an amine functional group with Pka > 7, and an alkali metal oxide (sodium oxide) with or without a source of alumina and water. The procedure for synthesis of ZSM-48 is presented in Figure 15. The composition ranges for the compounds comprising the reaction mixture are presented in Table 21 in terms of the mole ratios of the oxides. The mixture was maintained at 453 K in a stainless-steel autoclave until crystals of ZSM-48 were formed. The sodium-form of ZSM-48 was subsequently exchanged three times with a 1 N ammonium nitrate solution at 298 K. The ammonium-form of ZSM-48 was heated for 16 hours at 1023 K to obtain the hydrogen form of the catalyst.

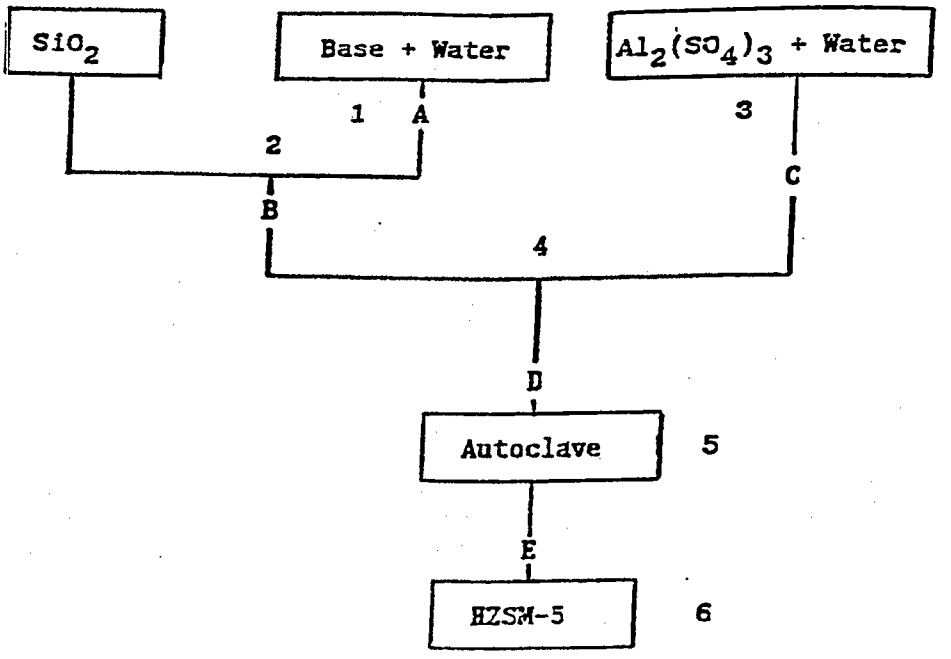

Step 1: An organic cation (C6DN) was dissolved in water at 353 K with magnetic stirring to form Solution A.

Step 2: Silica was partially dissolved in Solution A at 353 K with magnetic stirring to form Solution B.

Step 3: Aluminium sulfate was dissolved in water at 353 K with magnetic stirring to form Solution C.

Step 4: Solution B was mixed with Solution C at 353 K with magnetic stirring to form Solution D.

Step 5: Solution D was transferred to an autoclave and was heated in an oven at 453 K for 2 days without stirring to produce the precipitated/crystallized Zeolite E.

Step 6: The HZSM-5, as synthesized, was filtered and washed with distilled water. The hydrogen-form of ZSM-5 was then dried at 383 K for 16 hours and calcined at 813 K for 16 hours.

Figure 14

Procedure for the Direct Synthesis of the Hydrogen-Form of ZSM-5

Step 1: An organic cation (C6DN or C8DN) was dissolved in water at 353 K with magnetic stirring to form Solution A.

Step 2: Silica was partially dissolved in Solution A at 353 K with magnetic stirring to form Solution B.

Step 3: Sodium aluminate was dissolved in water at 353 K with magnetic stirring to form Solution C.

Step 4: Solution B was mixed with Solution C at 353 K with magnetic stirring to form Solution D.

Step 5: Sodium bromide was added to Solution D to adjust the sodium concentration at a temperature of 353 K with magnetic stirring to form Solution E.

Step 6: Solution E was transferred to an autoclave and was heated in an oven at 453 K for 2 days without stirring to produce the precipitated/crystallized Zeolite F.

Step 7: The NaZSM-48, as synthesized, was filtered and washed with distilled water. The sodium-form of ZSM-48 was then dried at 383 K for 16 hours and calcined at 813 K for 16 hours.

Step 8: The NaZSM-48 was exchanged using ammonium nitrate to produce the hydrogen-form of ZSM-48.

Figure 15

Procedure for the Synthesis of ZSM-48

PROCEDURE FOR SYNTHESIS OF HZSM-48

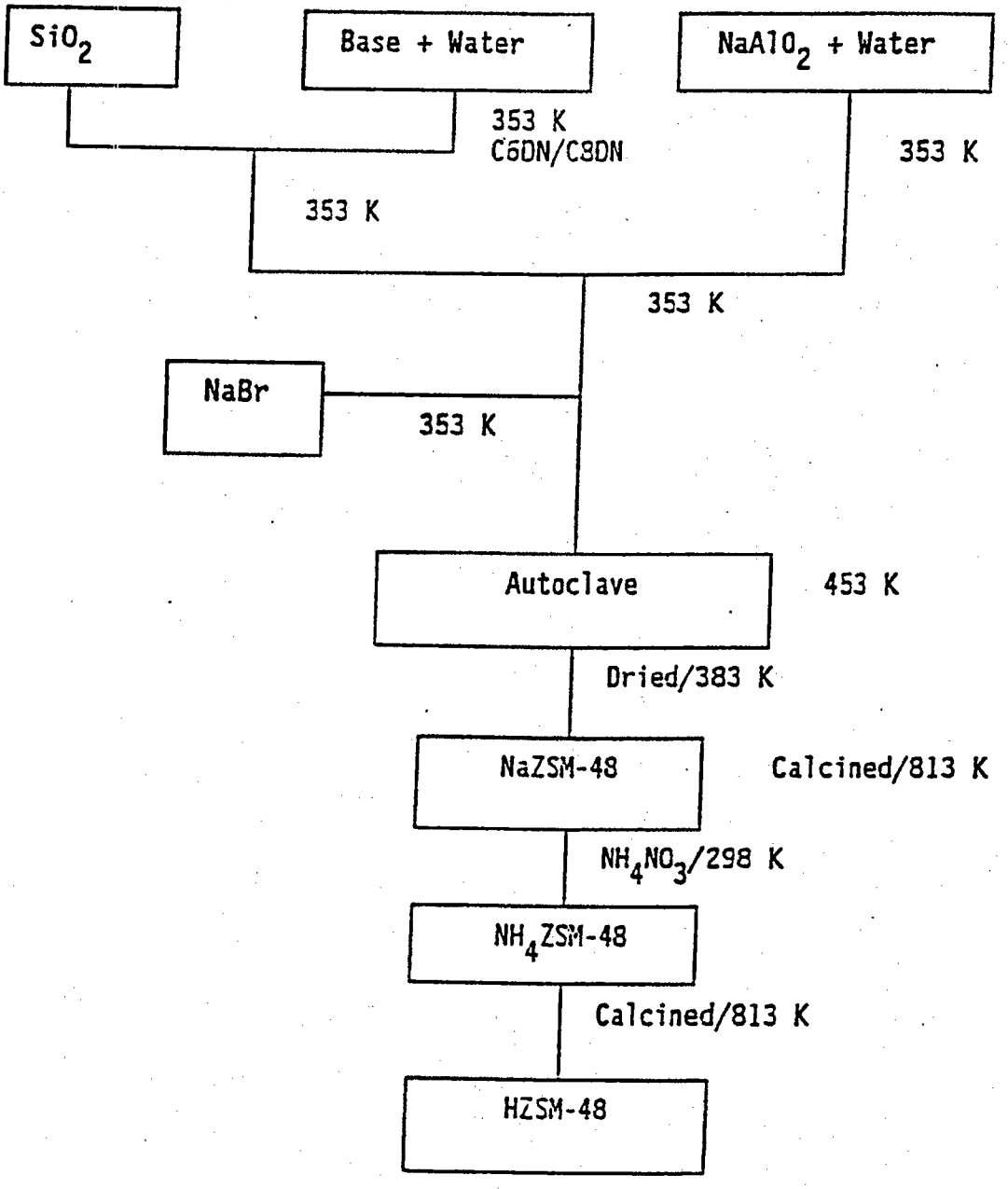

Table 21

Composition Ranges in Terms of Mole Ratios for the Synthesis of ZSM-48

Reactants	Broad[77]	Preferred[77]	This work
Al_2O_3/SiO_2	0 - 0.02	0 - 0.01	0.025 - 0.005
Na/SiO_2	0 - 2	0.1 - 1.0	0.6 - 0.3
RN/SiO_2	0.01 - 2.0	0.05 - 1.0	0.3 - 0.1
OH^-/SiO_2	10-100	20-70	40

Characterization of Synthetic Zeolites

Elemental Analysis of Synthetic Zeolites

The elemental analysis of the synthetic zeolites was determined using an electron microprobe method in an EMX-SM Spectrometer (Model-121000, Applied Research Laboratories, Inc.). A wavelength dispersive X-ray detection system (WDS) was used in this microprobe. Lithium fluoride (LiF) crystals with precise d-spacings are used to diffract narrow band X-ray wavelengths into the detector (Extron or Flow). The signals produced are then amplified and counted.

X-ray Diffraction

The structures of the synthetic zeolites were investigated using X-ray diffraction. A Phillips Norelco Electronic Instrument X-ray Diffractometer was used in this study. The incident beam was CuK_{α} X-ray radiation with a wavelength of 0.15405 nm. The diffracted X-ray was detected by an ionization chamber that could be rotated to determine the angle for constructive interference. The intensity of the diffracted X-ray was measured synchronously as the goniometer of the X-ray diffractometer rotated.

The synthetic zeolites were ground to a fine powder and placed in an aluminum sample holder. X-ray diffraction patterns were measured from 10° to 50° (2θ) at a scanning speed of 2°/min. The X-ray diffraction pattern of a ZSM-5 (ammonium-form) sample provided by the Mobil Research and Development Corporation was also determined for comparison with those of the synthetic zeolites prepared for this study.

Thermal Desorption

A schematic of the microreactor system that incorporated a thermo-conductivity detector to monitor feed and product streams is presented in Figure 16. The microreactor/TPD (MCR) apparatus was used to study normal-hexane cracking (α-test), the isobutane isomerization, temperature-programmed ammonia desorption, and alcohols conversion reactions.

Zeolite catalysts were saturated with ammonia by flooding the samples with a flowing stream of 5 percent ammonia/nitrogen for at least 30 minutes at room temperature. The catalysts were then heated at a linear heating rate of 5 K/min in a stream of helium and the amount of ammonia desorbed was continuously monitored by the thermal conductivity detector to give the TPD spectra.

Infrared Spectroscopy

Methanol adsorption and its subsequent reactions on zeolites ZSM-5 and ZSM-48 were studied using a diffuse reflectance infrared cell. The infrared cell (Figure 17) was used in a Digilab FT-IR spectrometer (model FTS-40). Zeolite samples were pretreated in flowing helium at 773 K for two hours. Since the optical path of the cell is very short, the spectra of adsorbed surface species can be measured in the presence of the reactant vapor.

The infrared spectra were measured during reaction and/or after pulse methanol injection with zeolite catalysts. The thermal desorption of methanol from ZSM-5 and ZSM-48 was also studied using the diffuse reflectance FT-IR method.

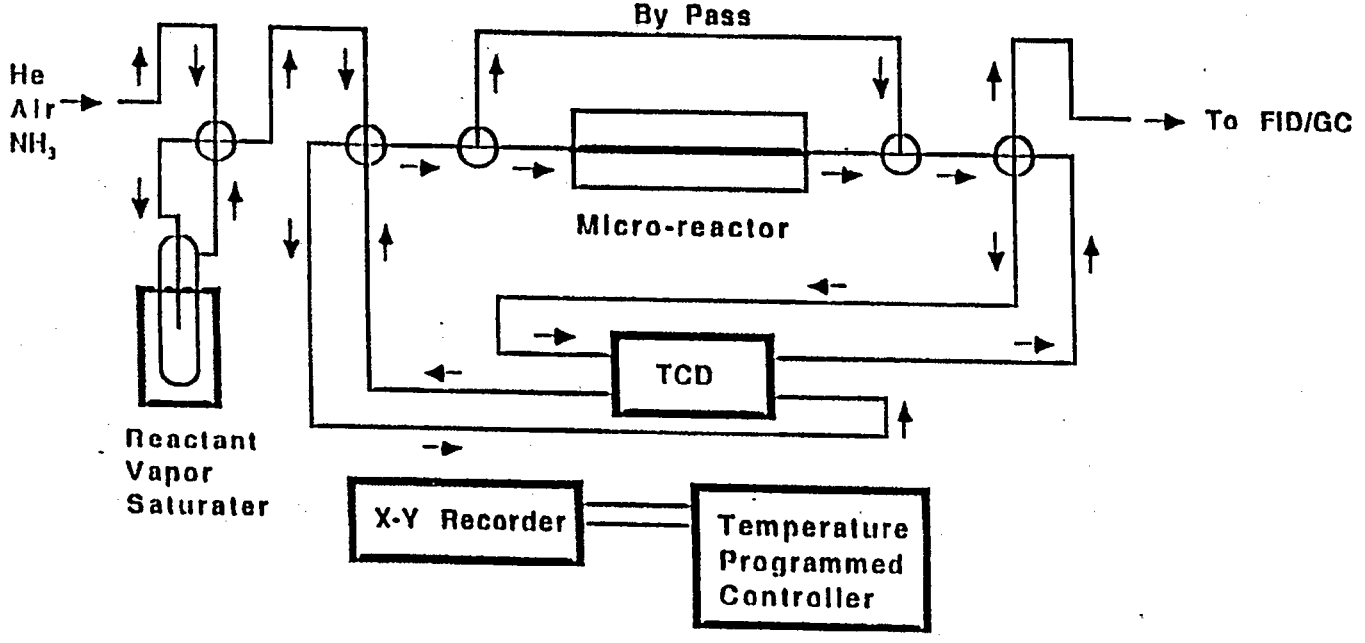

Figure 16. Schematic of Temperature-Programmed Desorption (TPD) and Microreactor Apparatus

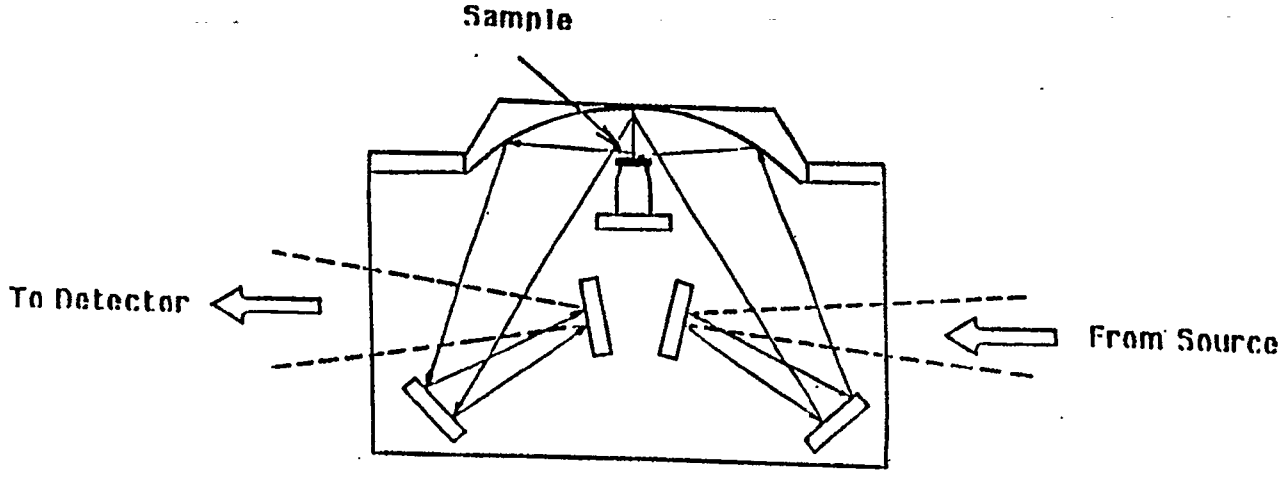

Figure 17. Diffuse Reflectance FTIR Cell and Optical Layout

SEM and the Morphology of Zeolites

The morphology of the zeolites prepared in this investigation was examined with an Hitachi S-530 Scanning Electron Microscope equipped with an X-ray detector (PGT System IV). The vacuum in the specimen chamber was below $5x10^{-6}$ torr. Samples were mounted on aluminum pegs and coated with a thin film of gold. For small particles analyzed directly on the support, the particle thickness was assumed to be roughly the same as the lateral dimension of the particle.

Energy Dispersive Analysis of X-ray (EDAX) is a rapid semiquantitative method for elemental analysis. Use of this system (PGH System IV) in conjunction with the SEM provides a powerful analytical tool for examining catalyst surfaces.

Channel Structure

The pores of ZSM-5 and ZSM-48 have openings of about 5.5 Å. They can admit linear and slightly branched paraffins, and simple naphthenes and aromatics. Isomerization of isobutane was studied at 623 K with a hydrogen/isobutane molar ratio of four in the microreactor to investigate the nature of the pore/channel structures of ZSM-5 and ZSM-48.

Acidity

The cracking of n-hexane provides a suitable test reaction for measuring the acidity of the zeolites since n-hexane is free of diffusion limitations for both zeolites ZSM-5 and ZSM-48. Measurements were carried out with n-hexane in a continuous flow microreactor at temperatures at which the conversion is above 5 percent, for accuracy of measurement, and below about 40 percent to avoid complications due to reactant and/or product transport limitations. The hexane cracking activities of crystalline aluminosilicates including HY, ZSM-5, and ZSM-48 were investigated.

Surface Area

The adsorption of nitrogen on the synthesized zeolite catalysts was measured by the volumetric adsorption method in a glass vacuum system (Figure 18). The apparatus consists of a diffusion pump (model PMCS-4B, CVC) backed up with a mechanical vacuum pump (GCA Precision Scientific D25 1/3 hp). The background pressure was monitored with a Penning Vacuum Gauge (Model GPH-320C, CVC) and was of the order of 10^{-4} torr. The pressures during the volumetric adsorption were measured using a MKS Baratron Absolute Pressure Gauge (Type 222B, 0-1000 Torr). A more detailed discussion of surface area measurement, the experimental apparatus, and the treatment of the data are presented in Section VIII and in the Appendices.

The external and internal surface areas of the zeolites were measured using the n-hexane filled-pore method.[159] Calcined zeolite samples were heated in vacuum at 623 K for eight hours. The amounts of adsorbed nitrogen molecules at 77 K were measured both before and after n-hexane filling of the pores of the zeolite samples. The dead volume of the system was measured and calculated from the free expansion of neon at room temperature and 77 K.

Reactivity of Methanol and Higher Alcohols over Zeolites

The activity and selectivity of the synthesized zeolites for alcohol conversion were studied in a stainless steel flow microreactor at a total pressure of one atmosphere and generally at 643 K. The catalysts (one gram reactor charge) were activated in flowing air for four hours at 773 K followed by cooling to the reaction temperature in helium. The reactant mixtures (flow rate of 30 cm^3/min) were fed to the reactor in a helium stream that had been saturated by passing the helium through a bubbler containing the alcohols at room temperature. The reactor effluent was analyzed by gas chromatography method in a Hewlett Packard Chromatograph (Model 5830) using an SP-2100 or Chrosorb-102 column.

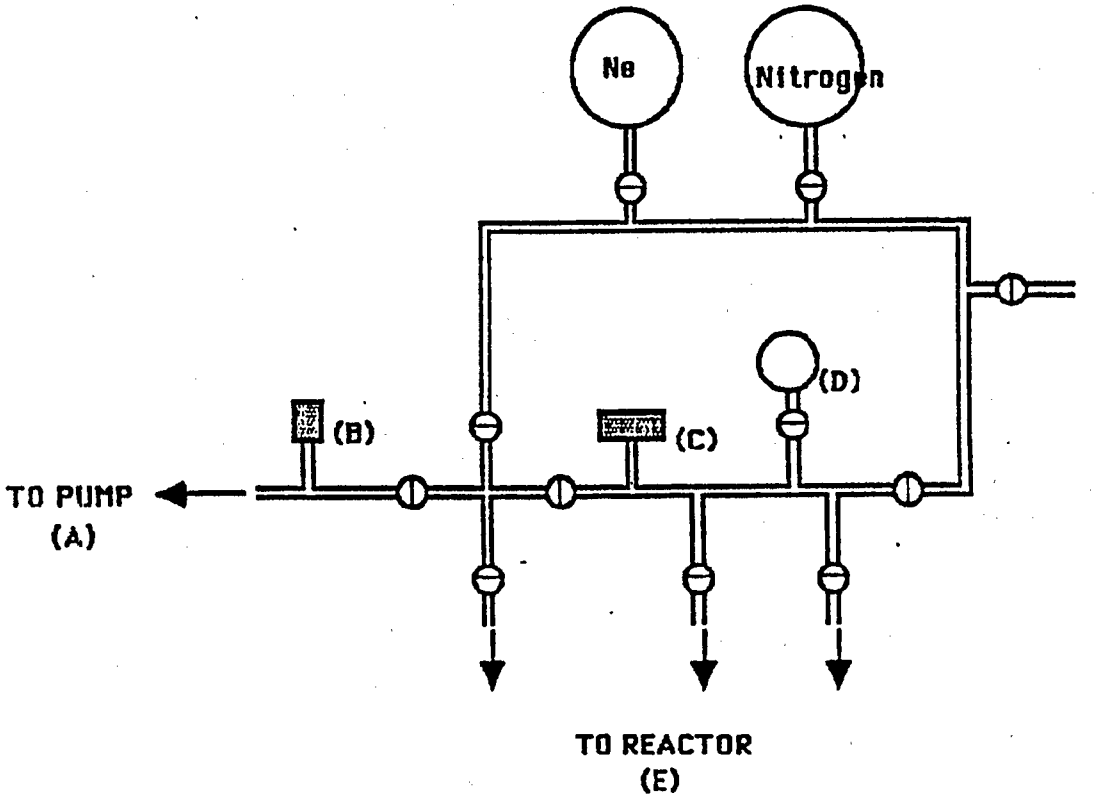

Figure 18. Volumetric Adsorption System for BET Surface Area Measurement

A fixed-bed flow reactor system (Figure 19) was used to study the reaction of methanol over ZSM-5 and ZSM-48 catalysts. The product from the catalytic reactor was cooled in a high-pressure separator. Light gases were metered through a wet test meter. An X-Y recorder was used to record and measure the temperature of the catalyst bed during reaction. The feed was pure methanol (reagent grade). The liquid products were analyzed using an SP-2100 column while the gaseous products were analyzed using a Chrosorb-102 column. A flame ionization detector was used in both cases.

A dual-stage process (Figure 19) was also studied. The product from the first reactor was conducted to a gas-liquid separator where the light gases were separated from water and liquid product. The light gases were compressed with a Whitey compressor (Model No. 5KC49FG1101EX, 1/2 HP) to the inlet pressure of the second reactor where the light gases reacted to form aromatics over ZSM-5.

Chemical Supplies

A listing of the chemicals and materials used in this work is presented in Table 22.

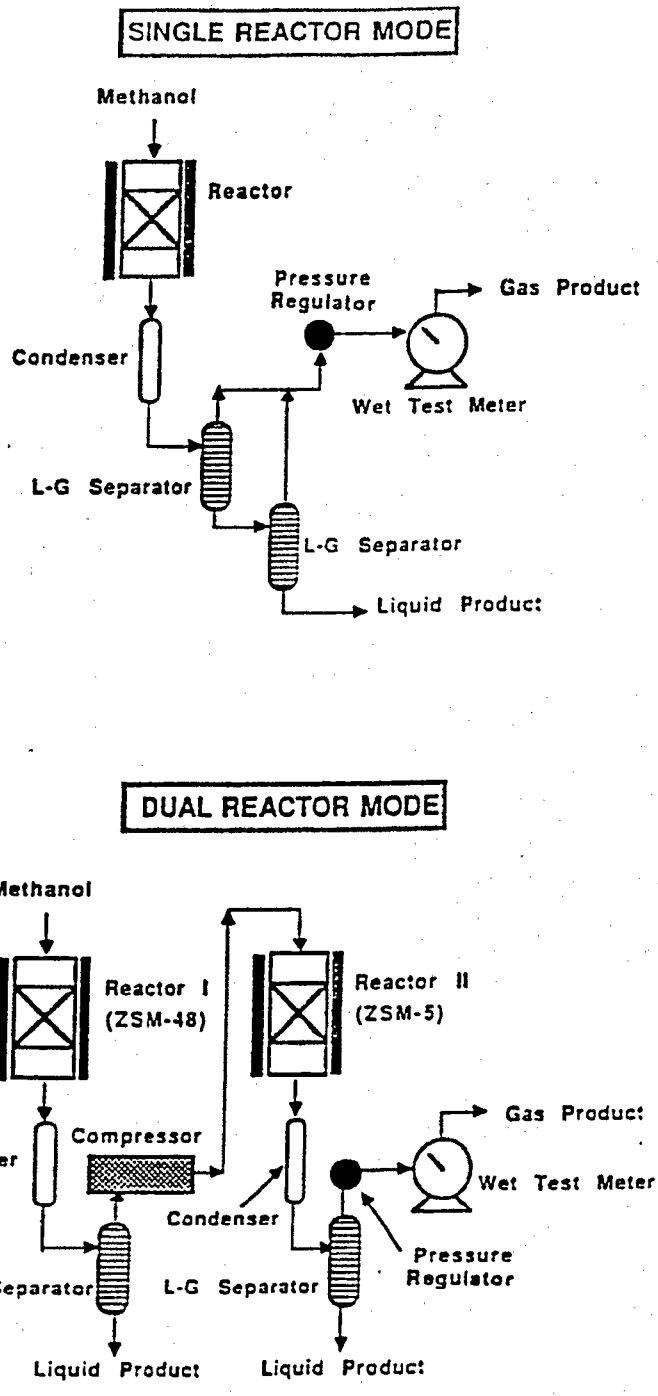

Figure 19. Reactor Systems for the Study of Methanol Conversion

Table 22

Chemicals Used in Catalyst Preparation

Chemical	Application	Purity	Source
Tetrapropylammonium Hydroxide	ZSM-5 prep.	1 M	Aldrich
Tetrapropylammonium Bromide	ZSM-5 prep.	98%	Aldrich
Sodium Aluminate	ZSM-5/48 prep.	pure	Amend
Aluminum Sulfate	ZSM-5 prep.	BG	Baker
Aerosil 200	ZSM-5/48 prep.	-	Degussa
Silica	ZSM-5/48 prep.	G-12	Aldrich
Sodium Bromide	ZSM-48 prep.	GR	EM Sci.
Sodium Hydroxide	ZSM-5 prep.	BG	Baker
Indium Nitrate	ZSM-5/48	99.999%	Aldrich
1,6-Hexanediamine	ZSM-5/48	98%	Aldrich
1,8-Diaminooctane	ZSM-48	98%	Aldrich
1,12-Diaminododecane	ZSM-48	98%	Aldrich
Ammonium Nitrate	Ion exchange	ACS	Aldrich
n-Hexane	α-test	HPLC G.	Mallinckrodt
Isobutane	Isomerization	99.5%	Union Carbide
Ammonium Gas	TPD	5%	Liquid Air
Methanol	TD & Reactions	Spect. G.	Mallinckrodt
Ethanol	Reactions	Spect. G.	Aldrich
n-Propanol	Reactions	Analy. G.	Mallinckrodt
i-Propanol	TGA/TPD	Spect. G.	Fisher
n-Butanol	Reactions	Analy. G.	Baker

Section IV: SELECTIVE SYNTHESIS OF AROMATIC HYDROCARBONS OVER ZEOLITE CATALYSTS

Research Personnel: Hong Paul Wang
Graduate Student

Francis V. Hanson
Associate Professor

Laboratory Preparation of ZSM-5 and ZSM-48 Zeolites

Synthesis of ZSM-5

ZSM-5-type zeolites were synthesized hydrothermally in this investigation. The crystallization of zeolites from hydrogels includes nucleation and crystallization (crystal growth) processes. The nucleation process is defined to be the formation of the initial crystalline phase. Virtually no information can be found regarding the detailed mechanism of formation of the ultrafine particles (diameters approx. 1-10 nm) in the nucleation process. Thus crystal growth is defined as the process that takes place after 50 percent conversion of the original solution to crystalline material.

The composition of zeolite ZSM-5b in terms of mole oxide ratios of components was $6TPA\text{-}2Na_2O\text{-}Al_2O_3\text{-}21SiO_2\text{-}460H_2O$. The source of silica was Aerosil (Degussa). The crystal formed after 6 days at a temperature of 423 K and an autogenous pressure of 13 atm was examined using the X-ray diffraction method. The crystalline material was identified as ZSM-5. A comparison of the X-ray diffraction pattern of ZSM-5b to that of Mobil ZSM-5 (ZSM-5M) and amorphous SiO_2 is presented in Figure 20. The patterns indicate that the ZSM-5b synthesized at typical reaction conditions has a crystalline structure similar to ZSM-5M.

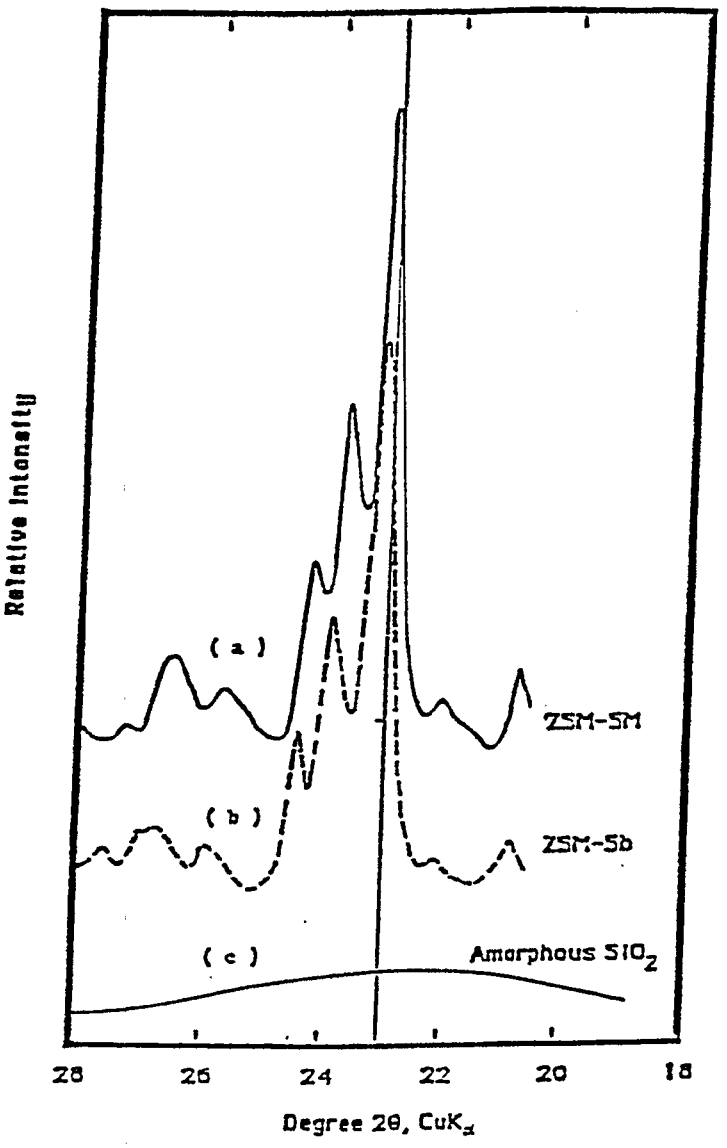

Figure 20. X-ray Diffraction Patterns for ZSM-5
(a) Mobil Standard ZSM-5
(b) Synthesized ZSM-5
(c) Amorphous SiO_2

The elimination of the organic cations such as tetrapropyl ammonium (TPA) ion from ZSM-5 was studied by differential scanning calorimetry (DSC). The DSC pattern obtained in air with the sodium form of ZSM-5b is presented in Figure 21. The broad exotherm between 630 and 820 K in the DSC profile is believed to be associated with the decomposition of the TPA ions. The profile indicates that the minimum temperature necessary to insure complete removal of the TPA ions was around 820 K. Thus it was concluded that the ZSM-5 synthesized in the presence of TPA ions can be activated by calcination at a temperature of 823 K. After calcination at 823 K for 16 hours, the synthetic ZSM-5 was a white crystal.

The influence of synthesis reaction variables on the synthesis of ZSM-5 was also investigated. The X-ray diffraction pattern of the Mobil ZSM-5 sample was used as the standard for characterizing the ZSM-5 zeolites prepared in this investigation. The degree of crystallization (crystallinity) was estimated by comparing the area under the X-ray diffraction bands (2θ = 22 - 25°) to that of ZSM-5M. The ZSM-5M was taken as the standard and was assumed to exhibit 100 percent crystallinity. The crystallinity was calculated from the following relationship:

$$\text{Crystallinity}(\%) = \frac{\text{peak area } (2\theta = 22\text{-}25) \text{ of ZSM-5}}{\text{peak area } (2\theta = 22\text{-}25) \text{ of ZSM-5M}} \cdot 100 \qquad (4\text{-}1)$$

The crystallinities of the various ZSM-5 zeolites synthesized in this study are presented in Table 23. It should be noted that the crystallite sizes were about the same (crystallite sizes should be about the same for the two samples if the crystallinity equation is to be valid) for ZSM-5M and zeolites ZSM-5 synthesized by using TPA cations.

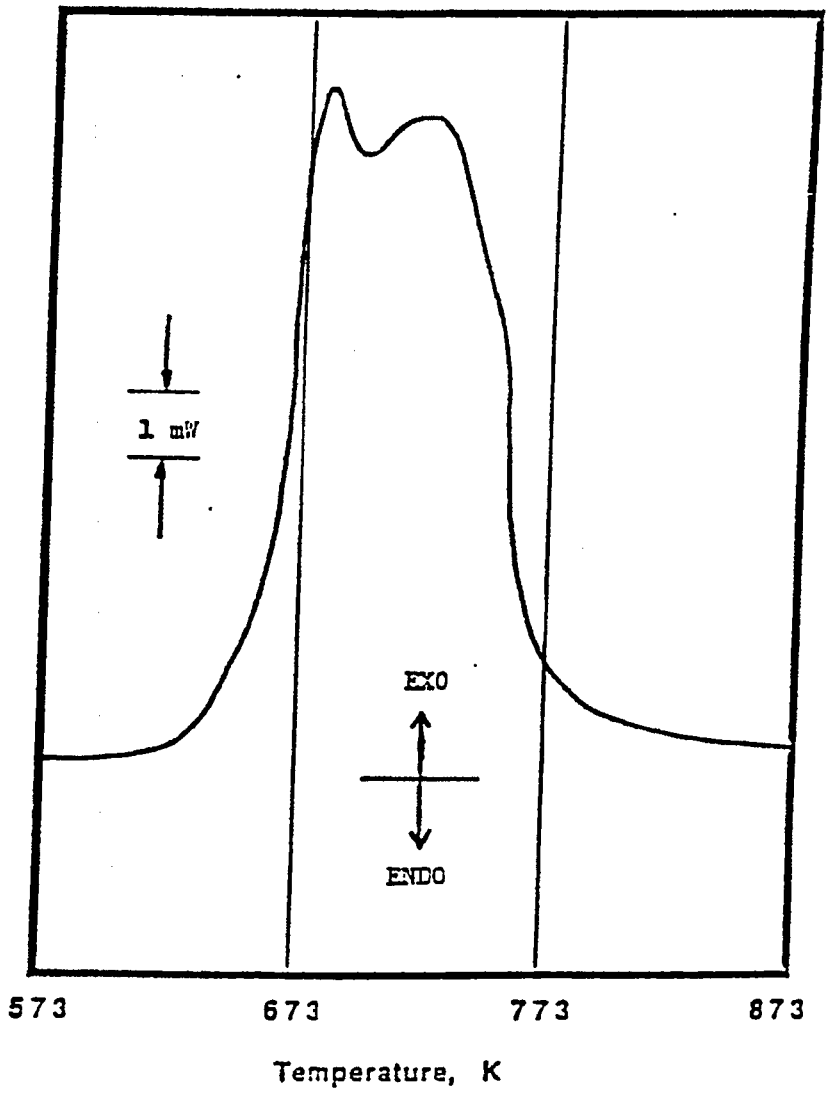

Figure 21. Differential Scanning Calorimetry Pattern for NaZSM-5.
Elimination of the Organic Cation (TPA)

Table 23

Degree of Crystallinity of Synthesized ZSM-5 Samples

Zeolite	Reaction Conditions			Cation[a]	Crystallinity[b]
	T (K)	P (atm)	Time (days)		%
ZSM-5M	-	-	-	-	100
ZSM-5a	425	11	6	TPAOH	86
ZSM-5b	425	11	10	TPAOH	91
ZSM-5c	453	1	6	TPAOH	70
ZSM-5d	453	13	6	TPAOH	99+
ZSM-5e	453	13	6	C6DN	95
ZSM-5D	453	13	6	C6DN	95
ZSM-5(70)	453	13	6	TPABr	99+

a Cation Identities

TPAOH	Tetrapropylammonium hydroxide
C6DN	1,6-hexane-diamine
TPABr	Tetrapropylammonium Bromide

The composition of synthetic ZSM-5

ZSM-5 a-d	$6TPA\text{-}2Na_2O\text{-}Al_2O_3\text{-}2lSiO_2\text{-}46OH_2O$
ZSM-5 e	$6C6DN\text{-}2Na_2O\text{-}Al_2O_3\text{-}2lSiO_2\text{-}46OH_2O$
ZSM-5D	$70C6DN\text{-}ONa_2O\text{-}Al_2O_3\text{-}70SiO_2\text{-}280OH_2O$
ZSM-5(70)	$18TPA\text{-}6Na_2O\text{-}Al_2O_3\text{-}70SiO_2\text{-}1400H_2O$

b Crystallinity computed from the following equation:

$$\text{Crystallinity (\%)} = \frac{\text{peak area } (2\iota=22\text{-}25) \text{ of ZSM-5}}{\text{peak area } (2\theta=22\text{-}25) \text{ of ZSM-5M}} \cdot 100 \qquad (3)$$

The autogenous pressure, due to the evaporation of the mother liquor that built during the synthesis of ZSM-5c at 453 K, was repeatedly released until atmospheric pressure was attained (> 6 days). The ZSM-5 sample produced in this experiment had a crystallinity of 70 percent. Rollmann[96] indicated that the initial mole ratio of water-to-silica in the reaction mixture strongly influences the mechanism and rate of crystallization of ZSM-5. It is presumed that the nucleation process was nearly complete during the early stages of the synthesis of ZSM-5c. The subsequent crystallization process may have been retarded due to the lack of hydrolysis in the reaction mixture thus preventing the formation of the ordered, three-dimensional network of ZSM-5.

Digestion time and digestion temperature also influence the structure of the synthesized zeolite. Highly crystalline ZSM-5 was obtained at reaction temperatures of 453 K. Low crystallization temperatures, e.g., 425 K and below, do not favor the formation of high crystallinity ZSM-5. Furthermore, if ZSM-5 remains in prolonged contact with the mother liquor at 425 K, a higher crystallinity ZSM-5 can be obtained in 4 days (Table 23).

It is believed that the organic content of {Na,TPA}ZSM-5 corresponds to one TPA ion per channel intersection and represents the maximum amount of the ion that can be encapsulated in the ZSM-5 structure. 1,6-Hexane-diamine (C6DN) is smaller and less hydrophobic than TPA. It seems likely that the packing of the C6DN in the ZSM-5 framework is not as highly ordered as that of the TPA ion. The accommodation of the cations in the structure provides little indication of the mechanism by which the organic host species influence the final structure of the zeolite, since both organic cations gave crystalline ZSM-5 (Table 23). However, it is well-known that the TPA ion causes the formation of ZSM-5 with a wide range of reaction mixture compositions and this may indicate that TPA ion is a strong structure directing species. It should be noted that the crystallization of ZSM-5 is determined by factors other than the availability of

a suitable template cation. C6DN seems to have the ability to promote the crystallization of ZSM-5 in the absence of sodium ions. A comparison of the scanning electron microscope (SEM) images of ZSM-5 synthesized in the presence of C6DN and TPABr is presented in Figure 22. The images indicate that the crystallite size (~4 μm) of ZSM-5 synthesized with C6DN was larger than that (~1 μm) of ZSM-5 synthesized with TPABr since C6DN was found to promote the crystallization of ZSM-5. However, it is not as effective as the TPA ion (crystallinity = 95 percent for ZSM-5D), and it may not be a true template species for ZSM-5.

Scanning electron microscope (SEM) micrographs indicated the growth of larger crystals (cubical aggregates in shape and 0.5 - 2 μm in size) of ZSM-5 when using a synthesis mixture with a lower aluminum content, as shown in Figure 23. Generally, zeolite crystallization is a nucleation-controlled process occurring in molecularly inhomogeneous, alkaline, aqueous gels. Thus an increase in crystallization rate is expected as the silica-to-alumina ratio is increased due to the fact that the ZSM-5 nuclei is ready to be formed in the high silica content mixture.

Synthesis of ZSM-48

A systematic study of the effects of the organic template and the composition of the reaction mixture on the synthesis of ZSM-48 was also conducted. The synthesis of high-silica ZSM-48 from a reaction mixture in which the only organic ion was C6DN was investigated. The reaction mixture containing C6DN and sodium has shown that the most readily obtained product is ZSM-5 at a low initial molar ratio (IMR) of SiO_2/Al_2O_3, although at 453 K when the aluminum content of the reaction mixture was very low (i.e., SiO_2/Al_2O_3 > 200) zeolite ZSM-48 crystals were

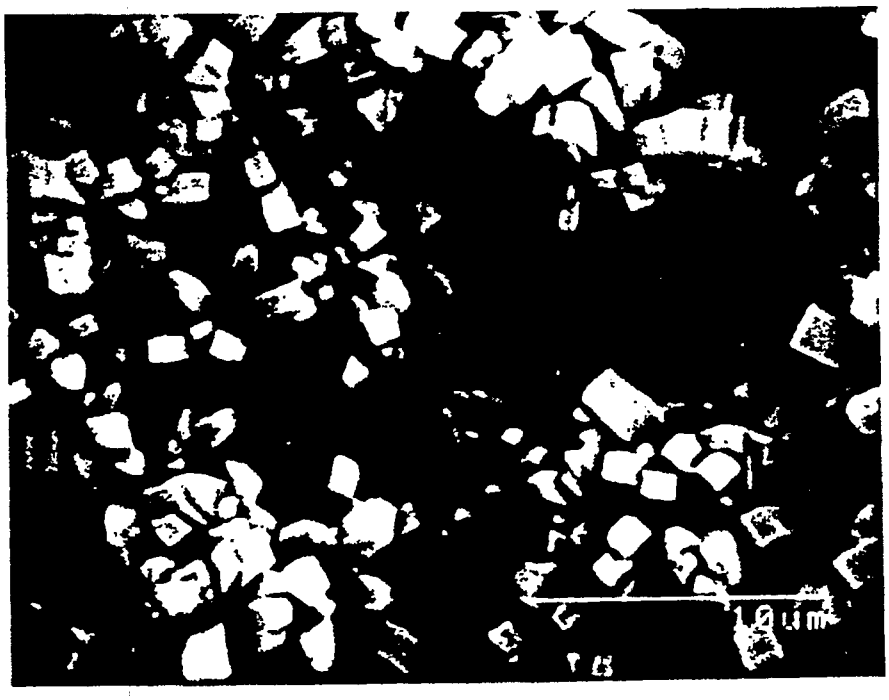

(a) C6DN

(b) TPABr and Exchanged with NH_4NO_3

Figure 22. Scanning Electron Microscope Images of HZSM-5. Effect of Organic Cations on Synthesis

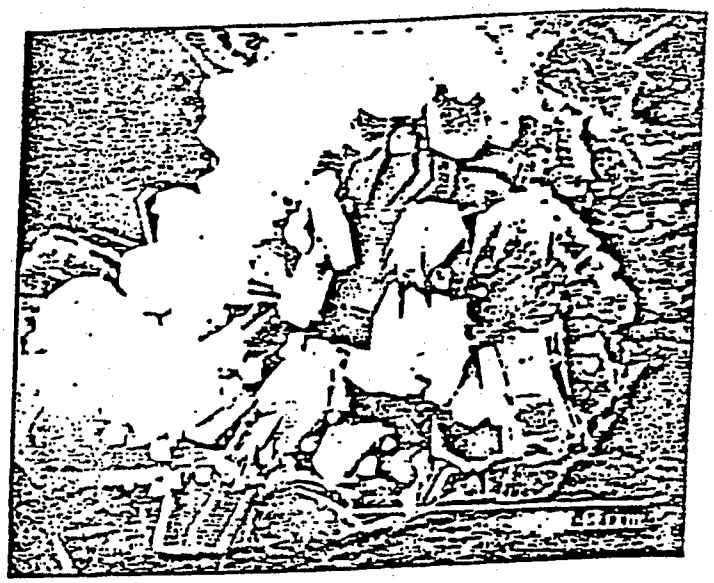

(a) SiO_2/Al_2O_3 = 105

(b) SiO_2/Al_2O_3 = 35

Figure 23. Scanning Electron Microscope Images of HZSM-5. Effect of SiO_2/Al_2O_3 Ratio.

formed. The reasons for the transition from pure ZSM-5 to a mixture of ZSM-5 and ZSM-48 to pure ZSM-48 are not understood at present. However, it should be noted that ZSM-48 was initially discovered as an impurity in crystalline ZSM-39.[49]

A comparison of the X-ray diffraction patterns for ZSM-5 with that for ZSM-48 formed using the same organic cation (i.e., C_6DN) are presented in Figure 24. The most intense peaks for the two samples are different. The positions of the two peaks were $2\theta = 23.8$ and $2\theta = 21.2$ for ZSM-5 and ZSM-48, respectively. This difference makes it possible to distinguish between ZSM-5 and ZSM-48.

The effect of the silica-to-alumina ratio on the synthesis of ZSM-48 is shown in Figure 25. It indicates that pure ZSM-48 could be obtained in this investigation only at initial molar SiO_2/Al_2O_3 ratios greater than 200. At an initial molar SiO_2/Al_2O_3 ratios between 25 and 200, a mixture of ZSM-5 and ZSM-48 was produced. The SEM image of ZSM-48/5(70), which is a mixture of ZSM-48 and ZSM-5, is shown in Figure 26. Interpretation of micrograph indicates that the ZSM-5 and ZSM-48 may not be an intergrowth crystal but rather are a physical mixture of the two zeolites.

Different organic cations were also used for the synthesis of ZSM-48. The X-ray diffraction patterns of ZSM-48 zeolites obtained from two different bases, namely, C_6DN (1,6-hexanediamine) and C_8DN (octane 1,8-diamine) are presented in Figure 27. The two samples exhibit almost identical X-ray diffraction patterns. The relative intensities of X-ray diffraction peaks and the diffraction angles of the ZSM-48 synthesized in this investigation are compared with X-ray diffraction patterns for the standard ZSM-48 (data available in reference [72]) which is presented in the insert of Figure 27. The organic cation, C12DN, used in the synthesis of ZSM-48 was not

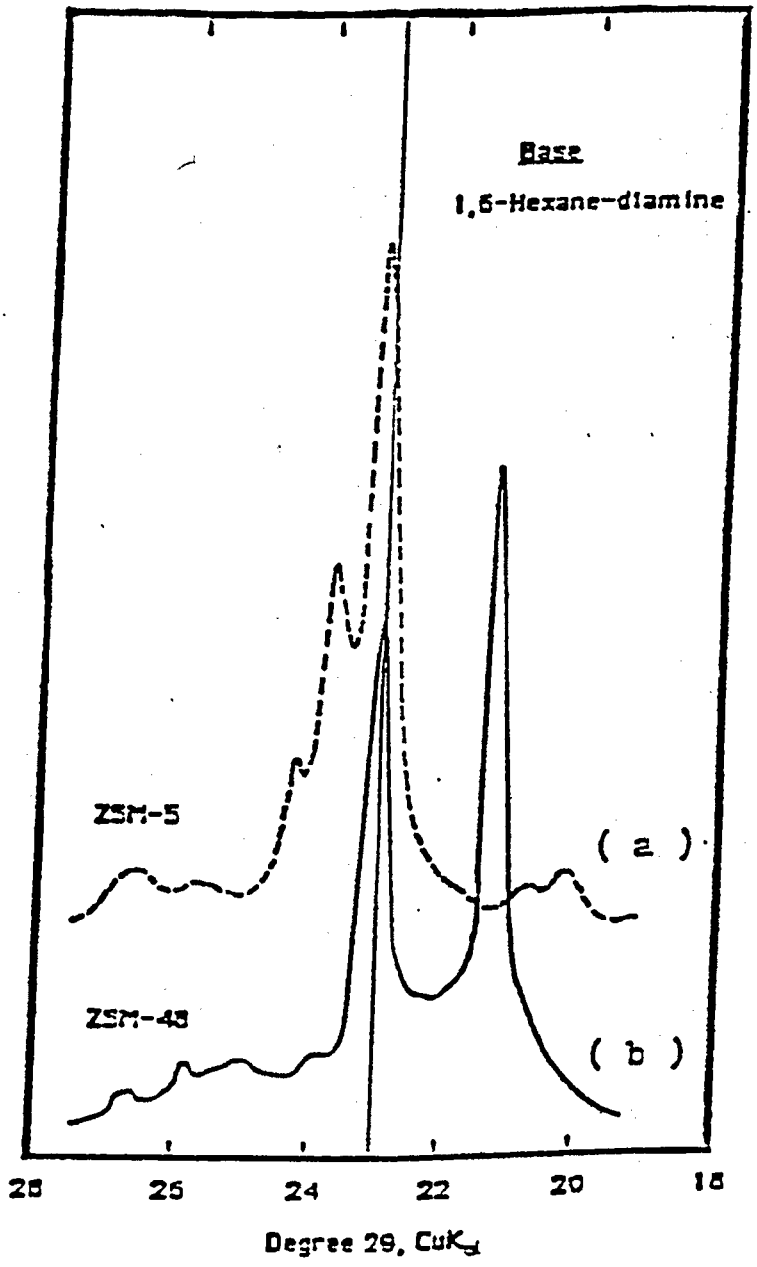

Figure 24. Comparison of the X-ray Diffraction Patterns for ZSM-5 and ZSM-48

(a) ZSM-5 (b) ZSM-48

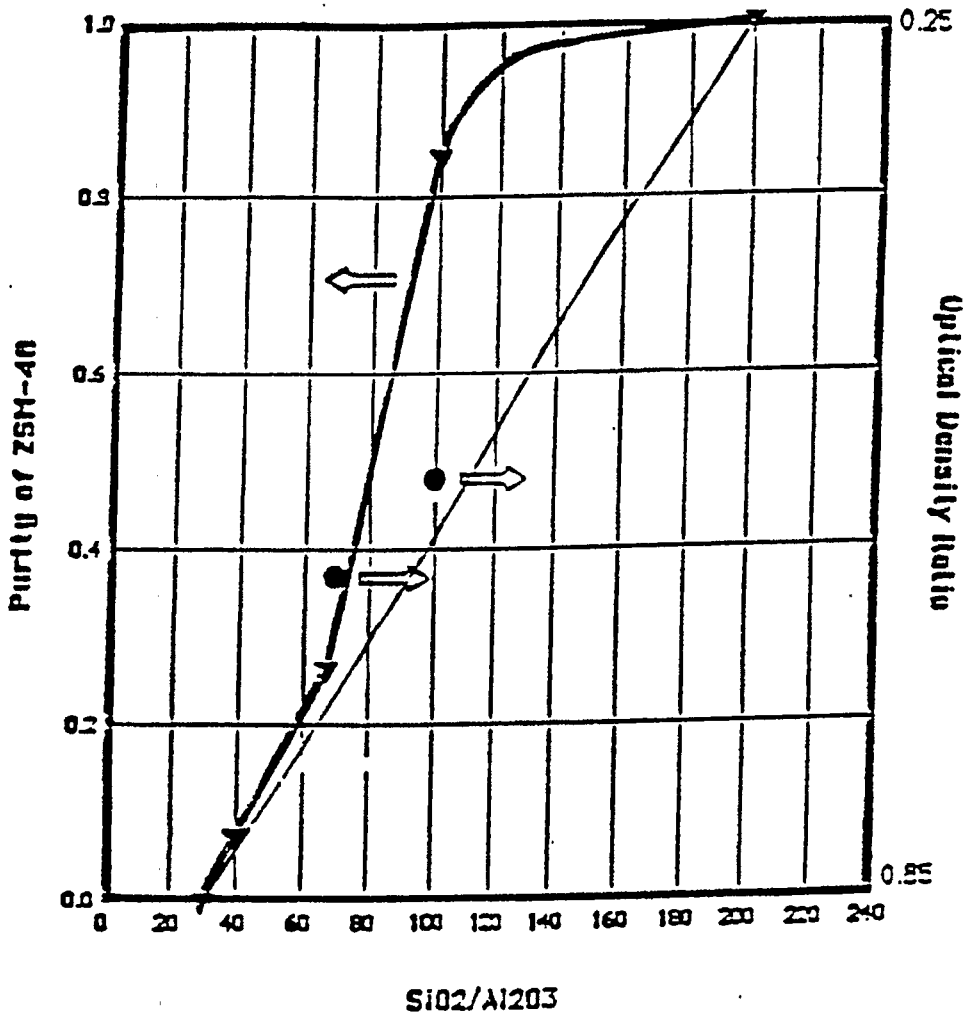

Figure 25. Effect of SiO_2/Al_2O_3 Ratio on the Synthesis of ZSM-48.

▲ denote X-ray diffraction crystallinity of zeolites.
● denotes optical density ratio of zeolites.

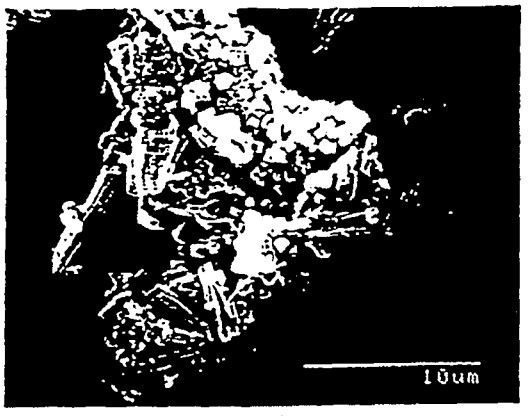

(a) SEM of HZSM-48/5 (70)

(b) SEM of ZSM-5

(a) SEM of ZSM-48

Figure 26. Scanning Electron Microscope Images of ZSM-48/5(70) ZSM-48 and ZSM-5

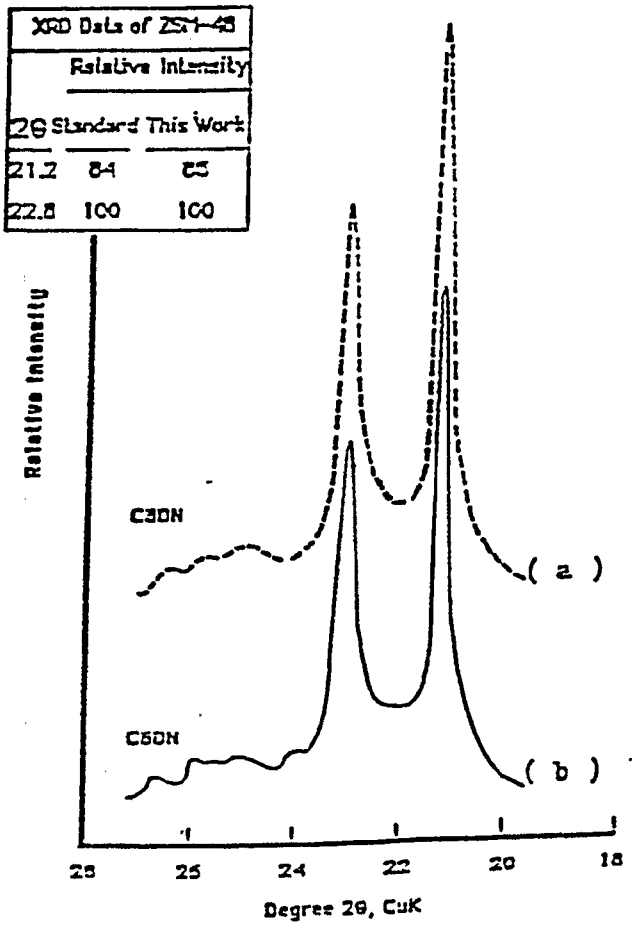

Figure 27. X-ray Diffraction Patterns for ZSM-48 Prepared with Different Organic Templates

(a) C8DN; (b) C6DN

as effective as C6DN or C8DN for synthesis of ZSM-48. It seems likely that the nature of synthesis of ZSM-48 is determined by channel filling by the organic cation at the nucleation stage.

The removal of C6DN and C8DN from the synthesized ZSM-48 was studied by DSC. The DSC patterns for the catalysts prepared with the C6DN and C8DN bases are presented in Figures 28 and 29, respectively. Neither of the organic cations could be completely removed at 873 K. The organic amines in ZSM-48 were eliminated by calcining the samples at 1023 K for 16 hours. White crystal ZSM-48 zeolites were obtained. The effect of calcination temperature on the thermal stability of ZSM-48 is presented in Figure 30. It is clear that the ZSM-48 is a thermally stable zeolite (up to 1323 K).

The organic cations present in a reaction mixture are often the major factor in determining which zeolite structure is obtained. The effect of the C6DN/SiO_2 ratio on the synthesis of ZSM-48 was investigated using X-ray diffraction. The X-ray patterns are presented in Figure 31. At an initial molar C6DN/SiO_2 ratio of 0.1, ZSM-48 could not be produced and the solid appeared to be X-ray amorphous. The ability of the organic ion, C6DN, to alter the course of the nucleation process is apparent. In addition, the effect of the initial molar Na/SiO_2 ratio on the synthesis of ZSM-48, shown in Figure 32, is of interest as a structure-directing function. A structure-unknown crystallite, namely ZSM-48X, was obtained at Na/SiO_2 = 0.45. However, it is very likely that ZSM-48 is one of the components in the ZSM-48X crystallite since all diffraction peaks appearing in the X-ray diffractogram of ZSM-48 are also present in the diffractogram of ZSM-48X.

The cation is said to have a structure-directing function and influences the structure of the zeolite that forms. In early work using alkali and alkaline earth cations, it was suggested that

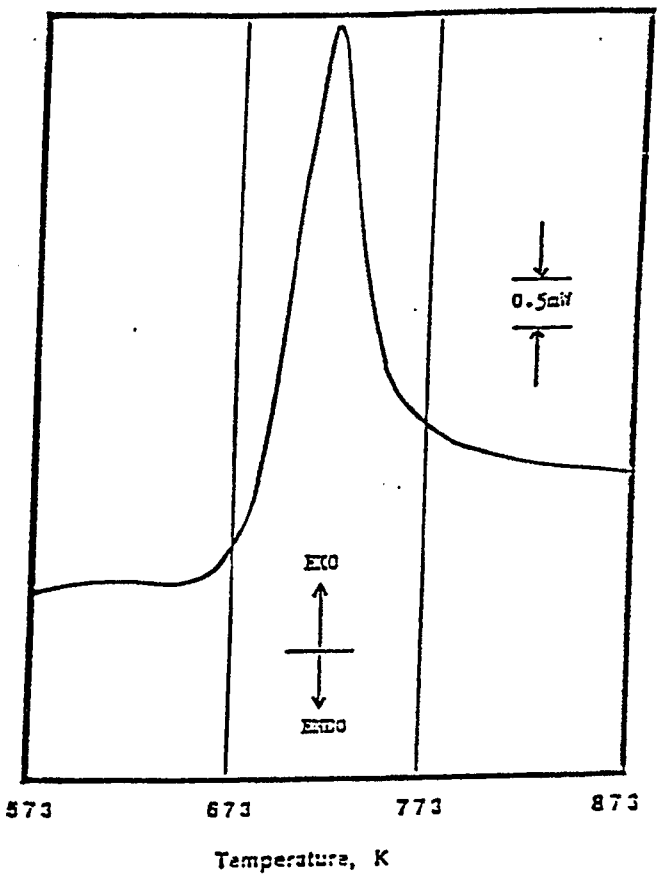

Figure 28. Differential Scanning Calorimetry (DSC) of NaZSM-48.
Elimination of the Organic Cation (C6DN) from Synthesized NaZSM-48

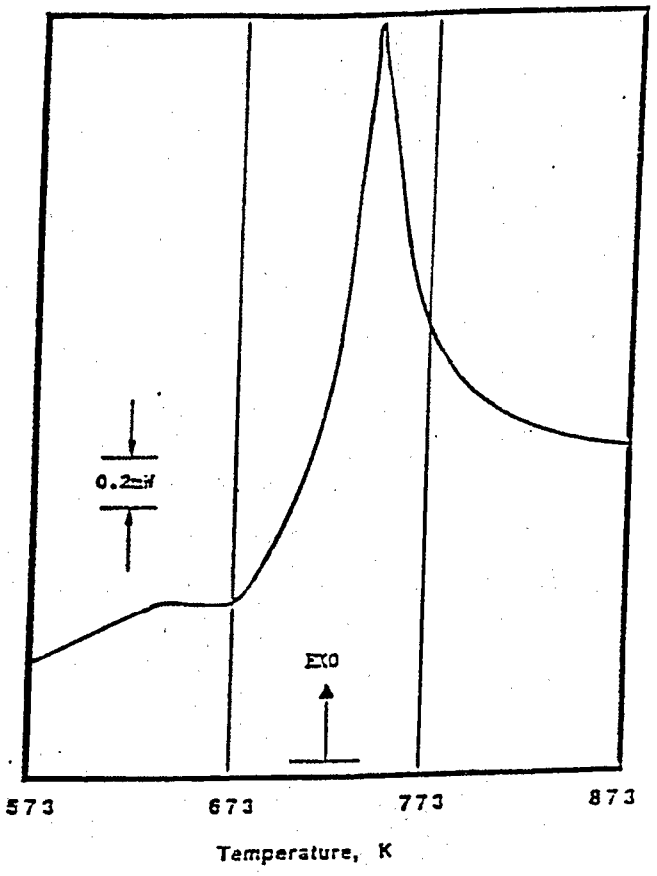

Figure 29. Differential Scanning Calorimetry Pattern for NaZSM-48. Elimination of the Organic Cation (C8DN) from Synthesized NaZSM-48

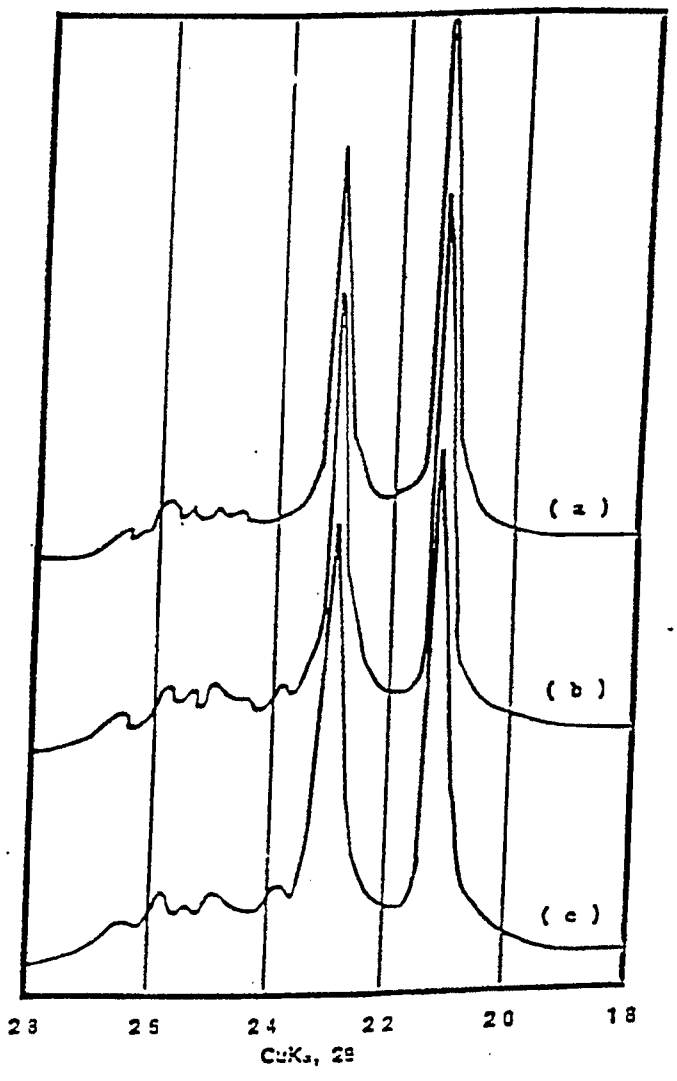

Figure 30. X-ray Diffraction Patterns for NaZSM-48(200). Effect of Calcination Temperature

(a) Calcination Temperature = 1323 K
(b) Calcination Temperature = 1023 K
(c) Calcination Temperature = 823 K

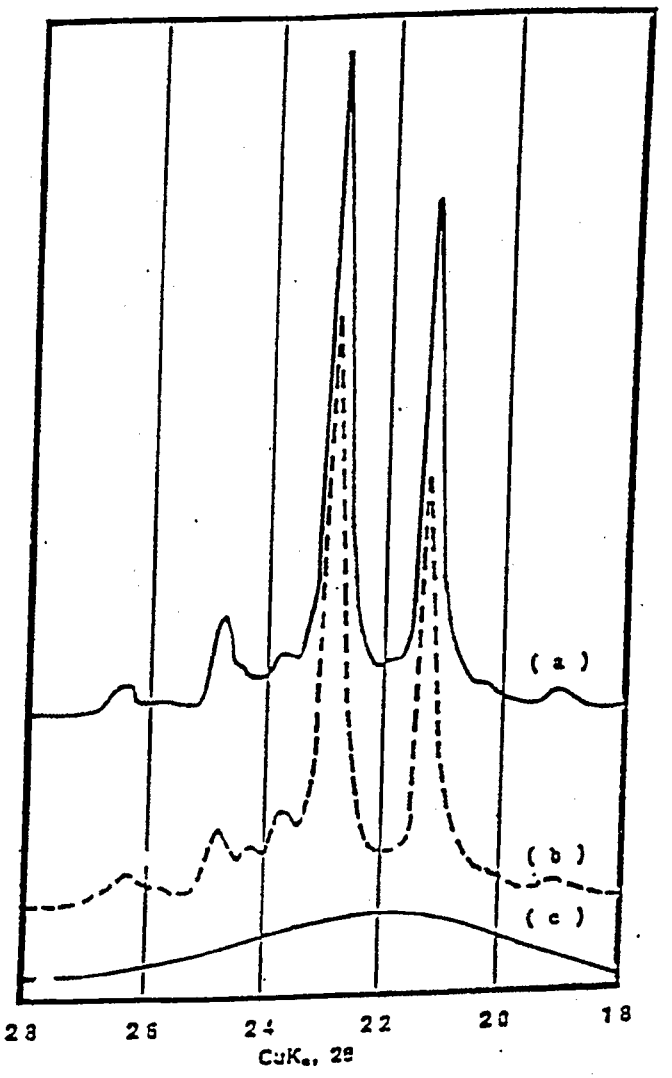

Figure 31. X-ray Diffraction Patterns. Effect of C6DN/SiO_2 on the Synthesis of ZSM-48.

(a) C6DN/SiO_2 = 0.3
(b) C6DN/SiO_2 = 0.2
(c) C6DN/SiO_2 = 0.1

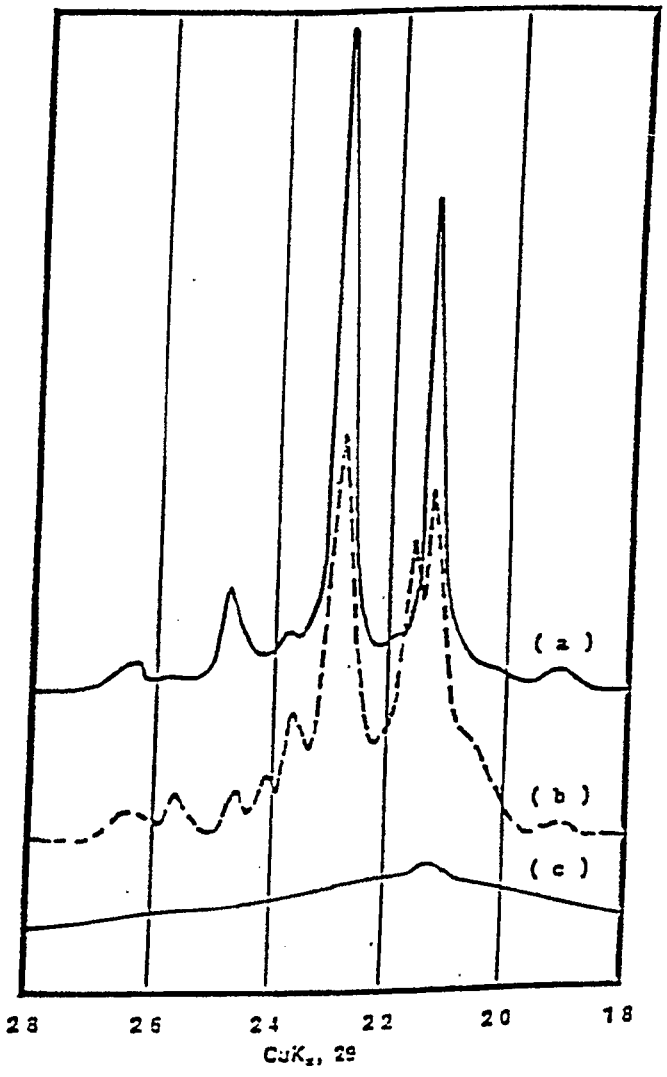

Figure 32. X-ray Diffraction Patterns. Effect of Na/SiO_2 Ratio on the Synthesis of ZSM-48.

(a) Na/SiO_2 = 0.59
(b) Na/SiO_2 = 0.45
(c) Na/SiO_2 = 0.30

the hydrated cation forms the nucleus of certain secondary building units.[20] For example, the dehydrated sodium ion influences the formation of a double four ring (D4R) or double six ring (D6R) and the hydrated sodium cation causes the formation of sodalite units. However, the relationship between the cation influence on the structure and the cation influence on gel chemistry is not well-understood. The major complication associated with the use of the cation in the synthesis of ZSM-48 may be that its incorporation results in a specific chemical environment could also affect the nucleation process, and hence the formation, of a particular zeolite, e.g., ZSM-48X.

The initial precipitation of gel and its subsequent conversion to a zeolite may be considered to be an example of Ostwald's rule of successive transformation.[230] According to this rule, the first phase to appear is always thermodynamically less stable than the phase that subsequently replaces it. The first crystals of ZSM-48X to nucleate and grow from the gel having an initial molar Na/SiO_2 ratio equal to 0.45 could not be replaced in the aqueous reaction mixture by another crystalline species such as zeolite ZSM-48. Since the sequence always occurs in the direction of increasing thermodynamic stability, replacement reactions that lead to the less stable zeolite ZSM-48X become possible when it is calcined at high temperatures. The effect of ZSM-48X calcination temperature on the phase transformation is shown in Figure 33. The formation of a thermally stable crystalline species (see Figure 33a) was observed at a calcination temperature of 1323 K. It should be noted that the pure ZSM-48, i.e., ZSM-48(200), was not involved in the phase transformation or structural change at 1323 K (shown in Figure 30a). The SEM images of synthetic ZSM-48X are presented in Figure 34. It should be noted that the topographies of the ZSM-48X calcined at 1323 or 823 K did not change significantly. This may result from a rearrangement of the framework of ZSM-48X (or phase transformation) at high temperatures,

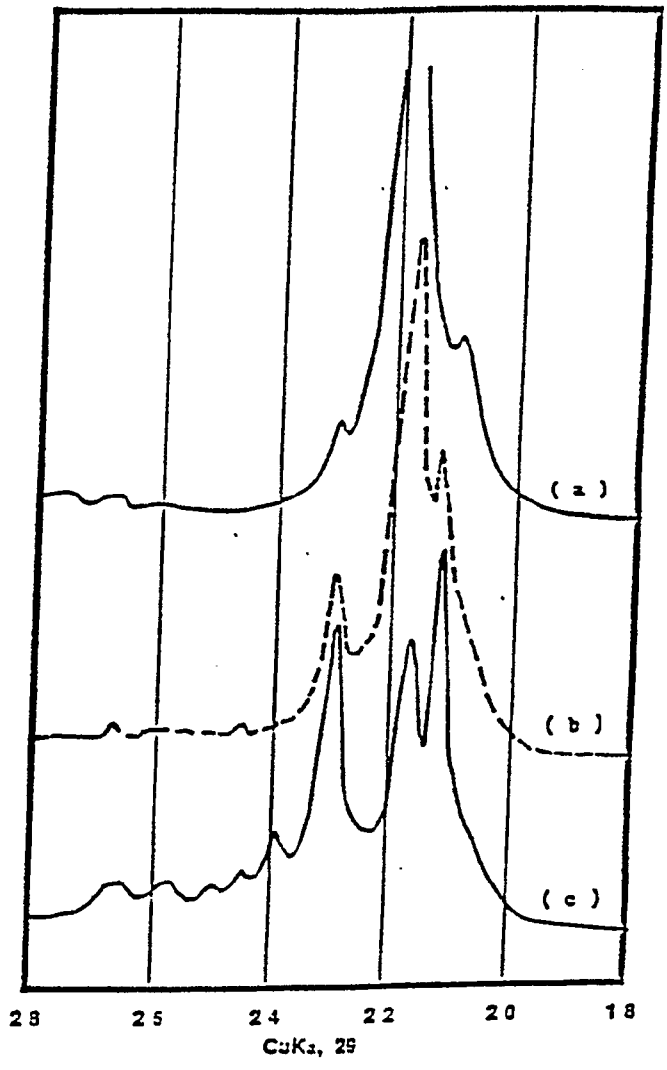

Figure 33. X-ray Diffraction Patterns of NaZSM-48X. Effect of Calcination Temperature on Phase Transformation.

(a) Calcination Temperature = 1323 K
(b) Calcination Temperature = 1023 K
(c) Calcination Temperature = 823 K

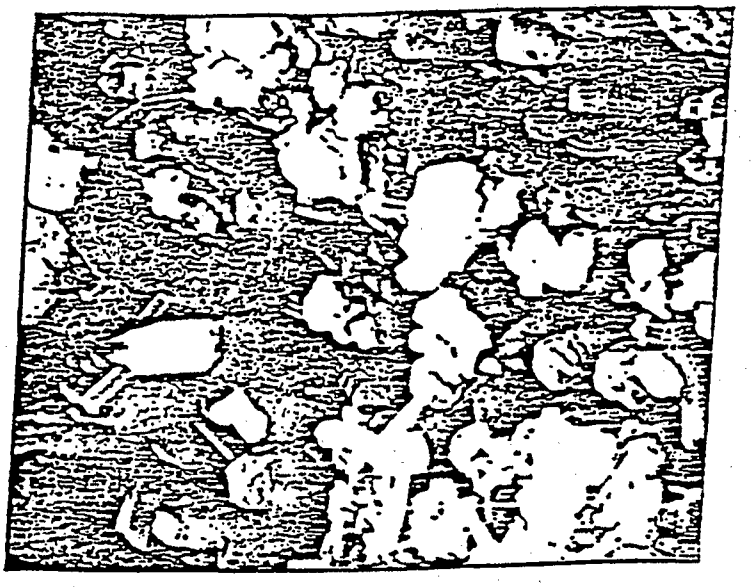

(a) Calcined at T = 823 K in air for 16 hours

(b) Calcined at T = 1323 K in air for 16 hours

Figure 34. Scanning Electron Microscope Images of NaZSM-48X. Effect of Calcination Temperature

which may not be distinguished from their topographies directly. A ZSM-48X-type crystalline material was also obtained from a similar reaction mixture at a crystallization temperature of 503 K. The comparison of the X-ray diffraction patterns for the ZSM-48X at zeolite crystallization temperatures of 503 and 453 K is presented in Figure 35. It appears that in the reaction sequence

$$\text{amorphous } SiO_2 \rightarrow \text{ZSM-48X} \rightarrow Z \qquad (4\text{-}2)$$

the system prefers to descend the ladder of relative thermodynamic stabilities in a series of steps rather than in a single step. The symbol Z represents a crystalline material of unknown structure. On the other hand, the necessity of the right gel chemistry in the formation of the zeolite ZSM-48, and the influence of the gel chemistry on the final crystalline material, can not be underemphasized. The structure-directing role of the alkali metal cations in the synthesis of ZSM-48 must also be considered. The crystalline material ZSM-48X was not evaluated catalytically.

The various methods for preparing ZSM-48 result in final products containing substantial amounts of sodium ion. The sodium form was ammonium exchanged to give the hydrogen-form of ZSM-48. A comparison of the SEM images of the hydrogen and sodium forms of ZSM-48 is presented in Figure 36. It was observed that both forms of the ZSM-48 have a similar morphology. The ZSM-48 crystalline material consisted of rod-like crystals with 0.2 - 0.4 μm in width and three-to-five μm in length.

Chemical Composition

The chemical compositions of the zeolites prepared in this study were measured by the electron microprobe analysis (Table 24). In most of the samples, the molar SiO_2/Al_2O_3 ratios of

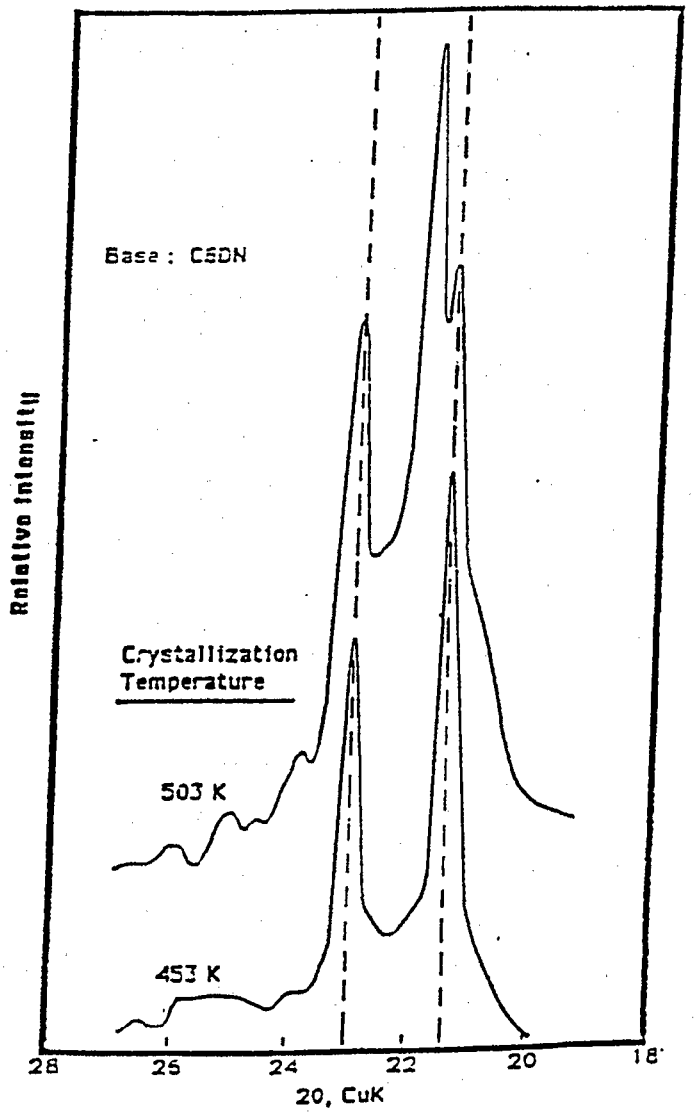

Figure 35. Effect of Crystallization Temperature on the Synthesis of ZSM-48

Sodium-form

Hydrogen-form

Figure 36. Scanning Electron Microscope Image of ZSM-48(200).

Table 24

Chemical Composition of Synthesized Zeolites

Zeolite	IMR SiO_2/Al_2O_3	FMR SiO_2/Al_2O_3
ZSM-5M	N/A	70
ZSM-5D	70	76
ZSM-5(35)	35	40
ZSM-5(70)	70	74
ZSM-5(105)	105	123
ZSM-48(200)	200	239
ZSM-48(100)	100	104
ZSM-48(70)	70	76
ZSM-48(40)	40	49

Note:

IMR: Initial Molar Ratio

FMR: Final Molar Ratio Measured by Electron Microprobe

the crystalline products were higher than the molar SiO_2/Al_2O_3 ratios of the parent hydrous gels. Considering the fact that the difference of the SiO_2/Al_2O_3 molar ratio between reaction mixture and product is great in these high-silica zeolites, it is presumed that generation of silicon-rich nuclei would be favored during crystallization and that the presence of aluminum in the reaction mixture is not always necessary.

Summary

1. The H-form ZSM-5 can be synthesized directly by the use of diamines as the organic ions.
2. Silicon-rich nuclei of ZSM-5 formed during the initial nucleation process.
3. No direct evidence was obtained to indicate that organic ions function as templates for the synthesis of ZSM-5 or ZSM-48.
4. Zeolite ZSM-48 could only be synthesized at $SiO_2/Al_2O_3 > 200$ at typical reaction conditions in this investigation.
5. A nonintergrowth mixture of ZSM-5 and ZSM-48 formed at $SiO_2/Al_2O_3 = 70$.
6. It is possible that the structure of ZSM-48 was directed highly by sodium ions during the crystallization of the sample.

Characterization of Synthesized Zeolites

Thermal Desorption

Temperature-programmed desorption was used to investigate the acidity of the zeolites prepared in this investigation. The zeolite samples were reacted with ammonia by exposure to ammonia for at least 30 minutes at room temperature. It is believed that the strong acid sites are completely saturated with ammonia since one can determine the excess weakly adsorbed ammonia on the high-silica zeolite surfaces. The excess physisorbed or weakly bonded ammonia

was removed by purging the catalyst with helium. The samples were then heated at a linear rate of (5 K/min) in flowing helium and the amount of ammonia desorbed was continuously monitored with a thermal conductivity detector.

The temperature-programmed desorption (TPD) profiles for ammonia desorption from fresh HZSM-5 (IMR SiO_2/Al_2O_3 = 70) and spent HZSM-5 (following the methanol conversion reaction) are presented in Figures 37 and 38, respectively. At least four discrete features at 410, 480, 700, and 830-860 K were observed corresponding to adsorption on Site I, Site II, Site III, and Site IV, respectively. Since the interactions between ammonia and Sites I and II are weak for both of fresh and spent ZSM-5, they are attributed to physisorbed ammonia on ZSM-5 surfaces. The uptakes of ammonia for the fresh ZSM-5 at Site III and Site IV are greater than that for the spent ZSM-5. This indicates that these two sites may be related to the catalytically active centers in ZSM-5 since they have been partially deactivated in the methanol conversion. It is believed that site III and site IV are the Brönsted acid sites and Lewis acid sites, respectively.[119]

The TPD profile for ammonia desorption from ZSM-48 is presented in Figure 39. The broadening of the desorption band in the temperature range assigned to Type III sites for ZSM-48 may be due to the influence of the channel system of ZSM-48 which could also play a role in molecular traffic control with desorbed ammonia. Furthermore, the differences in the ammonia desorption profiles in the temperature range from 300 to 550 K for ZSM-5 (Figure 37) and ZSM-48 (Figure 39) may also indicate a difference of channel structure for these two types of zeolites. It should be noted that ZSM-48 has an intermediate pore diameter and a two-dimensional non-intersecting channel system.[49]

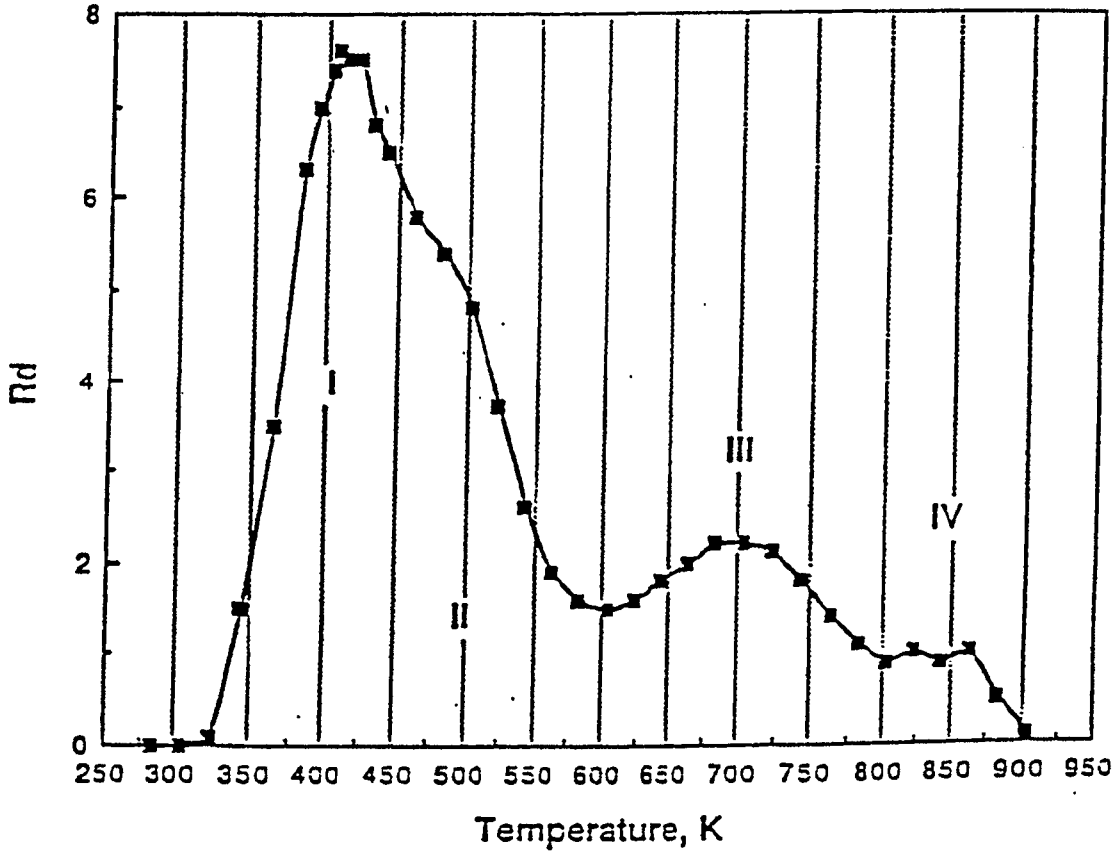

Figure 37. Temperature-Programmed Desorption Spectrum of Ammonia. Fresh ZSM-5 Catalyst

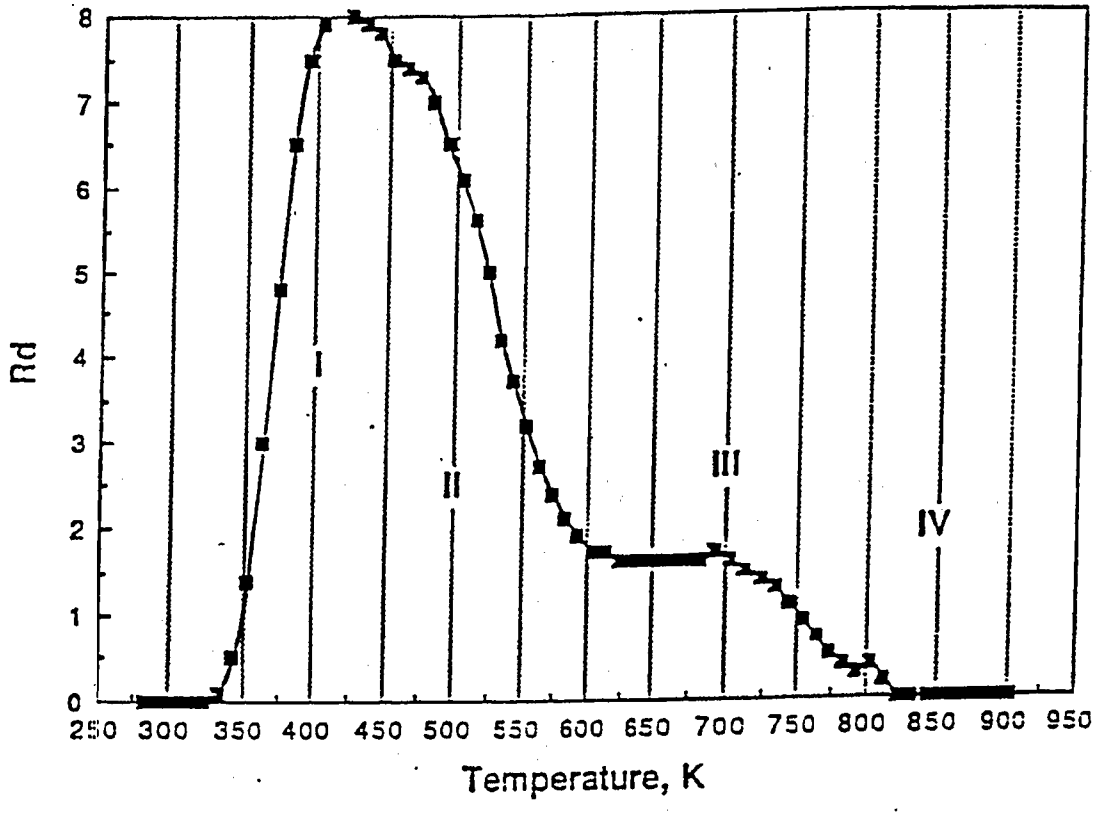

Figure 38. Temperature-Programmed Desorption Spectrum of Ammonia Spent ZSM-5 Catalyst

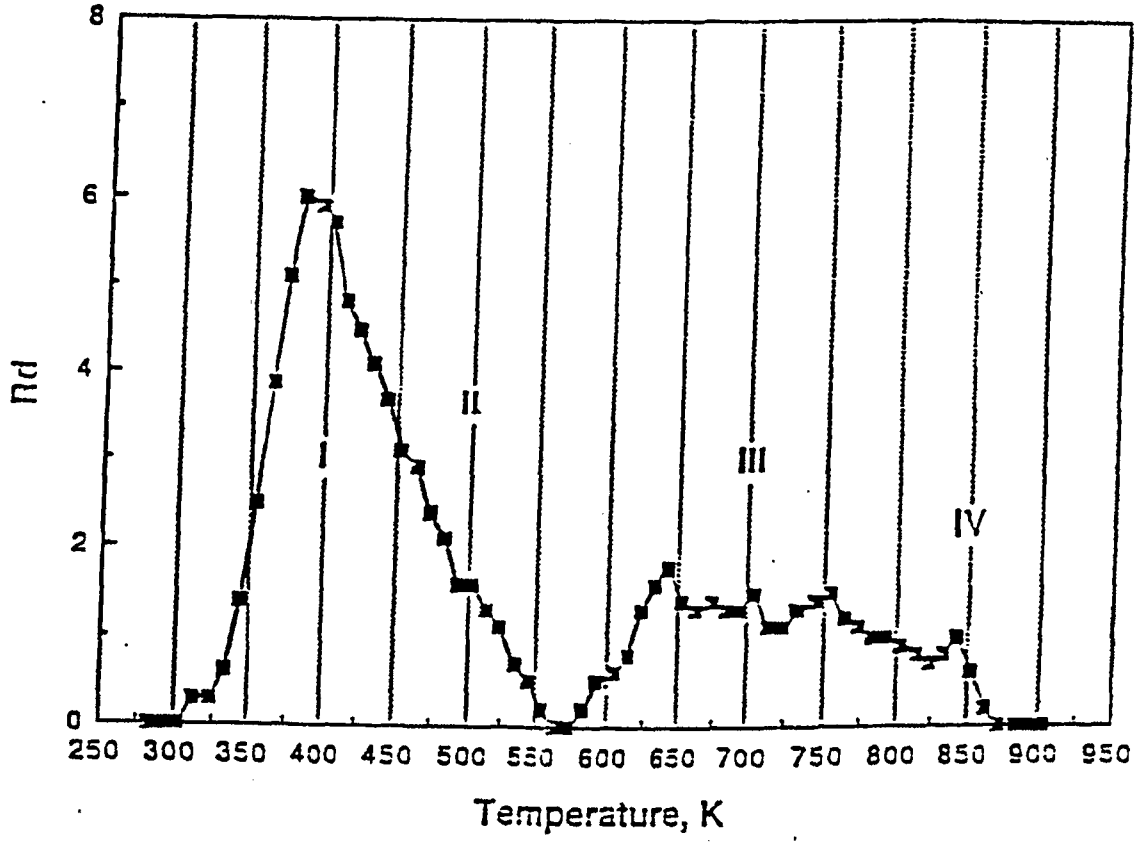

Figure 39. Temperature-Programmed Desorption Spectrum of Ammonia Zeolite ZSM-48/5(70)

The TPD profile for ammonia desorption from HZSM-48/5(70), which has been shown to be a physical mixture of ZSM-5 and ZSM-48, is presented in Figure 40. It is also consistent with the conclusions from the SEM study for zeolite ZSM-48/5(70) (Figure 26) indicating that the zeolite is not an intergrowth mixture of ZSM-5 and ZSM-48. Furthermore, it should be noted that the HZSM-48/5(70) consisted of at least 75 wt. percent of ZSM-5 and 25 wt. percent of ZSM-48 (see Figure 25).

Alcohol desorption from ZSM-5 was studied on a therm-gravimetric analyzer (TGA) equipped with a temperature-programmed controller. The thermal desorption profiles are presented in Figure 41. Physisorbed and chemisorbed methanol were desorbed from ZSM-5 surface in the temperature ranges 323 - 473 K and 473 - 523 K, respectively. Other higher alcohols (C_2 - C_4 normal-alcohols) produced corresponding alcohols, olefins, and oligomers via surface reactions when desorbed from ZSM-5. This indicates that the minimum temperature for the reaction of alcohols over ZSM-5 was around 625 K.

Infrared Spectroscopy

Infrared spectroscopy has been widely used to identify species adsorbed on solid surfaces. During the last decade, there has been increasing use of infrared spectroscopy in structural investigations of zeolites, particularly when the powder X-ray diffraction method may not be suitable for measuring structural information of zeolites with different crystalline sizes. Furthermore, infrared spectroscopy is concerned with short-range order that is only slightly different for zeolites of the same group.

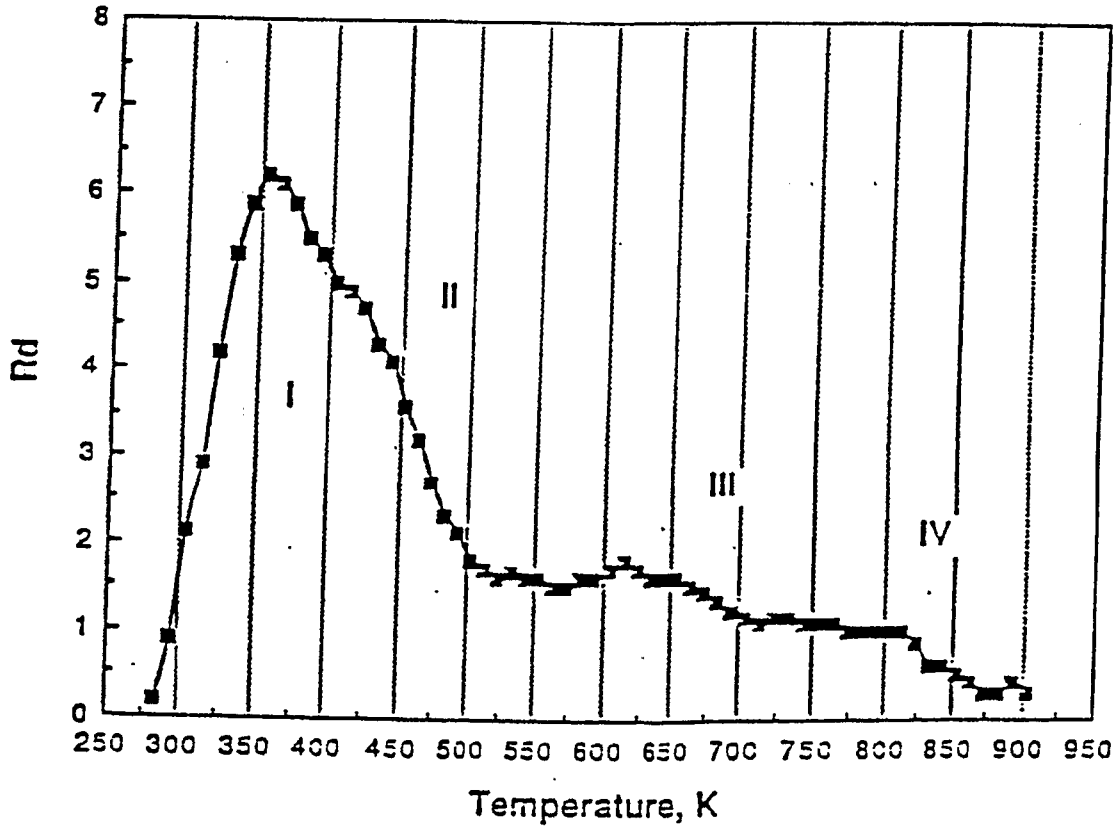

Figure 40. Temperature-Programmed Desorption Spectrum of Ammonia Zeolite ZSM-48/5(70)

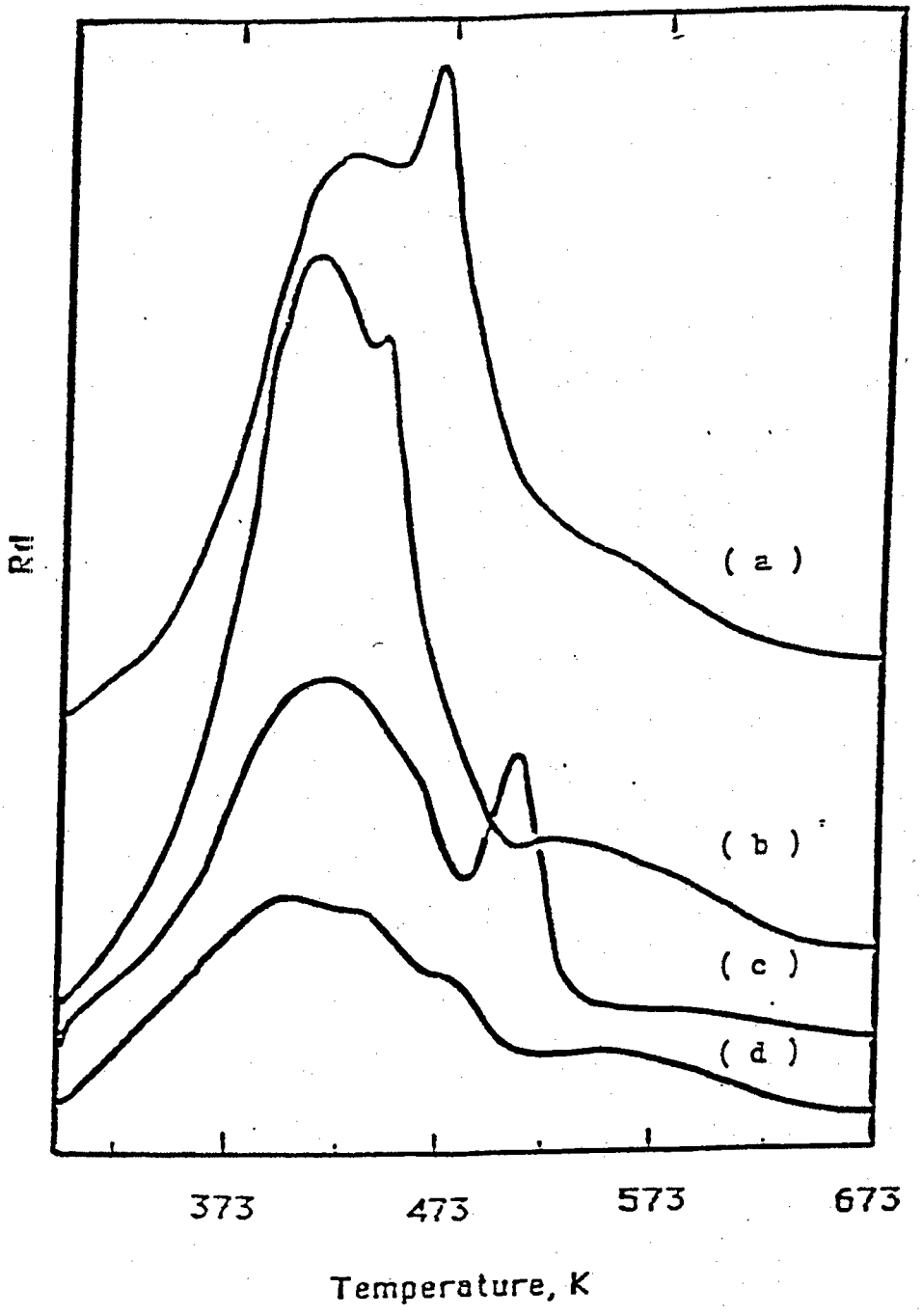

Figure 41. Temperature-Programmed Desorption Spectra of Alcohols from HZSM-5:

(a)	n-Butanol	(c)	Ethanol
(b)	n-Propanol	(d)	Methanol

The diffuse reflectance FTIR spectra of the zeolites prepared in this investigation are presented in Appendix A. According to the Flanigen-Khatami-Szymanski correlation,[231] the 650-550 cm^{-1} band was empirically assigned to the presence of double-rings of tetrahedra in the framework of a zeolite. A band around 500 cm^{-1}, which was not observed in silica, may be attributed to internal vibrations of ZSM-5 or ZSM-48. The optical density ratios of the A (~600 cm^{-1}) and B (~500 cm^{-1}) bands determined from normal coordinate calculations are presented in Table 25. It appears reasonable to use the optical density ratio, A/B, as a criterion for determining the structural characteristics of the zeolite frameworks since the ratio depend on the variety of the external vibrations of the zeolites. Thus, one may predict that the A/B ratio increases as the degree of the external vibrations, which are assigned to linkages of the TO_4-tetrahedra, increases. This is true that for high crystallinity zeolites, the A/B ratio of ZSM-5 is equal to ~0.8 and that of ZSM-48 is equal to ~0.3. These data also fit quite well in Figure 25, which shows the effect of the SiO_2/Al_2O_3 ratio on the synthesis of ZSM-48. This indicates that infrared spectroscopy also has a potential for offering structural information of zeolite materials.

Infrared spectra were measured using an in situ diffuse reflectance FTIR method during and after pulse methanol reaction with zeolites ZSM-5 and ZSM-48 at 643 K. The difference spectra are shown in Figure 42. The negative features at 3600 and 3745 cm^{-1} observed during methanol reaction may be correlated to the positive feature around 3000 cm^{-1} which is attributed to adsorbed hydrocarbons. The strong broad positive feature between 3000 and 3700 cm^{-1} corresponds to absorption of water (free water plus weakly adsorbed water molecules) produced during methanol reactions. Irreversibly adsorbed hydrocarbons were observed only with ZSM-48 following the methanol reaction.

Table 25

IR Structural Characteristics of the Zeolite Frameworks

Zeolite	Optical Density Ratio,[a] A/B	XRD Crystallinity
HZSM-5M	0.80	100
HZSM-5D	0.81	95
HZSM-5b	0.74	91
HZSM-5(35)	0.84	99^+
HZSM-5(70)	0.83	99^+
HZSM-5(105)	0.82	99^+
H{In}ZSM-5	0.81	99^+
HZSM-48(200)	0.25	ZSM-48
HZSM-48/5(100)	0.51	ZSM-5/ZSM-48
HZSM-48/5(70)	0.65	ZSM-5/ZSM-48
H{In}ZSM-48	0.33	ZSM-48
SiO_2	0	0

[a]Optical Density Ratio, A/B, is defined in the text.

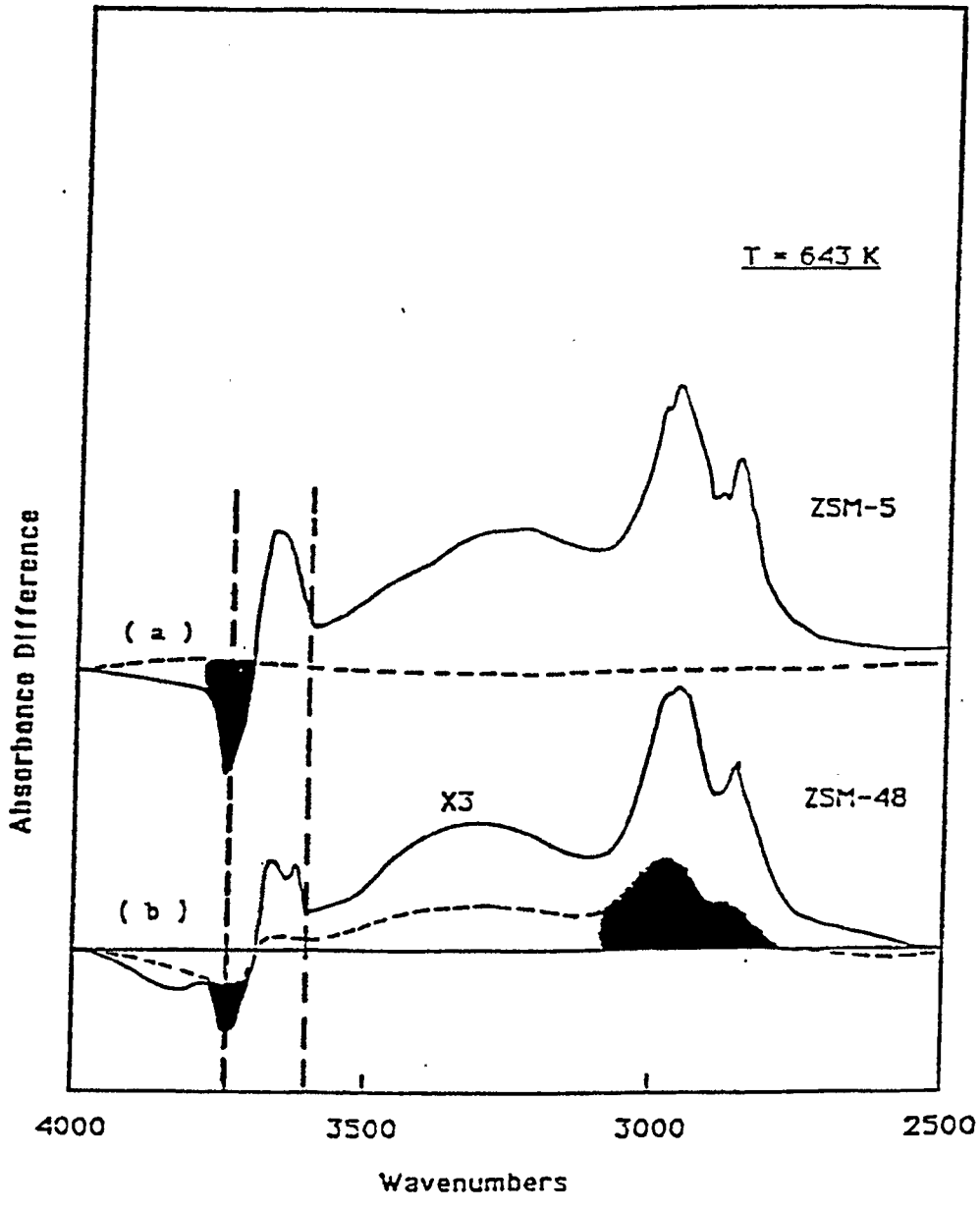

Figure 42. In-situ Diffuse Reflectance FTIR Study of Methanol Conversion over ZSM-Type Zeolites

The thermal desorption of methanol from ZSM-5 and ZSM-48 was also studied using diffuse reflectance FT-IR. The zeolite sample was exposed to methanol vapor at room temperature and heated to the desorption temperatures in the flowing helium. The infrared difference spectra for thermal desorption of methanol from ZSM-5 are presented in Figure 43. The background spectrum was measured on a fresh ZSM-5 sample at room temperature. Methanol interacted with the silanol group at 3710 cm^{-1} and strongly with the hydrogen cation (Brönsted acid site) at 3600 cm^{-1}. Similar results are also observed for ZSM-48 which is presented in Figure 44. However, because of the interference of the hydrogen-bonded hydroxyl groups, the behavior of aluminum-bonded hydroxyl groups (Brönsted sites) could not be observed clearly enough to interpret the difference in the distribution of Brönsted sites between ZSM-5 and ZSM-48 which was observed by ammonia-TPD spectroscopy.

Catalytic Cracking of n-Hexane

The cracking of n-hexane provides a suitable test reaction that is free of diffusion limitations for both intermediate pore size zeolites ZSM-5 and ZSM-48. Primary data (Appendix B) on catalytic cracking activity were obtained from measurements of n-hexane conversion to C_1 - C_5 hydrocarbons (mostly C_3 and C_4 aliphatics) in a continuous flow microreactor. A suitable choice of reaction temperature was made for each zeolite so as to maintain conversion within a limited range (5-40 percent) because of the wide range of activities encountered or measured by hexane conversion. At a given temperature the magnitude of the first-order rate constant (k) was obtained from the expression:

$$k = (1/t)\ln[1/(1-\varepsilon)] \qquad (4\text{-}3)$$

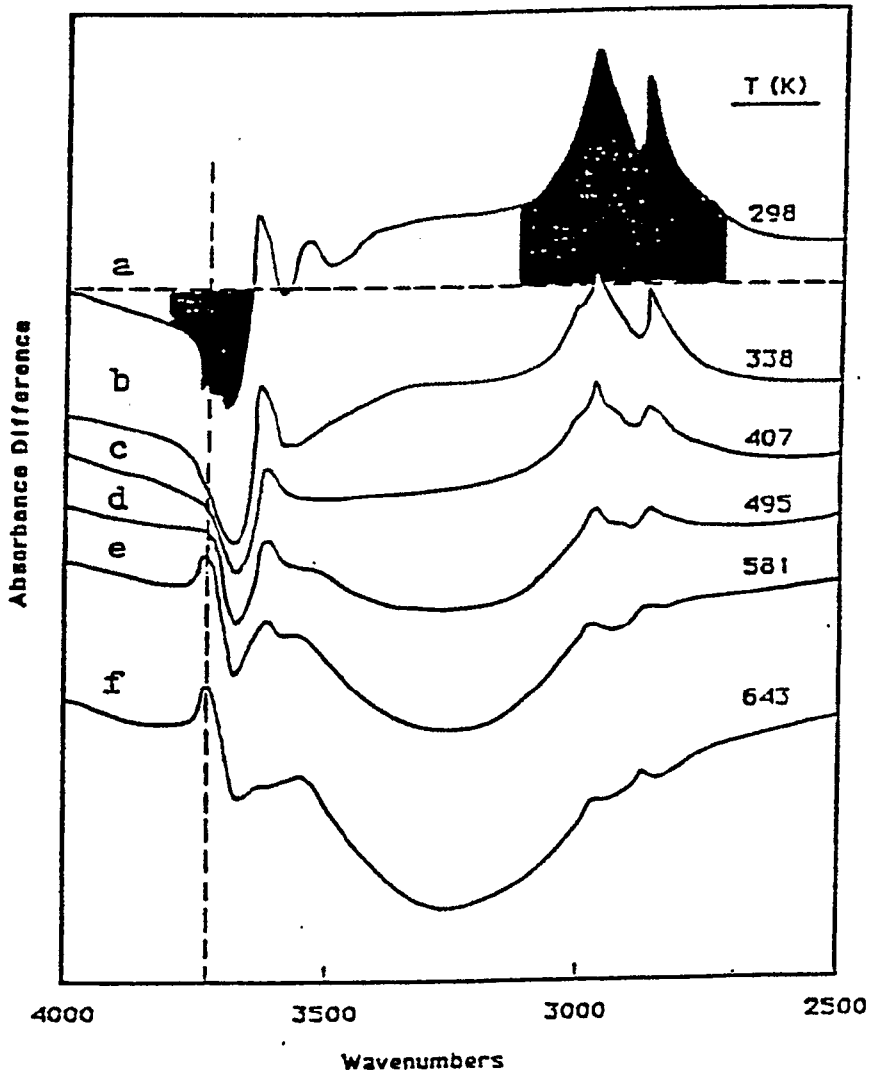

Figure 43. Diffuse Reflectance FTIR Study of the Thermal Desorption of Methanol from Zeolite ZSM-5

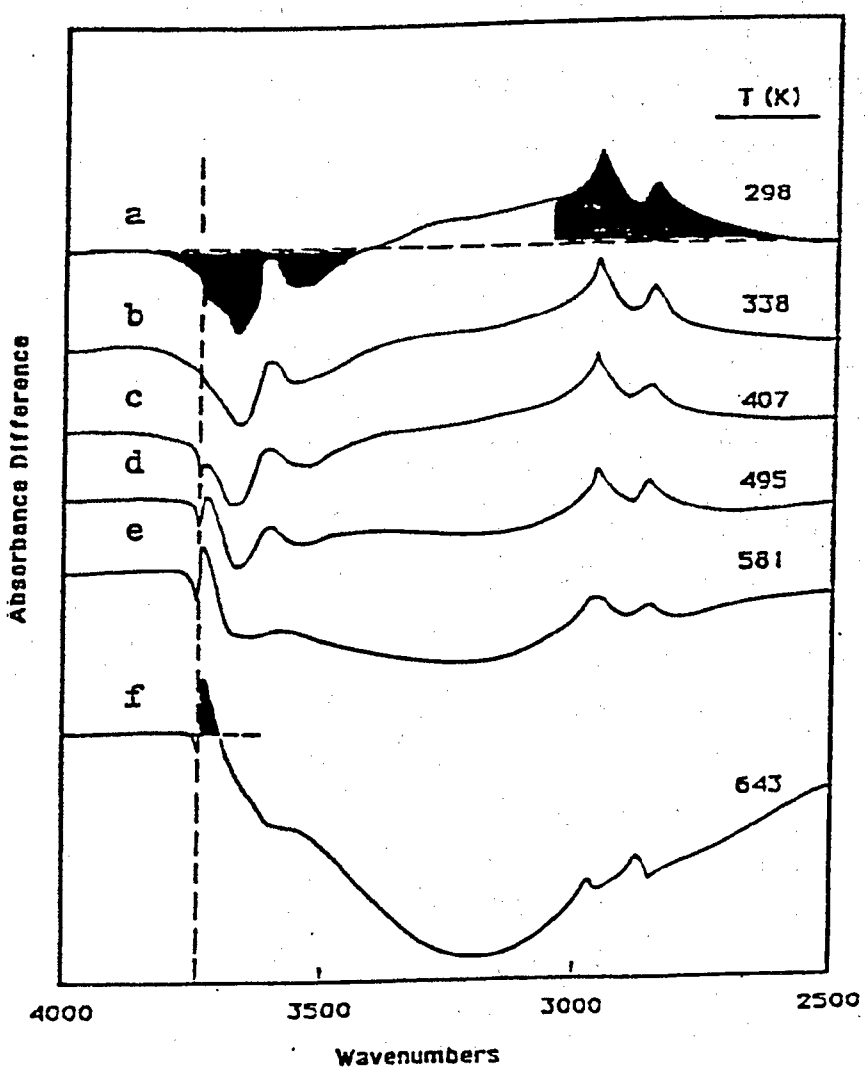

Figure 44. Diffuse Reflectance FTIR Study of the Thermal Desorption of Methanol from Zeolite ZSM-48

where ε is the observed fractional conversion and t is the contact time.[150]

The results of hexane cracking over crystalline aluminosilicates including HY, ZSM-5, and ZSM-48 are presented in Figure 45. Attainable levels of superactivity of the order of magnitude of $\alpha > 10{,}000$ (relative to amorphous silica-alumina, $\alpha = 1$) were obtained for both ZSM-5 and ZSM-48. The zeolites Y and ZSM-5 showed a normal apparent activation energy of 30 kcal/mole. Interestingly, a deviation in apparent activation energy from the generally prevailing behavior for the ZSM-48-type zeolites was found. The slopes of the lines in Figure 45 indicate that the apparent activation energy for cracking of n-hexane over ZSM-48/5(70) is approximately one-half of the value (30 kcal/mol) for the ZSM-5 and the HY zeolite. Such a depression of the slope may be expected for a situation where diffusion inhibition corresponds to a utilization factor or Thiele modulus $n < 0.5$. This indicates that the true intrinsic rate constant of the ZSM-48-type zeolites was even greater than measured. The results may be attributed to the two-dimensional channel structure reported for the ZSM-48 which is expected to be different from other zeolites with three-dimensional pore/channel structure.

Isomerization of Isobutane

Product distributions in shape selective catalysis are governed by the size and shape of the pores or channels within the zeolite structure. These pores or channels restrict the diffusion of larger reactant and product species in addition to restricting the formation of larger transition states and hence limiting the size of the molecules that can react or form. The pores of ZSM-5 and ZSM-48 have openings of about 5.5 A. They can admit linear and slightly branched paraffins, and simple naphthenes and aromatics.

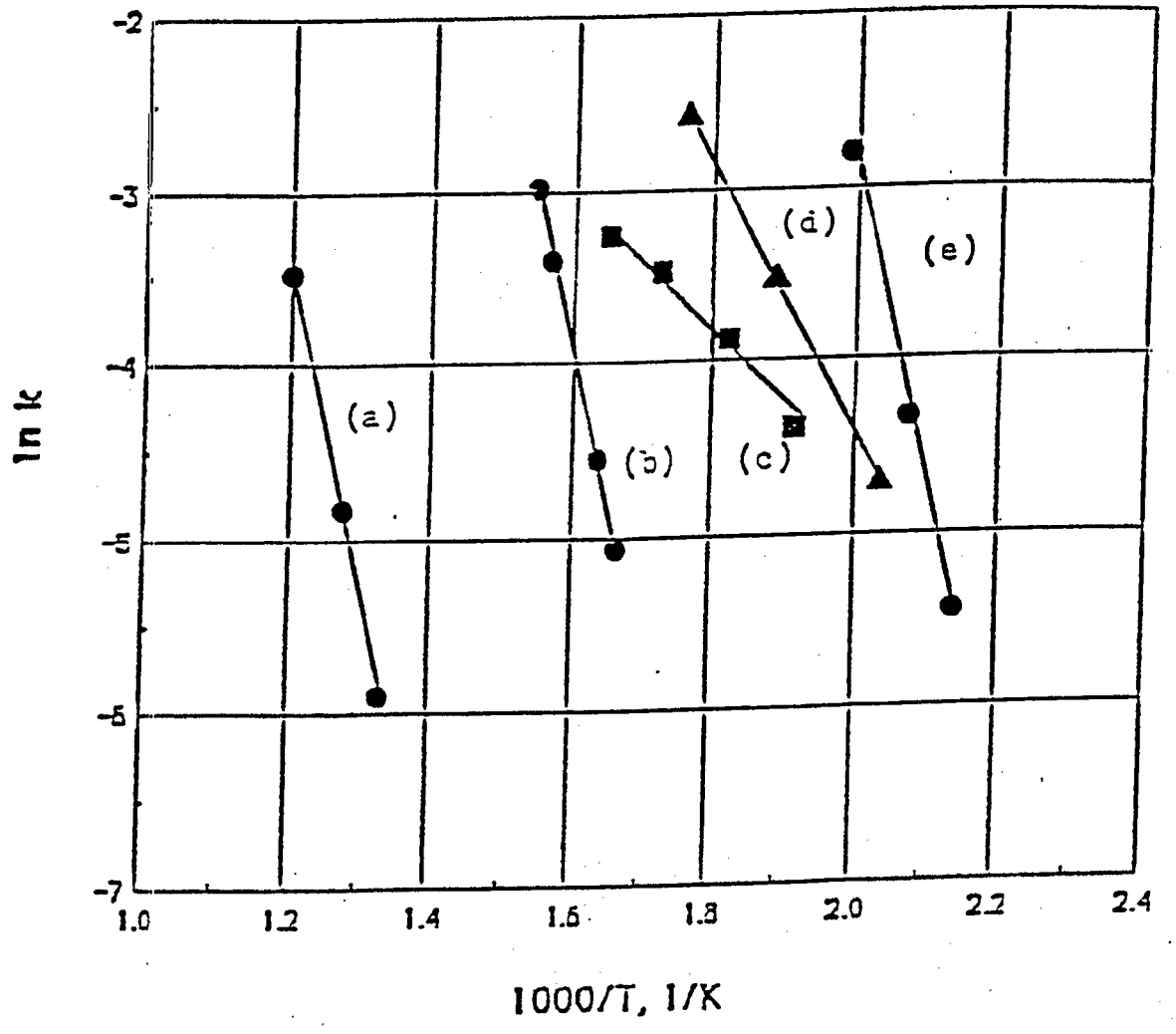

Figure 45. Alpha Test - Normal-Hexane Cracking Activity with Crystalline Aluminosilicates

(a) Aluminosilica
(b) HY
(c) ZSM-48(200)
(d) ZSM-48/5(70)
(e) ZSM-5(70)

Isomerization of isobutane was studied at 623 K with a hydrogen/isobutane molar ratio of four in a microreactor to investigate the pore/channel structure of ZSM-5 and ZSM-48. The results are shown in Table 26. Pentanes were absent from the reaction product. This result is in agreement with the conclusion reached by Hilaireau et al.[154] that two isobutane molecules cannot be accommodated simultaneously at the channels intersections of ZSM-5. Thus it also suggests a mono-molecular reaction mechanism for isomerization of isobutane over ZSM-48. In other words, there is not enough space for a bimolecular (isobutane) transition state in the pores of ZSM-5 or ZSM-48.

Surface Area Measurement

The possible modes of nitrogen adsorption on the external and internal (pore system) surface of an intermediate pore zeolite ZSM-5 is illustrated in Figure 46. It also illustrates normal-hexane filling the pore/channel system of a zeolite. Thus, the external surface area can be measured with pores which are filled with normal-hexane. Furthermore, it is noted that it is impossible to form multiple layers of adsorbed nitrogen on the internal surfaces. Thus, even the use of the Langmuir isotherm may not be an appropriate method for the study of adsorption of nitrogen on the surfaces of a microporous (pore diameter < 20 Å) zeolite such as ZSM-5 or ZSM-48. A modified Langmuir method combined with a SEM geometrical method was used to investigate the surface area of the synthetic zeolites in this study.

The mean pore diameter for both ZSM-5 and ZSM-48 is believed to be 5.4 Å. Thus the internal surface area corresponding to a mole of N_2 adsorbed at 77 K in the channel can be calculated as following.

Table 26

Isomerization of Isobutane at 623 K

Hydrogen/Isobutane Molar Ratio of Four

Zeolite	Product Distribution, wt%			Ref.
	Propane	n-Butane	Pentanes	
Mordenite	41	24	11	(128)
HY	7	2	7	This Work
HZSM-5(70)	0	0	0	This Work
HZSM-48(200)	0	0	0	This Work

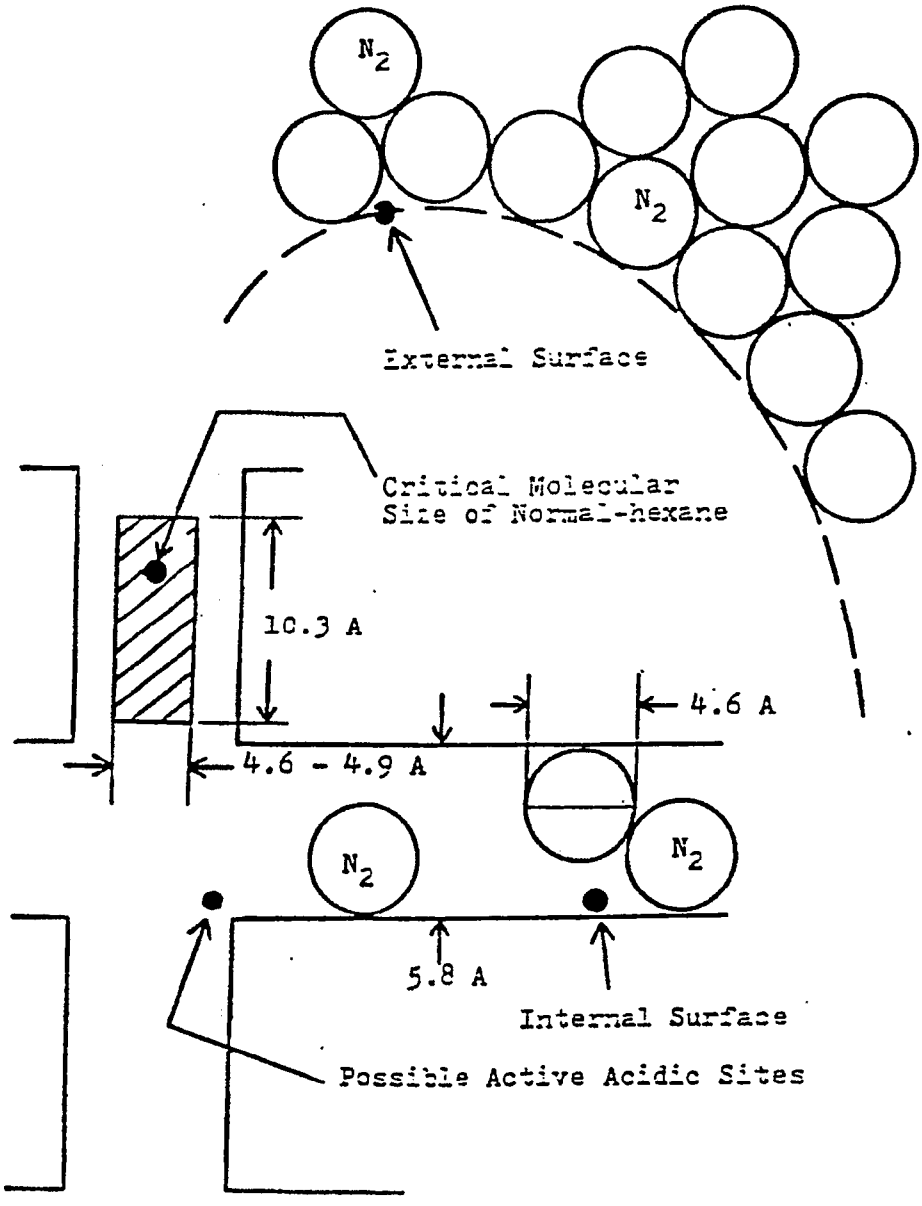

Figure 46. Possible Model for N_2 Adsorption of Zeolites with Intermediate Pore Structure

Channel Diameter (Dc) = 5.4×10^{-10} m

Nitrogen Diameter (Dn) = 4.6×10^{-10} m

Channel Surface Area $= \pi DcDn(6.02 \times 10^{23})$

$= 3.14 \times (5.4 \times 10^{-10}) \times (4.6 \times 10^{-10}) \times (6.02 \times 10^{23})$

$= 4.7 \times 10^{5}$ (m^2/mole N_2 adsorbed)

Thus the internal surface area can be calculated.

Weight of ZSM-5 = 0.222 g

Weight of ZSM-48 = 0.217 g

Adsorption of N_2 at p/p_o = 0.63 and T = 77 K

Adsorbed N_2 on Fresh ZSM-5 = 1.17×10^{-3} mole

Adsorbed N_2 on Pore-filled ZSM-5 = 1.00×10^{-3} mole

Adsorbed N_2 in the Channel of ZSM-5 = 1.7×10^{-4} mole

Adsorbed N_2 on Fresh ZSM-48 = 7.37×10^{-4} mole

Adsorbed N_2 on Pore-filled ZSM-48 = 4.76×10^{-4} mole

Adsorbed N_2 in the Channel of ZSM-48 = 2.61×10^{-4} mole

Internal Surface Area of ZSM-5

$= (1.70 \times 10^{-3}) \times (4.7 \times 10^{5})/0.222$

$= 359.9$ (m^2/g)

Internal Surface Area of ZSM-48

$= (2.61 \times 10^{-3}) \times (4.7 \times 10^{5})/0.217$

$= 565.3$ (m^2/g)

The external surface areas of synthetic zeolites were measured geometrically by SEM images. The SEM pictures of zeolites revealed identifiable cube, sphere, or rod forms. Zeolite ZSM-5 exhibited cubic-like crystals 0.5 - 2 μm in diameter while zeolite ZSM-48 appeared to be a bundle of rod-like crystals. Based on these SEM images, the external geometrical surface area could be calculated as follows.

Calculation of external surface area of ZSM-5

$$D = 1 \times 10^{-6} \text{ m}$$

$$\text{Density } (o) = 1.8 \text{ g/cm}^3$$

$$\text{External Surface Area } (A) = 6/RD$$

$$A = 6/[(1 \times 10\text{-}6) \cdot (1.8 \times 10^6)] = 3.3 \text{ (m}^2\text{/g)}$$

Calculation of external surface area of ZSM-48

$$D = 3 \times 10^{-7} \text{ m}$$

$$\text{Length } (L) = 4 \times 10^{-6} \text{ m}$$

$$o = 1.7 \text{ g/cm}^3$$

$$\text{External Surface Area } (A) = (1 + 4L/D)/Lo$$

$$A = [1 + (4 \times 10\text{-}6)/(3 \times 10\text{-}7)] \div [(4 \times 10\text{-}6) \times (1.7 \times 10\text{-}6)] = 2.1 \text{ (m}^2\text{/g)}$$

A summary of the surface area measurements for ZSM-5 and ZSM-48 is presented in Table 27. The total surface area measured for ZSM-5 in this work is generally consistent with the reported data.[159] Furthermore, one may expect that zeolite ZSM-48 could be effectively filled with normal-hexane since ZSM-48 has an one-dimensional channel structure while ZSM-5, with three-dimensional channel structure, may not be blocked all its pores by adsorbed normal-hexane.

Table 27

Surface Area Measurements of ZSM-5 and ZSM-48

	Surface Area (m^2/g)	
	Internal (Filled-pore Method)	**External (SEM Geometrical)**
ZSM-5	359.9	3.3
ZSM-48	565.3	2.1

It is true that a higher internal surface area for ZSM-48 than that for ZSM-5 was obtained. In addition, it is believed that most of the active centers of ZSM-5 are located in the interchannel; thus blocking all its pores of ZSM-5 by adsorbed normal-hexane is impossible. A high normal-paraffin (molecular length > 15 Å) such as normal-dodecane should be able to block all its pores of ZSM-5 theoretically during surface area measurements.

Summary

1. The Brönsted acid sites of synthesized zeolites were characterized by an ammonia desorption feature near 700 K.
2. For high crystallinity zeolites, the optical density ratio, A/B (a criterion for determining the structural characteristics of the zeolite frameworks), for ZSM-5 is equal to 0.8 and that for ZSM-48 is equal to 0.3.
3. The interactions between active acidic sites and methanol molecules were observed by in situ and thermal desorption FTIR (diffuse reflectance) spectroscopy.
4. Attainable levels of superactivity of the order of magnitude of $\alpha > 10{,}000$ were observed for ZSM-5 and ZSM-48.
5. It appears that the pore structures of both synthesized ZSM-5 and ZSM-48 have intermediate pore diameters and may not have cages around interchannels.
6. A modified method for measuring the surface area of zeolites with micropores is reported. The relatively low external surface area measured indicates that the catalytic reactions mostly occur on the internal surfaces.

Reaction of Alcohols over Zeolites

Since the development of the process for the conversion of methanol to hydrocarbons by Mobil,[30] the reactions of higher alcohols over ZSM-5 catalysts have been widely studied.[173,181,183] A review of these studies revealed that essentially the same product distribution was obtained for C_1 to C_6 alcohols which indicates that a common reaction network/pathway may be followed.[173] However, the effect of the channel structure of the ZSM-5 family of zeolites on the selectivity of alcohol reactions has not been described in the literature. The mechanisms of alcohol reactions are not fundamentally different over zeolite catalysts than they would be with any other acidic oxides from a purely chemical standpoint. Zeolites introduce molecular shape selectivity due to pore structure effects. In the course of this work, ZSM-5, ZSM-48, and related zeolites have been used for the systematic study of C_1 - C_4 alcohol reactions. The product distributions are summarized in Appendix III. It should be noted that ZSM-5 and ZSM-48 have similar pore diameters; however, they appear to have different channel structures. Thus these two catalysts were thought to be useful for this type of study.

The alcohol reactions were studied in a fixed-bed continuous flow microreactor operating at atmospheric pressure. Alcohols were fed to the reactor from a saturator by means of helium carrier gas. Reaction product distributions were recorded after 40 minutes on-stream. The most significant aspect of the methanol reaction over both ZSM-5 and ZSM-48 is the cut-off point in the hydrocarbon product distribution at C_{10} aromatics in the reaction temperature range of 594-759 K (shown in Figures 47 and 48, respectively). The aromatic fractions consisted mainly of xylenes and toluene with a smaller amount of benzene, ethylbenzene, and higher alkylated aromatics. The distribution of substituted aromatics is, of course, controlled by the dimensions of

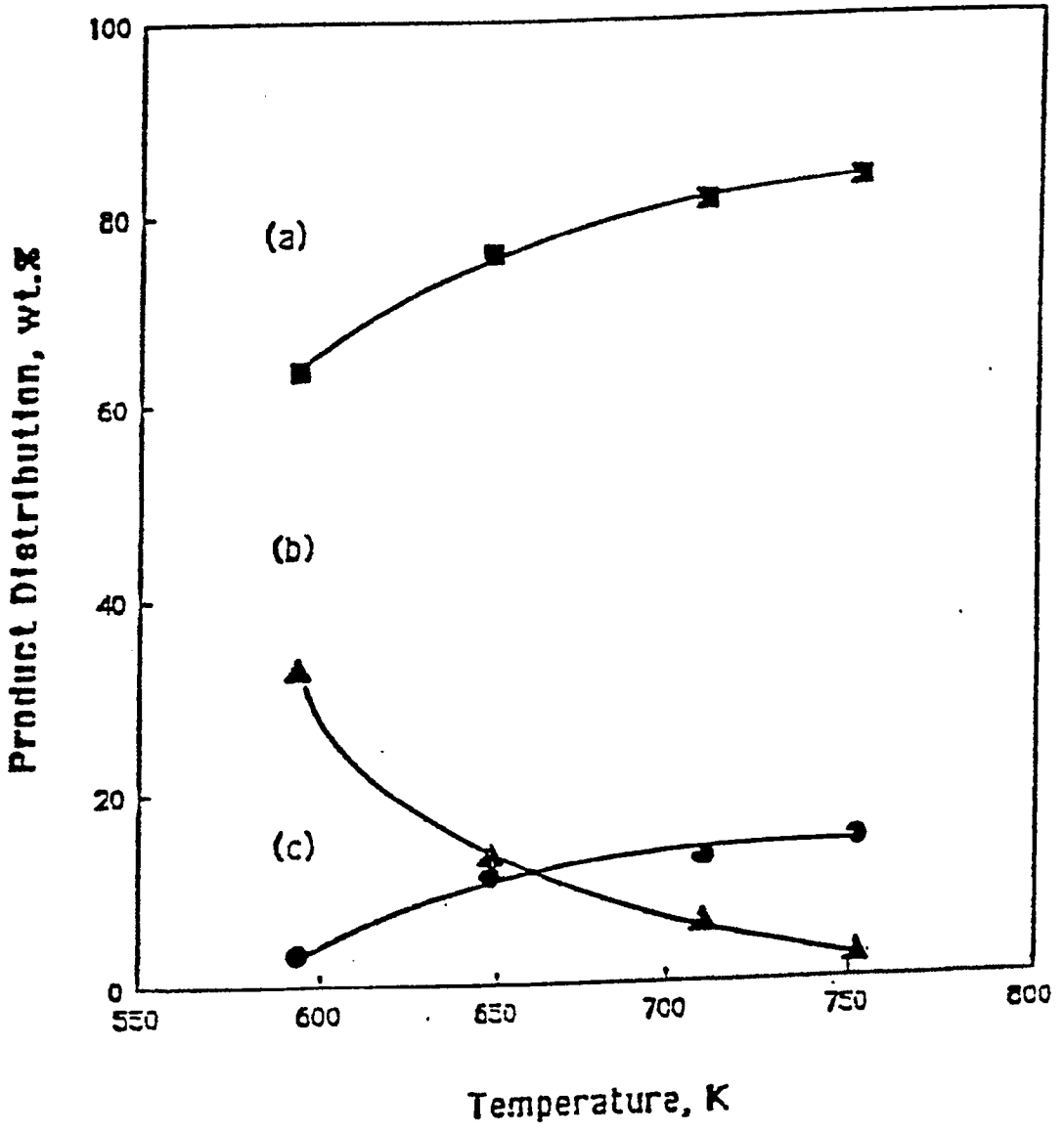

Figure 47. Product Distribution from Methanol Conversion over Zeolite HZSM-5(70) Helium Carrier Gas

(a) $C_1 - C_5$; (b) C_6^+; (c) Total Aromatics

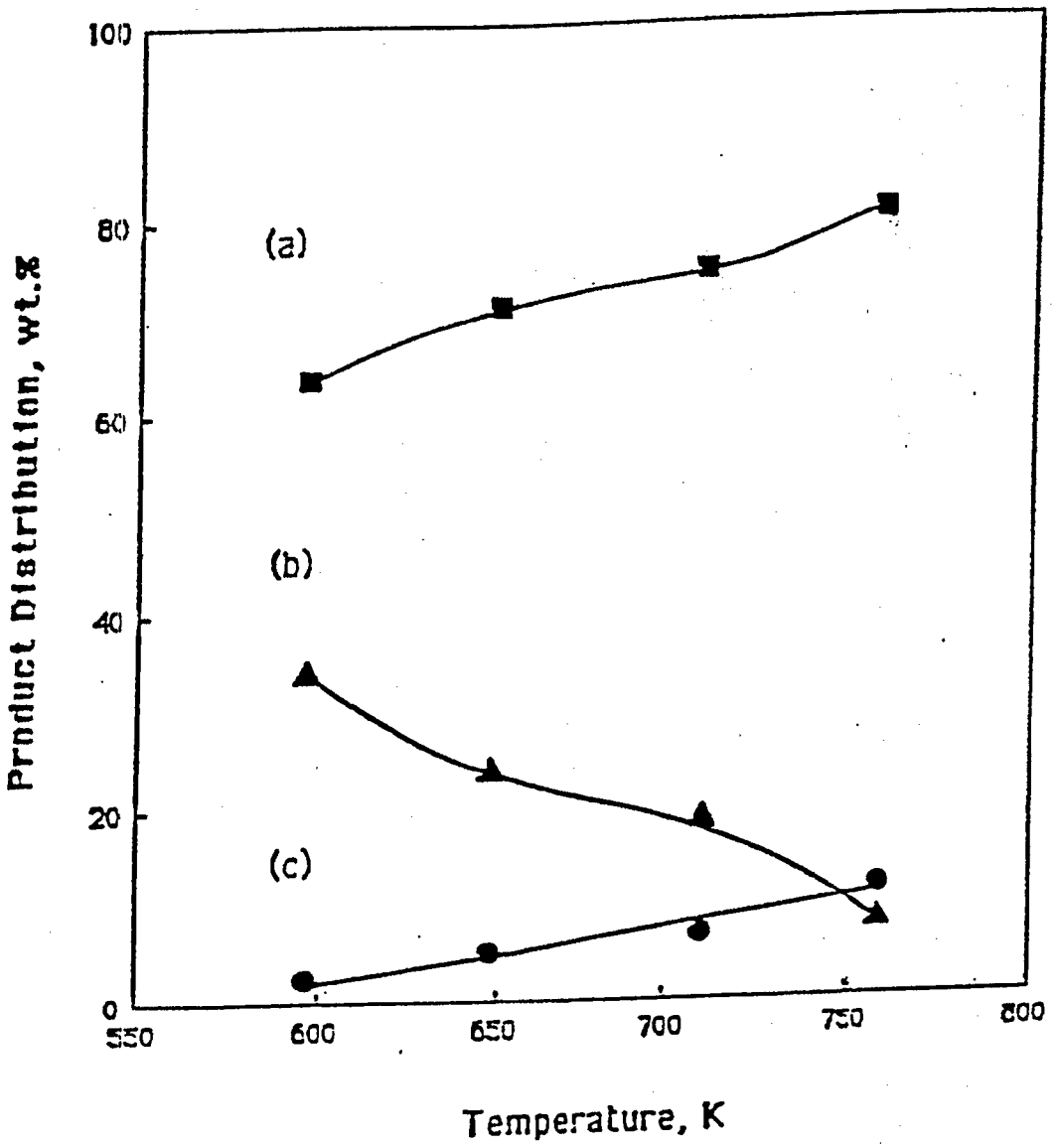

Figure 48. Product Distribution from Methanol Conversion over Zeolite HZSM-48(200)
Helium Carrier Gas

(a) C_1 - C_5; (b) C_6+; (c) Total Aromatics

the intracrystalline pore structure. Catalysis on unconstrained exterior sites would not account for the observed aromatic yields nor for the cut-off at C_{10} aromatics. Moreover, the surface area of the synthetic zeolites on the exterior is at least two orders of magnitude less than that on the interior (Table 27). Therefore, methanol would be expected to have access to the internal acidic sites and it is likely that most of the conversion to hydrocarbons occurred on these sites.

At a temperature of 594 K the reaction of methanol over ZSM-5 gave a low yield of aromatics, which were mainly xylenes. The main products were C_1 to C_8 aliphatic hydrocarbons. These aliphatics were further converted to aromatics as the temperature was increased up to 648 K; however, as the temperature was increased up to 752 K, the light gas yield increased as a result of secondary cracking. A similar trend was observed with ZSM-48; however, aromatic selectivity was lower (Table 28). The aromatic distribution is believed to be very sensitive to structural differences between the two zeolites. These differences may be attributed to the larger space available at the channel intersections of ZSM-5, which allowed the formation of larger carbonium ion intermediates for further reactions. The size and shape of the channel intersections are essential to explain the effects of transition state selectivity in the conversion of various feedstocks with ZSM-5 catalysts. As noted previously, ZSM-48 does not have channel intersections that permit formation of larger intermediates.[49] The absence of channel intersections in the intracrystalline pore structure of ZSM-48 could therefore account for the unique shape selective properties of this novel high silica zeolite.

Table 28

Product Distribution from Methanol Conversion over ZSM-5 and ZSM-48 in a Microreactor

(Reaction Temperature = 648 K)

	Product Distribution, wt%	
	ZSM-5	ZSM-48
C_5^- aliphatics	56.4	61.0
C_6^+ aliphatics	32.6	33.7
Aromatics	11.0	5.3

Zeolite channels are generally viewed as spaces where large electrostatic fields and gradients prevail.[232] Such environments can be described as ionic solvents, capable of promoting high energy ionization. It is possible to visualize the formation of carbonium (or carbene) species in this environment; therefore, an investigation of the effect of the presence of hydrogen in the reactant mixture on the yield of unsaturated hydrocarbons was undertaken. Helium was replaced by hydrogen as the carrier gas in this study. Typical hydrocarbon distributions from the reaction of methanol over ZSM-5 and ZSM-48 in the presence of hydrogen are presented in Figures 49 and 50, respectively. Essentially no hydrocarbons above C_{11} were produced and the aromatics are mostly methyl-substituted benzene. We believe that the product distribution is also shape selective in the hydrogen atmosphere. It is clear that hydrogen as well as helium behaved primarily as diluents. This point is illustrated for methanol conversion over ZSM-5 and ZSM-48 in Figures 51 and 52.

It has been noted that the formation of the first C-C bond from methanol requires the participation of Brönsted acid sites stronger than those required for subsequent steps.[16] A series of consecutive steps involving isomerization, oligomerization, cracking, cyclization, and hydrogen transfer are operative after the formation of propylene or of a higher olefin molecule in the initial stages of the reaction. The acidity of ZSM-5 and ZSM-48 was investigated by ammonia-TPD and α-test measurements. The results indicated that both types of zeolite are very acidic in the catalytic sense. The effect of the silica-to-alumina ratio on the aromatic selectivity for the methanol reaction over ZSM-5 is shown in Figure 53. The aromatic selectivities for methanol conversion over ZSM-5 were virtually independent of the silica-to-alumina ratio in the range of silica-to-alumina ratios investigated (35 to 105). The data also indicated that the limited number of active sites at the

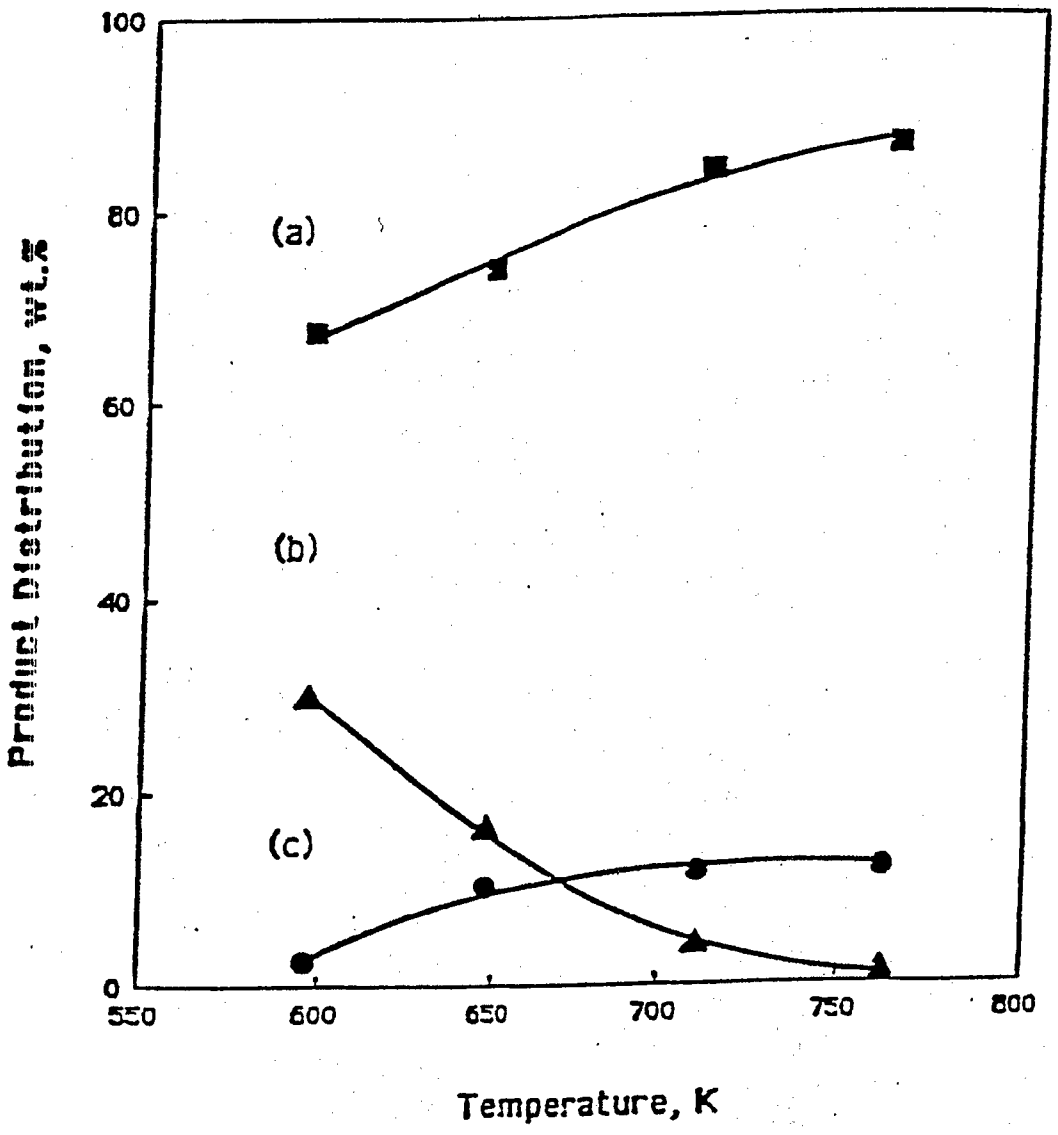

Figure 49. Product Distribution from Methanol Conversion over Zeolite HZSM-5(70)
Hydrogen Carrier Gas
(a) C_1 - C_5; (b) C_6+; (c) Total Aromatics

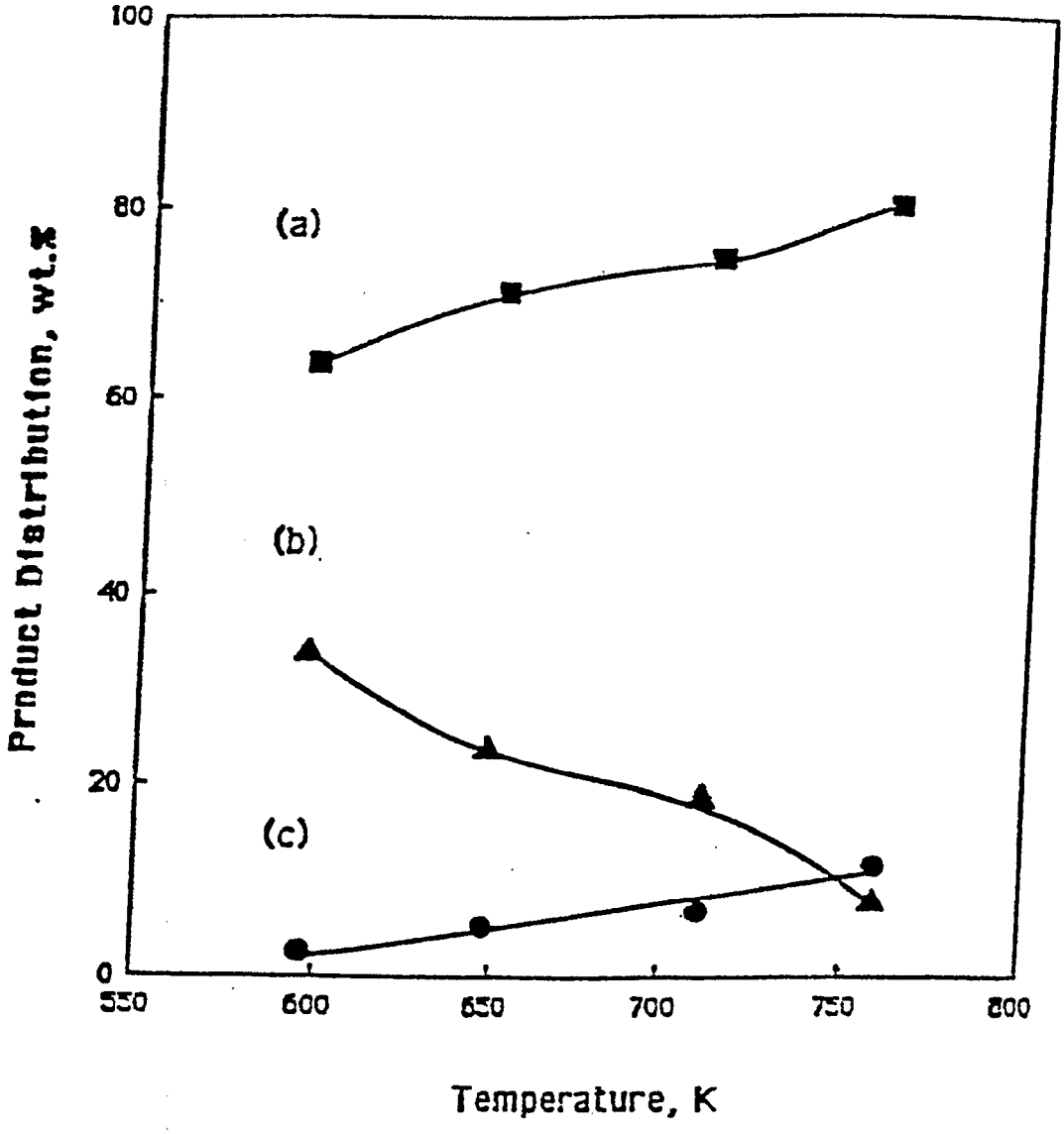

Figure 50. Product Distribution from Methanol Conversion over Zeolite HZSM-48(200)
Hydrogen Carrier Gas

(a) C_1 - C_5; (b) C_6+; (c) Total Aromatics

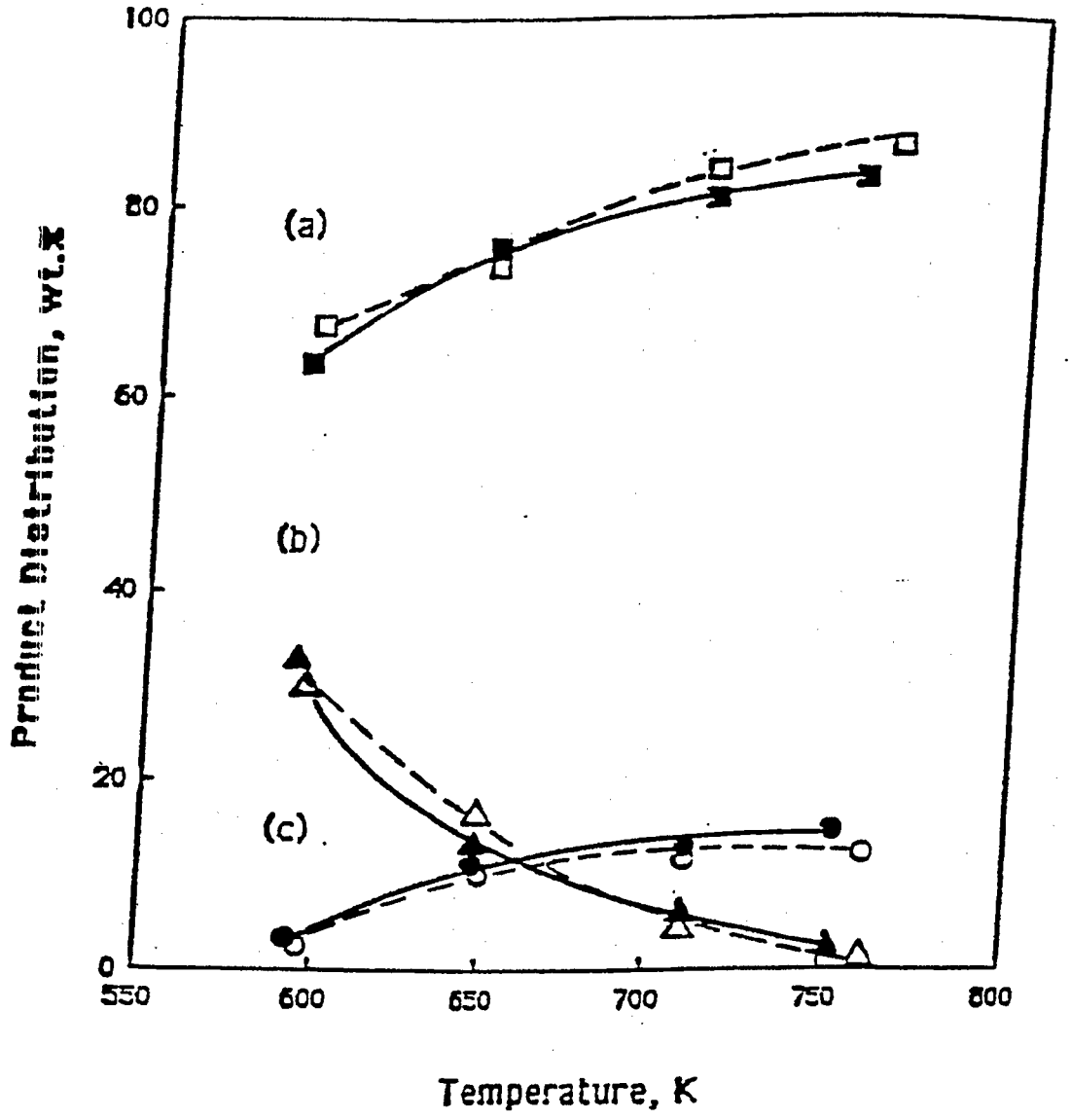

Figure 51. Product Distribution from Methanol Conversion over HZSM-5(70)

(a) C_1 - C_5; (b) C_6+; (d) Total Aromatics

(Solid lines denote product distribution from methanol conversion in helium carrier gas, and dashed lines denote that in hydrogen carrier gas)

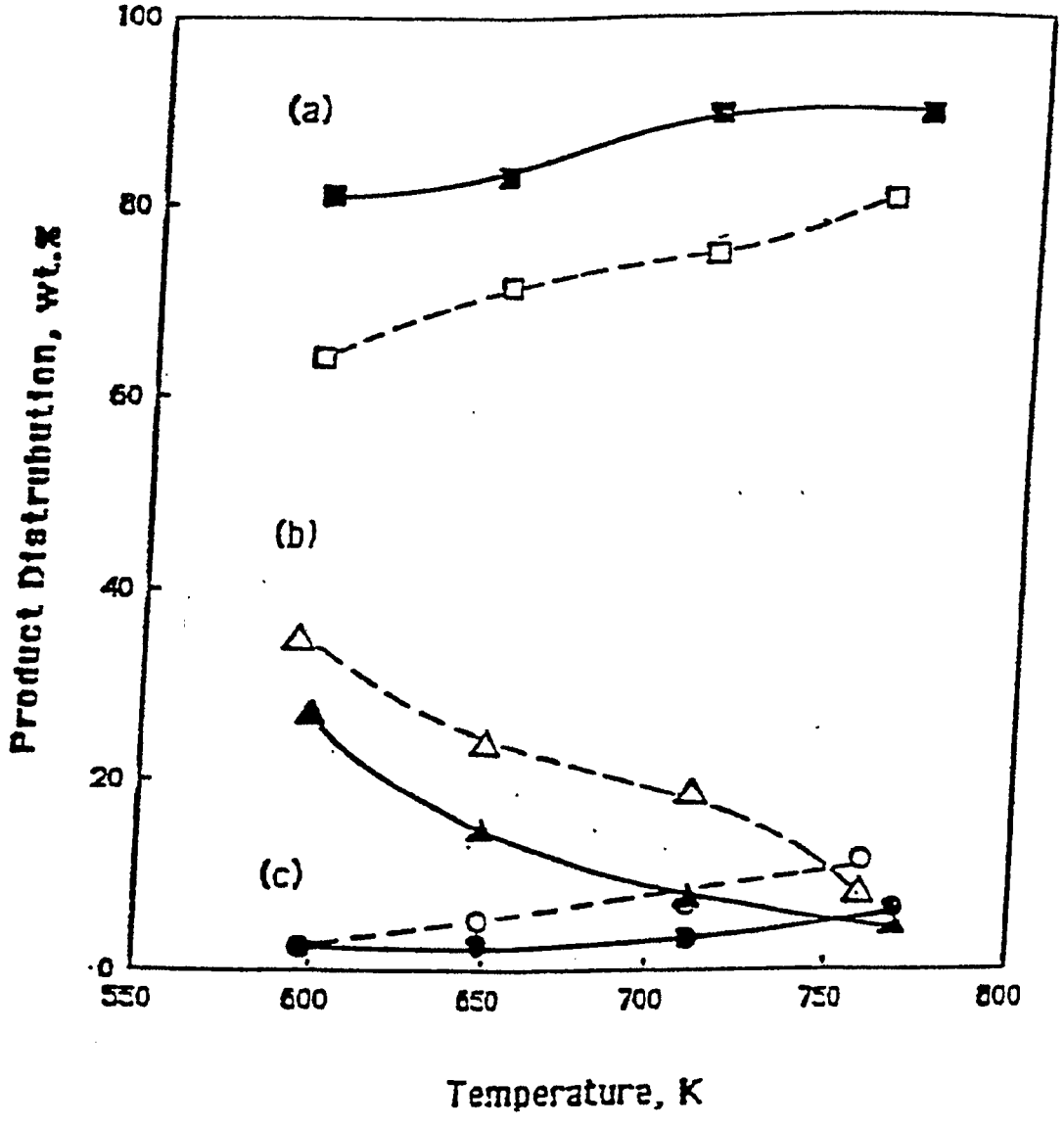

Figure 52. Product Distribution from Methanol Conversion over HZSM-48(200)

(a) C_1 - C_5; (b) C_6+; (c) Total Aromatics

(Solid lines denote product distribution from methanol conversion in helium carrier gas, and dashed lines denote that in hydrogen carrier gas)

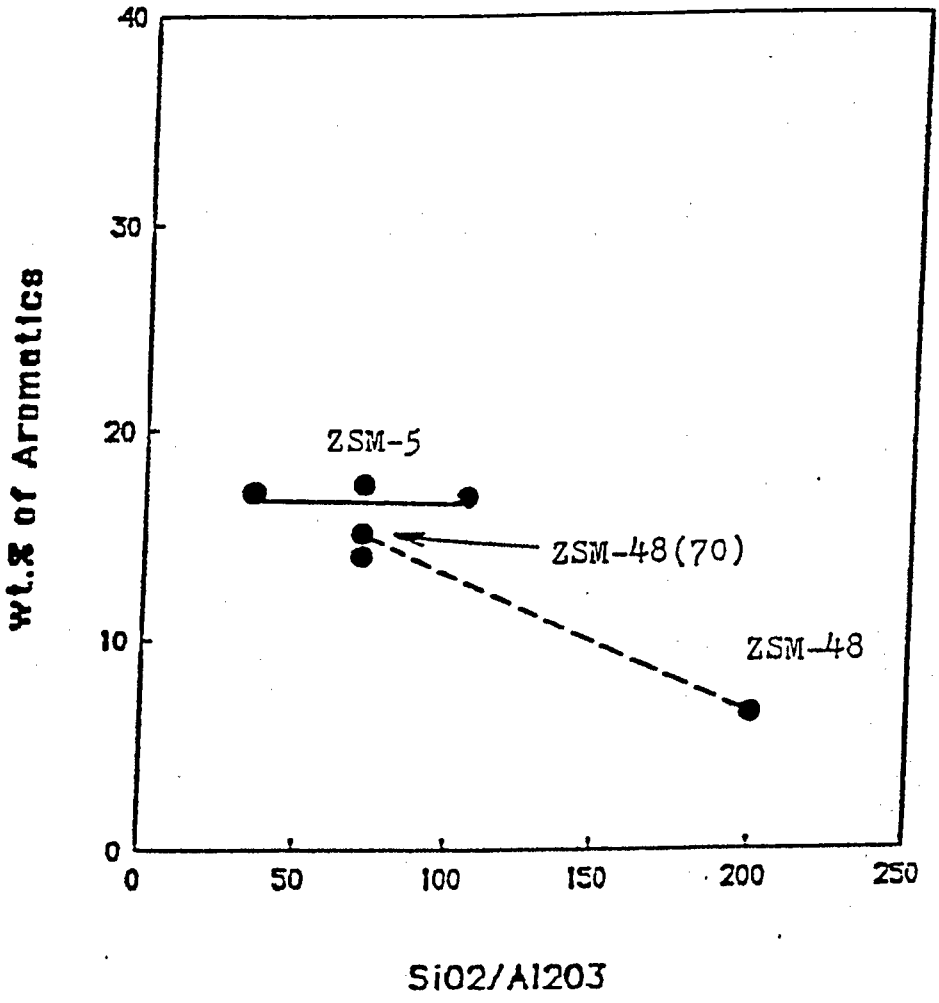

Figure 53. Effect of SiO_2/Al_2O_3 Ratio on Aromatic Selectivity for Methanol Conversion over ZSM-5.

channel intersections is essential to explain the observed transition state selectivities. It may be true that the limited number of active acidic sites in the channel intersections are expected since organic cation, such as TPA^+, may completely occupy the channel intersections of ZSM-5 during the synthesis of the zeolite. It should be noted that methanol was converted first to dimethylether followed by conversion of the dimethylether to olefins. The olefins are transformed into longer chain aliphatics which cyclize and dehydrogenate to form aromatics. The channel intersections of ZSM-5 may provide the necessary space as well as acidity for the formation of aromatics from methanol.

The low aromatic selectivity of ZSM-48 is attributed to local configuration constraints, imposed by the immediate environment of the active centers, which decrease the probability of the formation of the necessary transition state characteristic of the elementary step in the formation of aromatics. The preliminary results reported in the present work may indicate that the difference in the shape-selective properties of a series of pentasil zeolites is due to definitive differences in the zeolite channel structure.

The restricted environment near the active centers may play a distinct role in the ordering of reaction products. The reactions of C_1 - C_4 alcohols over ZSM-5 synthesized in the presence of TPABr (i.e., ZSM-5(70)) or C6DN (i.e., ZSM-5D) were investigated in an attempt to better understand aromatic selectivity. A comparison of their aromatic selectivities is presented in Figure 54. A higher aromatic selectivity is observed for zeolite ZSM-5D as the carbon number of reactant alcohol increases when compared to that for ZSM-5(70). Since both of the zeolites have an identical pore/channel structure, such an observation may result from the difference in the environment of the active centers. In addition, the aromatic selectivity of ZSM-5 during

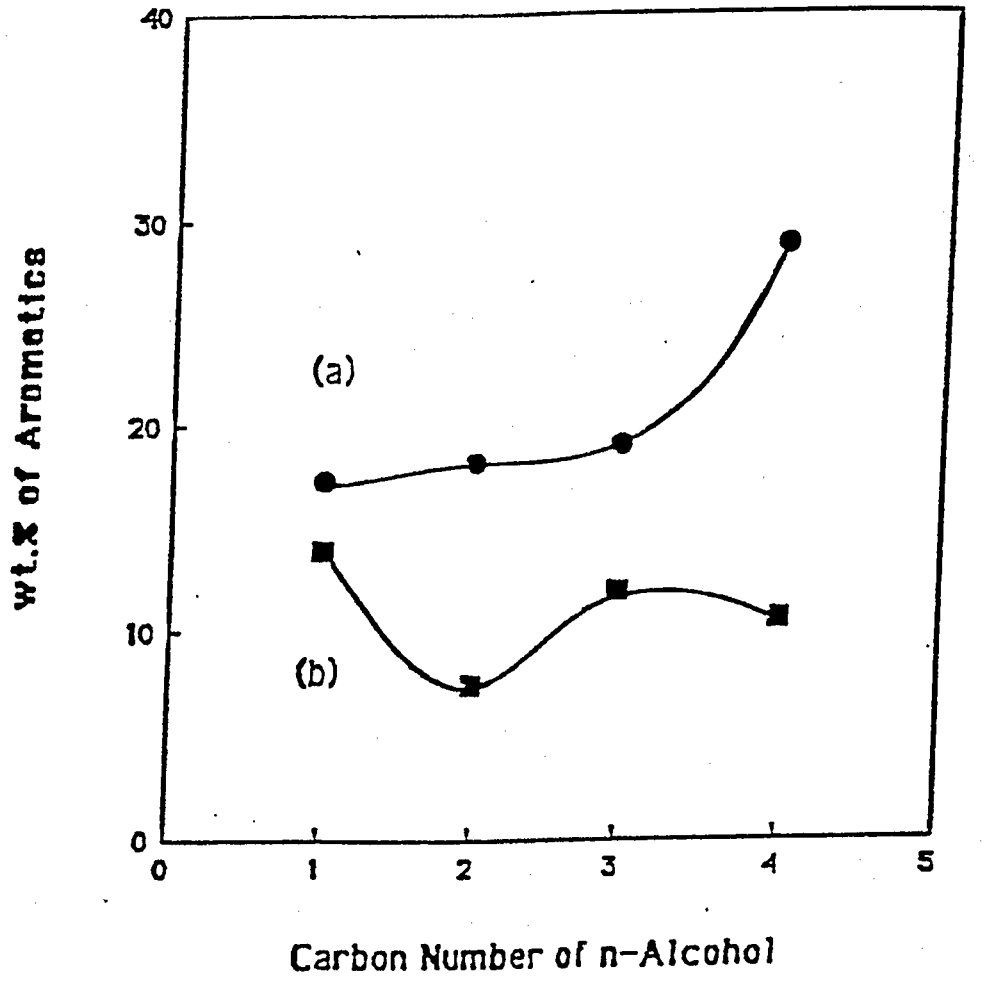

Figure 54. Effect of Organic Ions Used in the Synthesis of ZSM-5 on the Aromatic Selectivity for Alcohol Reactions

(a) C6DN; (b) TPABr

ethanol conversion, which formed ethylene over the ZSM-5 at the initial step in the reaction sequence, was low. This is consistent with other investigations, which indicated that the formation of hydrocarbons may not occur via intermediate ethylene, as free ethylene is less reactive than methanol itself.[16]

Thus, as expected, the aromatic selectivities of ZSM-48/5(70), which was determined to be a physical mixture of ZSM-5 and ZSM-48 crystals, were found to lie between those of ZSM-5 and ZSM-48 (shown in Figure 55). Parallel results were also observed in the ammonia-TPD experiments.

Summary

1. The cut-off point in the hydrocarbon product distribution for the methanol reaction over both ZSM-5 and ZSM-48 was found at C_{10} aromatics.
2. The difference in the shape-selective properties of the pentasil zeolites ZSM-5 and ZSM-48 may be due to differences in the zeolite channel structure.
3. Zeolites synthesized in the presence of different organic ions may induce different environments in the vicinity of active centers even when they have similar pore/channel structure.
4. The restricted environment about the active centers may impose shape selective constraints on the local site reaction mechanism.

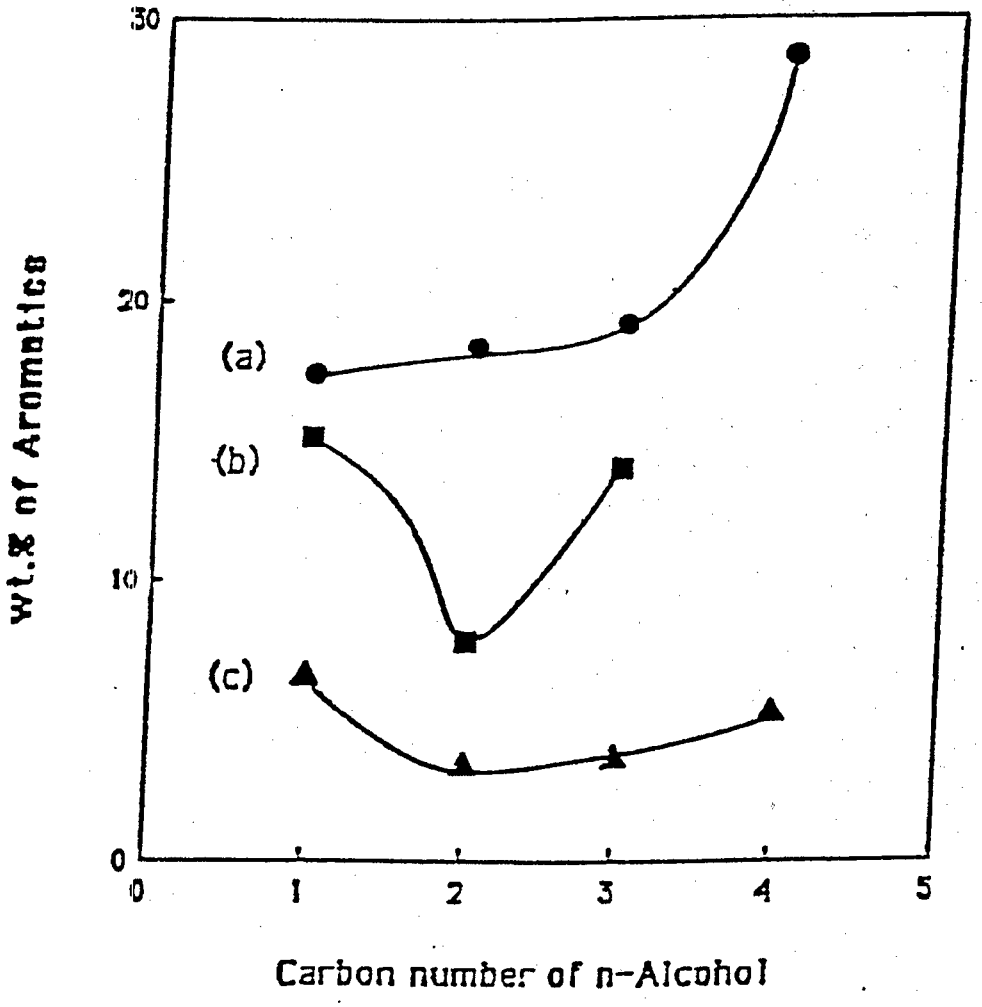

Figure 55. Effect of Channel Structure on the Aromatic Selectivity in Alcohol Reactions

(a) ZSM-5D; (b) ZSM-48/5(70); (c) ZSM-48(200)